INVESTIGATION OF THE RELATIONSHIP BETWEEN EXTREME WEATHER EVENTS AND AIR POLLUTION CONCENTRATION

BY

DEBADITYA SAHA

EXAM ROLL NO – M4CIV24020

CLASS ROLL NO – 002210402023

Registration number: 131941 of 2015 - 2016

MASTER OF ENGINEERING (ENVIRONMENTAL ENGINEERING)

2ND YEAR

UNDER THE GUIDANCE OF

DR. ABHISEK ROY

ASSISTANT PROFESSOR

DEPT. OF CIVIL ENGINEERING

AT

DEPT. OF CIVIL ENGINEERING

FACULTY OF ENGINEERING AND TECHNOLOGY

JADAVPUR UNIVERSITY

KOLKATA, 700032.

DECLARATION

This thesis titled "**INVESTIGATION OF THE RELATIONSHIP BETWEEN EXTREME WEATHER EVENTS AND AIR POLLUTION CONCENTRATION** "is prepared and submitted for the partial fulfillment of the continuous assessment of Master of Engineering in Civil Engineering at Jadavpur University for the session 2023 – 2024.

Date:

Place: Civil Engineering Department,

Jadavpur University, Kolkata

DEBADITYA SAHA

M.E. CIVIL ENGINEERING 2ND YEAR

EXAM ROLL NO.: M4CIV24020

CLASS ROLL NO: 002210402023

REGISTRATION NO.: 131941 of 2015-2016

JADAVPUR UNIVERSITY

DEPARTMENT OF CIVIL ENGINEERING

KOLKATA – 700032

RECOMMENDATION CERTIFICATE

I hereby approve this thesis report "**INVESTIGATION OF THE RELATIONSHIP BETWEEN EXTREME WEATHER EVENTS AND AIR POLLUTION CONCENTRATION**" is prepared and submitted foe the partial fulfillment of the continuous assessment of Master of Engineering in Civil Engineering Course at Jadavpur University under my supervision and guidance by Debaditya Saha (Exam roll no.- **M4CIV24020** and Class roll no. – 002210402023) , it is also declared that no part of this thesis work has been presented or published elsewhere.

_____

DR. ABHISEK ROY
(THESIS SUPERVISOR)
ASSISTANT PROFESSOR
DEPT. OF CIVIL ENGINEERING
JADAVPUR UNIVERSITY

Countersigned by

_____ _____

Dean **Head of the Department**

Faculty of Engineering and Technology
Jadavpur University

Department of Civil Engineering
Jadavpur University

CERTIFICATE OF APPROVAL

I hereby approve this seminar report titled **INVESTIGATION OF THE RELATIONSHIP BETWEEN EXTREME WEATHER EVENTS AND AIR POLLUTION CONCENTRATION** has been prepared under my supervision by Debaditya Saha (Exam roll no.- **M4CIV24020** and Class roll no. – 002210402023), entitled by me as a creditable study of an engineering subject, carried out and presented in a manner satisfactory to warrant its acceptance in partial fulfillment of the requirements for master of civil engineering

DR. ABHISEK ROY
ASSISTANT PROFESSOR
DEPT. OF CIVIL ENGINEERING
FACULTY OF ENGINEERING AND TECHNOLOGY
JADAVPUR UNIVERSITY
KOLKATA - 700032

ACKNOWLEDGEMENT

I would sincerely like to express my deepest sense of gratitude to my guide, **Prof. Dr. Abhisek Roy** for enlightening me with his expertise and his guidance throughout this project. I would also like to thank him for constantly helping and supporting me whenever I encountered a problem and for his continuous encouragement to improve my work.

I am deeply indebted to all my faculty members, all of my friends and every concerned person of this department as well as of this university for their cooperation

Date:

Place: KOLKATA

DEBADITYA SAHA

Exam roll no.- M4CIV24020

Class Roll No. – 002210402023

Registration number: 131941 of 2015 - 2016

PG-II, M.E. (2ND YEAR) Civil Engineering

Jadavpur University, Kolkata - 700032

Structure of the thesis

The thesis of 8 chapters contains.

Chapter 1: Introduction

Chapter 2: Review of Literature

Chapter 3: Overview of the study area

Chapter 4: Data collection and Methodology

Chapter 5: Results and Discussions

Chapter 6: Statistical Analysis (Pearson Correlation Coefficient)
Scatter Plot Matrix

Chapter 7: Conclusion and Future aspects

Chapter 8: References

APPENDIX A: RAW DATA IN TABULAR FORM
APPENDIX B: METEOROLOGICAL DATA IN TABULAR FORM

ABBREVIATIONS

TABLE OF CONTENTS

LIST OF TABLES AND FIGURES

1. Introduction

1.1 General

In recent years, air pollution has become one of the major risks to human health [1]. In 2019, 99% of the world's population was living in places where the WHO air quality guidelines were not met. Globally, Ambient(outdoor) air pollution is estimated to have caused 4.2 million premature deaths worldwide in 2019, and around 90% of those premature deaths occurred in low- and middle-income counties. Major air pollutants include Particulate matter (PM), Carbon monoxide (CO), Ozone (O_3), Nitrogen dioxide (NO_2) and Sulfur dioxide (SO_2). Exposure to high concentrations of PM for prolonged time periods can have severe health effects such as premature deaths in person with residual cardiovascular disease, non-fatal heart attacks, irregular heartbeat, aggravated asthma, decreased lung function [2]. Despite progress in some regions, many developing countries continue to face significant air quality challenges due to rapid urbanization, industrialization, and inadequate pollution control measures. In these areas, air pollution levels may have worsened in recent years. Even after enforcing stringent measures in developing countries like **India,** the cumulative levels of emission of these pollutants are still in the rise which is expected as the country is urbanizing at a faster rate, adequate cleaner energy resources cannot keep up with the demand as a result new thermal power plant are still being constructed and the new renewable sources are now being used as an assist to take up the loads during less demand peak hours. Another trend that has been seen in the recent years is the reduction of a few pollutants due to shift into cleaner sources of energy generation for example, as countries transition to cleaner and greener energy sources and more efficient power generation technologies, the sources of air pollution may change. For instance, a shift from coal-based thermal power generation to natural gas or renewable energy can lead to reductions in emissions of pollutants like sulfur dioxide and particulate matter.

Another important source of these pollutants is vehicular emission in the transportation sector, here also a shift in the types of pollutants has been observed and are expected to change in the upcoming decade. Vehicle emissions remain a major contributor to urban air pollution in many places. While advancements in vehicle technology have led to cleaner engines, the growth in the number of vehicles on the road can offset these gains. The rise of electric vehicles (EVs) and the adoption of stricter emissions standards are expected to impact air pollution trends in the transportation sector, another recent study suggest that the small rubber particles left from the tyres of the vehicles as they accelerate are also responsible for air pollution.

In recent years another major source of air pollution emission is natural disasters such as the combined effects climate change and raging wildfires which is being increasingly common in the continent of North America and Europe. In recent years, there have been instances of extremely intense and widespread wildfires in various parts of the world. These fires release large amounts of pollutants into the atmosphere, including particulate matter and harmful gases. Climate change can exacerbate wildfire risk, potentially impacting air quality. It is evident from all the different sources and different changing patterns that this problem of air pollutants cannot be traced backed to a single source or due to a single reason, rather it is cumulative effects of multiple effects of multiple sources. Urbanization, industrialization, and population growth continue to drive air pollution challenges worldwide and these parameters are expected only to rise in the upcoming years as more and more country starts to emerge from low-income economy to middle-income and those from middle-income to high-income economy, lifestyles changes are expected and as a result higher power requirement to fulfill their needs, these trends can lead to increased energy consumption, greater vehicle use, and more industrial emissions, all of which can impact air quality. As a result, strict air quality monitoring techniques need to be enforced to the major emitters and liable them to penalty if they fail to operate within emission limits guidelines. Advances in technology and data collection have led to improved air quality monitoring capabilities**. Real-time data** from monitoring stations and **satellite observations** allow for better tracking of pollution levels and sources, enabling more informed decision-making.

Different meteorological process occurring over a large spatial and temporal scales strongly affect the movement and concentration of various air pollutants and can affect the dispersion mechanism of these pollutants. Extreme weather events such as severe storms (category 3* and above), drought, heat waves, air stagnation becomes a thing of concern when the air pollutants are unable to disperse properly and remain in their emitted vicinity therefore through various different weather mechanism, climate anomalies may directly affect air quality parameters by affecting the dispersion patterns. Changes in time duration, frequency of the event, and spatial extent(reach) have been reported by the IPCC [3]. For e.g., Severe heat waves that are becoming more frequent over land areas are causing elevated average temperature, more aerosols emission triggered by forest fires, organic emissions and faster chemical reaction contributes to increase in various air pollutants, but climate projections and modelling have vast assumption basis which leads to significant uncertainties.

In order to improve future climate projection modelling, understanding the relationship between different air pollutant concentration and extreme weather events in the past becomes a crucial step.

A better understanding between the correlation of various meteorological parameters with various air pollutant concentration is strongly desired and can help in predict future weather anomalies.

Since most of the meteorological departments in our country nowadays are equipped with powerful supercomputers so if a direct correlation can be found in between different pollutants and meteorological parameters then we will be able to predict the changes in meteorological parameters via the respective study models.

Our first goal would be to establish any correlation between the pollutant concentrations and the meteorological parameters via statistical tools. We will be using the Pearson correlation coefficient in this case, its is a type of descriptive as well as an inferential statistical tool. As a result, although its main use is in descriptive research to summarize the associations between variables, it can also be applied to inferential research to draw more general statistical conclusions.

In 2022, the Delhi-based non-profit Centre for Science and Environment (CSE) and *Down to Earth (DTE)* Data Centre tracked the extreme weather events that took place throughout the year in India. It found that the country, on the whole, experienced extreme weather events on 314 out of the 365 days. This means that at least one extreme weather event was reported in some part of the country on each of these days.

In 2022, extreme weather events cumulatively claimed 3,026 human lives, affected at least 1.96 million hectares (ha) crop area, destroyed 423,249 houses and killed over 69,899 animals. The year was also the fifth warmest for the country, according to the India Meteorological Department (IMD).

Heavy rains, floods and landslides was the most recurring extreme weather event type (reported on 214 days in the year), followed by lightning and storms (185 days), heatwaves (66 days), cold wave / cold days (46 days), cloudbursts (11 days), snowfall (4 days) and cyclones (3 days). The analysis relies on the number of days per extreme weather event as it shows the spread of such events across the year.

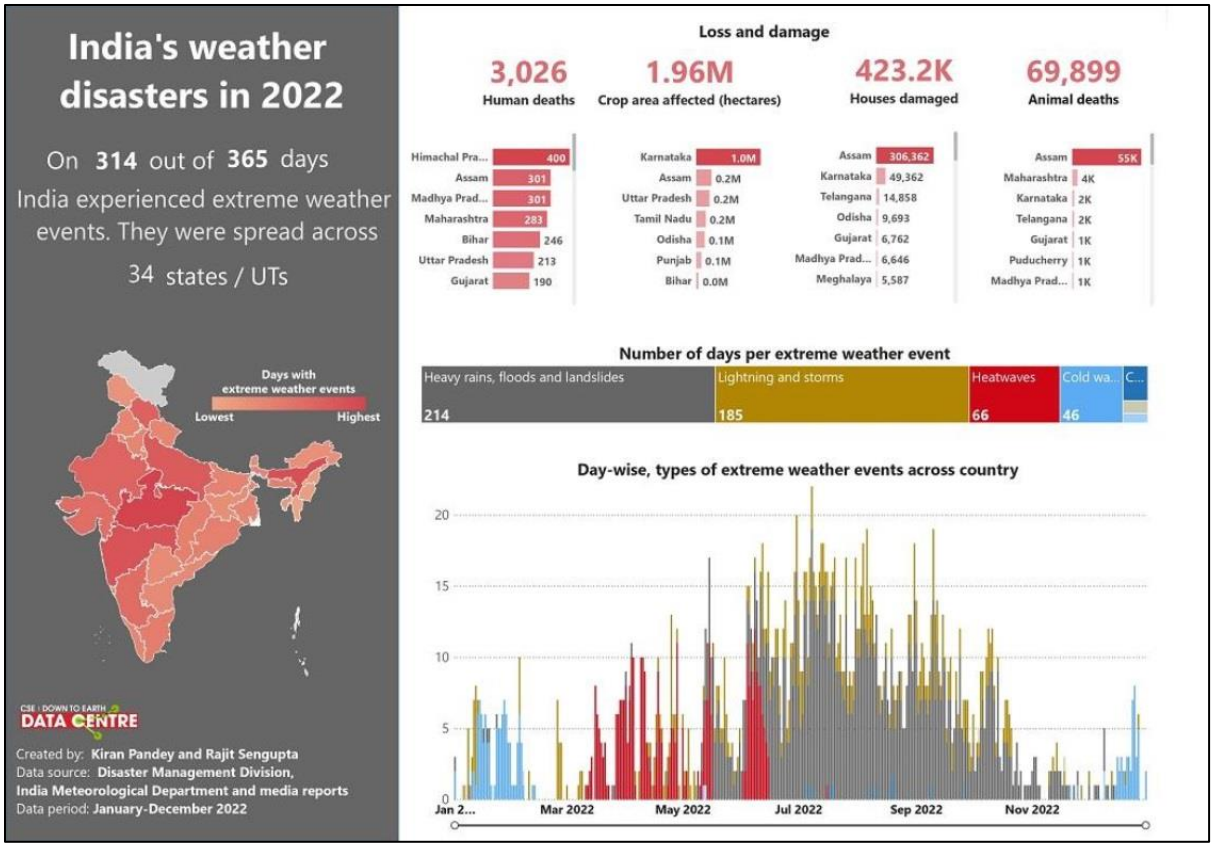

FIG 1: Quantifying the damage done by extreme weather events in 2022, by data from Centre for Science and Environment (CSE) and *Down to Earth (DTE)* Data Centre

In the above FIG 1, the following definitions were used to describe the events.

Heavy rains, floods and landslides: Heavy rainfall happens when a region receives 64.5-115.5 mm rain in 24 hours. In the case of very heavy rainfall, the threshold increases to 115.6-204.4 mm and in extremely heavy rainfall it is 204.5 mm or more. The report has considered all very heavy and extremely heavy rainfall events as well as heavy rainfall events only when they have caused damages.

Heatwave: These conditions signify a certain rise in temperature at a given place with respect to normal climatological value. The report has considered heatwaves (4.5-6.4°C departure of the maximum temperature from normal) and severe heatwaves (departure of more than 6.4°C)

Cloudburst: It occurs when there is very heavy rainfall (100 mm per hour) over a localised area. It is accompanied with strong winds and lightning.

2. Literature Review

2.1 Extreme Weather Events.

Extreme weather events refer to unusual and severe weather phenomena that deviate significantly from the norm for a particular region or a selected time period. These events can result from natural variability in the climate system, and in some cases, they may be influenced by anthropogenic activities, such as the emission of greenhouse gases that contribute to climate change. Extreme weather events can have a significant impact on communities, ecosystems, and economies, often leading to significant property damage, loss of life, and disruption of essential services.

2.1.1 Classification of Extreme Weather Events.

Examples of extreme weather events include:

1. Hurricanes and Typhoons: These are powerful tropical storms characterized by strong winds and heavy rainfall. They can cause storm surges, flooding, and extensive damage along coastlines or even urban areas if it passes over. Hurricanes are further classified into various categories based on their wind speed as follows:

Table 1: Categorization of Hurricanes based on speed. [5]

	Wind Speed
Category 1	74 – 95 mph (119 – 153 km/h)
Category 2	96 – 110 mph (154 – 177 km/h)
Category 3	111 – 129 mph (178 – 208 km/h)
Category 4	130 – 156 mph (209 – 251 km/h)
Category 5	> 157 mph (>252 km/h)

How climate change intensifies tropical storms?

1. Warming oceans – More than 90% of the excess heat from human-caused global warming over the past 50 years has been absorbed by the oceans. Since 1901, sea surface temperatures have risen an average **of 0.14 degrees Fahrenheit (0.077°C)**
2. Higher surface temperatures allow hurricanes to reach higher levels of maximum sustained wind.
3. **Rate of intensification –** Warmer oceans makes the rate of intensification more rapid.
4. **Rapid intensification** refers to an increase of at least 56 km/h, in the maximum sustained winds over a 24-hour period.
5. For example, in 2021, Hurricane Ida (landfall – Florida coastline, USA) strengthened from a Category 1 with 136 km/h winds into a near- Category 5 hurricane with excess of 250 km/h winds less than 24 hours later. This rapid intensification was later attributed to strong winds from the Atlantic Ocean.

As climate warms, the typical season for hurricanes is shifting and more months of the year are prone to storms. The Seasons for tropical storms are usually between June and November, but now they start three weeks earlier. Hurricanes are also shifting its landfall pattern farther north than in the past. Amid rising global air and ocean temperatures, there is a poleward shift in the landfall of hurricanes.

Major Hurricanes reported In India in last few decades are Bhola (1970), SCS BOB 01(1990), Odisha (1999), BOB 03 WB (2002), Pyarr (2005), Nisha (2008), Phyan (2009), Nilam (2012), Phailin (2013), Hudhud(2014), Vardah(2016), Ockhi(2017), Fani(2019), Amphan(2020), Tautake(2021), Yaas(2021). [9]

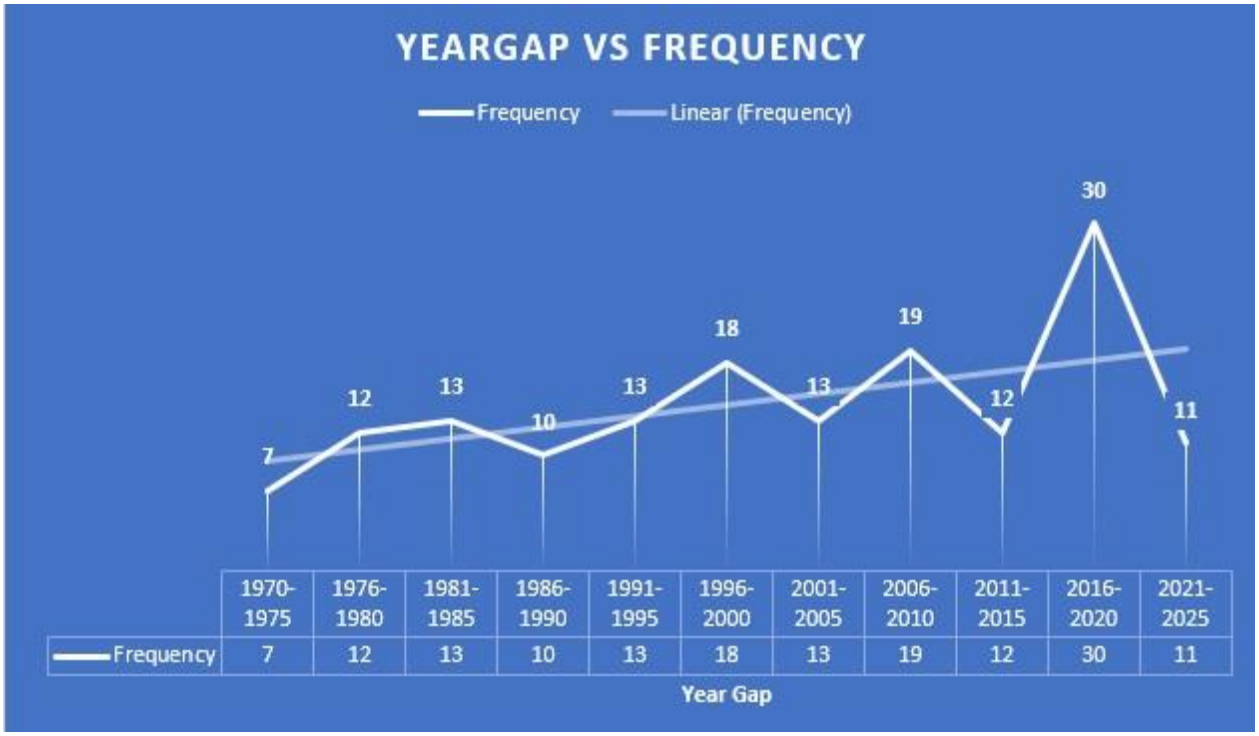

Table 2: Year gap vs frequency of tropical cyclones.

Year Gap	Frequency
1970-1975	**7**
1976-1980	**12**
1981-1985	**13**
1986-1990	**10**
1991-1995	**13**
1996-2000	**18**
2001-2005	**13**
2006-2010	**19**
2011-2015	**12**
2016-2020	**30**
2021-2025	**11***

Above Fig 2, illustrates how there is a trend of increasing frequencies of these hurricanes which make landfall with the Indian Coast

*2021-2025 data contains recorded values Upto December 2022.

2. Tornadoes: Tornadoes are rapidly rotating columns of air extending from a thunderstorm to the ground. They are known for their destructive winds and can cause extensive damage in a localized area. (Primarily occurring between summer and spring). Tornadoes come in many shapes and sizes, and they are often (but not always) visible in the form of a condensation funnel originating from the base of a cumulonimbus cloud, with a cloud of rotating debris and dust beneath it. Most tornadoes have wind speeds less than 180 kilometers per hour, are about 80 meters across, and travel several kilometers (a few miles) before dissipating. The most extreme tornadoes can attain wind speeds of more than 480 kilometers per hour, are more than 3 kilometers in diameter, and stay on the ground for more than 100 km. [7]

Meteorologists still do not know the exact mechanisms by which most tornadoes form, Research programs, including field projects such as the **VORTEX** projects (Verification of the Origins of Rotation in Tornadoes Experiment), deployment of **TOTO** (the TOtable Tornado Observatory), Doppler on Wheels **(DOW),** and dozens of other programs, hope to solve many questions that still plague meteorologists

Table 3: Classification of Tornadoes:

F0/EF0	F1/EF1	F2/EF2	F3/EF3	F4/EF4	F5/EF5
Weak		Strong		Violent	
		Significant			
			Intense		

The **Fujita scale** and the **Enhanced Fujita Scale** rate tornadoes by damage caused. The Enhanced Fujita (EF) Scale was an update to the older Fujita scale, using engineered wind estimates and better damage descriptions. The EF Scale was designed so that a tornado rated on the Fujita scale would receive the same numerical rating, and was implemented starting in the United States in 2007. An EF0 tornado will probably damage trees but not substantial structures, whereas an EF5 tornado can rip buildings off their foundations leaving them bare and even deform large skyscrapers.

3. Heatwaves: Heatwaves are prolonged periods of excessively high temperatures, often accompanied by high humidity. They can lead to health issues, such as heat-related illnesses, and strain on power systems. The **IPCC** defines heatwave as "a period of abnormally hot weather, often defined with reference to a relative temperature threshold, lasting from two days to months.

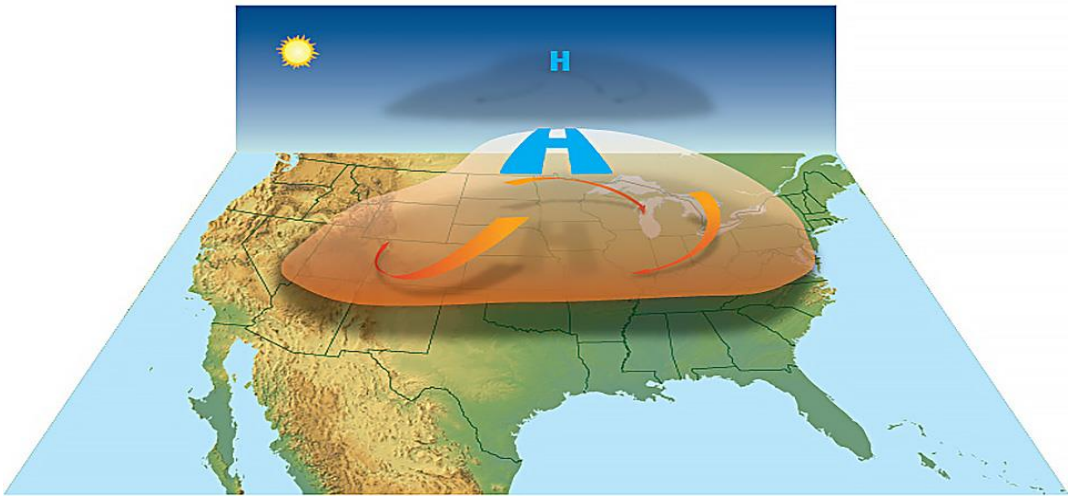

FIG 3: Visual representation of a Heatdome.

High pressure in the upper atmosphere traps heat near the ground, forming a heatwave. Mainly measured by a parameter known as **Heat Index (HI), one of the formulas for the calculation is given below [9]**

$$\mathrm{HI} = c_1 + c_2T + c_3R + c_4TR + c_5T^2 + c_6R^2 + c_7T^2R + c_8TR^2 + c_9T^2R^2$$

- HI = heat index (in degrees Celsius)
- T = ambient dry-bulb temperature (in degrees Celsius)
- R = relative humidity (percentage value between 0 and 100)

$$\begin{aligned} c_1 &= -8.784\,694\,755\,56, & c_2 &= 1.611\,394\,11, & c_3 &= 2.338\,548\,838\,89, \\ c_4 &= -0.146\,116\,05, & c_5 &= -0.012\,308\,094, & c_6 &= -0.016\,424\,827\,7778, \\ c_7 &= 2.211\,732 \times 10^{-3}, & c_8 &= 7.2546 \times 10^{-4}, & c_9 &= -3.582 \times 10^{-6}. \end{aligned}$$

For example, using this last formula, with temperature **32 °C** and relative humidity (RH) of **85%**, the Heat Index will be **46.05 °C**.

4. Cold Snaps (Cold Wave): Cold snaps involve abnormally cold temperatures over a specific area. They can result in frost, freezing conditions, and damage to crops and infrastructure. a cold wave is a rapid fall in temperature within a 24-hour period requiring substantially increased protection to agriculture, industry, commerce, and social activities. In the US, a cold spell is defined as national average high temperature falling below -7 °C, A cold wave of sufficient magnitude and duration may be classified as CAO (cold air outbreak).

5. Droughts: Droughts are extended periods of significantly reduced precipitation, leading to water shortages for agriculture, drinking water, and other essential uses. Annual dry seasons in the tropics significantly increase the chances of a drought developing and subsequent wildfires. The IPCC, NIDIS, NOAA all defines drought as "drier than normal conditions".

They are further divided into three major categories:

5.1 Meteorological drought is defined when there is a prolonged time with less than average precipitation.

5.2 Hydrological drought is brought about when the water reserves available in sources such as aquifers, lakes and other natural reservoirs **fall below a locally significant threshold**. Effect of Hydrological drought tends to show up more slowly because it involves stored water that is used but not replenished. Like an agricultural drought, this can be triggered by more than just a loss of rainfall

5.3 Agricultural or ecological droughts affect crop production or **ecosystems** in general. This condition can also arise independently from any change in precipitation levels when either increased irrigation or soil conditions and erosion triggered by poorly planned agricultural endeavors cause a shortfall in water available to the crops.

Main causes are General precipitation deficiency, Dry season, El Nino – Southern Oscillation (ENSO)

5.4 Role of Erosion and anthropogenic activities

Human activity can directly trigger exacerbating factors such as over-farming, excessive irrigation, deforestation, and erosion adversely impact the ability of the land to capture and hold water. Erosion can also be triggered by movement of strong winds.

They are severe Environmental and economic consequences if droughts are not managed properly.

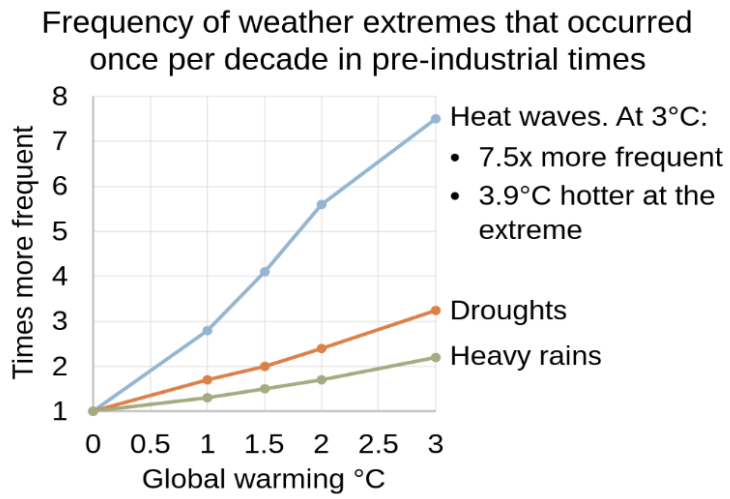

FIG 4: Multiplicative increases in the frequency of extreme weather events compared to the pre-industrial era for heat waves, droughts and heavy precipitation events, for various climate change scenarios

6. Floods: Floods occur when there is an excessive amount of water that overwhelms a region, often due to heavy rainfall, rapid snowmelt, or the failure of dams or levees. In particular climate change's increased rainfall and extreme weather events increases the severity of other causes for flooding, resulting in more intense floods and increased flood risk.

7. Blizzards: Blizzards are severe snowstorms characterized by strong winds, heavy snowfall, and reduced visibility. They can lead to transportation disruptions and power outages. A ground blizzard is a weather condition where snow is not falling but loose snow on the ground is lifted and blown by strong winds. Blizzards can have an immense size and usually stretch to hundreds or thousands of kilometers. To be classified as a blizzard, a snow storm must have sustained winds or frequent gusts that are greater than or equal to 56 km/h with blowing or drifting snow which reduces visibility to 400 m and must last for a prolonged period of time – typically three hours or more. The Australia Bureau of Meteorology describes a blizzard as, "Violent and very cold wind which is laden with snow, some part, at least, of which has been raised from snow covered ground." [14]

8. Wildfires: Wildfires are uncontrolled fires that spread rapidly through vegetation. They can be fueled by dry conditions and high winds, often causing destruction to forests and property. Wildfires are often classified by characteristics like cause of ignition, physical properties, combustible material present, and the effect of weather on the fire.. The initial ignition is mainly due to two reasons that is natural causes or due to interference from humans such as Sources arson, accidental ignition (from industrial equipment), or the uncontrolled use of fire in land-

clearing and agriculture such as the slash-and-burn farming in Southeast Asia. The type of wildfire can be classified from the flammable material present such as **Ground fires** are fed by subterranean roots, duff on the forest floor, and other buried organic matter they can burn slowly for days or even months. **Crawling or surface fires** are fueled by low-lying vegetation on the forest floor such as leaf and timber litter, debris, grass, and low-lying shrubbery. **Ladder fires** consume material between low-level vegetation and tree canopies, such as small trees, downed logs, and vines. Crown, canopy, or aerial fires burn suspended material at the canopy level, such as tall trees, vines, and mosses. The ignition of a crown fire, termed crowning, is dependent on the density of the suspended material, canopy height, canopy continuity, sufficient surface and ladder fires, vegetation moisture content, and weather conditions during the blaze. [16]

It's important to note that while individual extreme weather events can occur naturally, there is growing scientific evidence that some of these events have been **exacerbated by human-induced climate change** and majority of these climate change is being credited to **massive amounts of pollutants** that are being disposed in the atmosphere every day. Climate change can influence the frequency, intensity, and distribution of extreme weather events, making them more severe and frequent in some cases.

2.2 Role of Meteorological Parameters

2.2.1 Meteorological Parameters

Meteorological parameters are quantitative measurements used to describe various aspects of the Earth's atmosphere and weather conditions. These parameters provide valuable information about the state of the atmosphere, its behavior, and its interactions with the environment. Meteorological parameters play a crucial role in understanding weather patterns, forecasting, climate studies, and air quality assessments. Meteorological properties also change significantly with based on the Spatial scale that we are trying to study; the study of the atmosphere can be divided into distinct areas that depend on both time and spatial scales. At one extreme of this scale is climatology. In the timescales of hours to days, meteorology separates into micro-scale, meso-scale, and synoptic scale meteorology. Respectively, the geospatial size of each of these three scales relates directly with the appropriate timescale.

Table 4: Typical Scales of Atmospheric Motion Systems. [17]

Type of motion	Horizontal scale(meter)
Molecular mean free path	10^{-7}
Minute turbulent eddies	10^{-2} to 10^{-1}
Small eddies	10^{-1} to 1
Dust devils	1 to 10
Gusts	10 to 10^{2}
Tornadoes	10^{2}
Thunderclouds	10^{3}
Front, squall lines	10^{4} to 10^{5}
Hurricanes	10^{5}
Synoptic Cyclones	10^{6}
Planetary waves	10^{7}
Mean zonal winds and Atmospheric tides	10^{7}

.2.1.1 Microscale meteorology is the study of atmospheric phenomena on a scale of about 1 kilometer (0.62 mi) or less. Individual thunderstorms, clouds, and local turbulence caused by buildings and other obstacles (such as individual hills) are modeled on this scale.

2.2.1.2 Mesoscale meteorology is the study of atmospheric phenomena that has horizontal scales ranging from 1 km to 1000 km and a vertical scale that starts at the Earth's surface and includes the atmospheric boundary layer, troposphere, tropopause, and the lower section of the stratosphere. Mesoscale timescales last from less than a day to multiple weeks. The events typically of interest are thunderstorms, squall lines, fronts, precipitation bands in tropical and extratropical cyclones, and topographically generated weather systems such as mountain waves and sea and land breezes.

2.2.1.3 Synoptic scale meteorology predicts atmospheric changes at scales up to 1000 km and 10^5 seconds, in time and space. At the synoptic scale, the Coriolis acceleration acting on moving air masses (outside of the tropics) plays a dominant role in predictions. The phenomena typically described by synoptic meteorology include events such as extratropical cyclones, baroclinic troughs and ridges, frontal zones, and to some extent jet streams. All of these are typically given on weather maps for a specific time. The minimum horizontal scale of synoptic phenomena is limited to the spacing between surface observation stations.

2.2.1.4 Meteorological factors have an important effect on the amount of pollution in the atmosphere. Temperature and solar radiation affect the quantities of pollutant emitted by their influence on the amount of space heating required. Sunshine is required in a photochemical production of oxidants forming smog. The wind velocity, turbulence and stability affect the transport, dilution and dispersion of the pollutants. The rainfall has a scavenging effect in washing out ("rainout") particles in the atmosphere. Finally, the humidity is a frequent and important factor in determining the effect that concentrations of pollutants have on property, vegetation and health.

In view of these effects, meteorologists are involved in the following aspects of air pollution control:

1. Forecasting air pollution potential (Stackpole, 1967) so that the concerned air pollution control agencies may alert industry to carry out temporary abatement action.

2. Selecting sites and designing emission systems for large industrial sources.

3. Establishing air monitoring surveys.

4. Carrying out research in air pollution control methods.

2.2.1.5 Classes of sources of Pollutants are further divide into two separate groups, Low-level emitters comprising of vehicles, combustion sources for space heating houses and small commercial buildings and privately owned incinerators, whereas High-level emitters comprising of stacks serving: industrial sources, central heating systems for industrial, commercial and institutional multi-building complexes, municipal incinerators. These emitters are stacks at least 50 meters high.

Meteorological parameters affect differently the ground or "living" level concentrations of pollutants which are produced by these two classes of emitters. A knowledge of the micrometeorology and topography of the area, as well as the characteristics of the principal sources of emissions of pollutants and their locations in the area, must be known in order to provide satisfactory forecasts of air pollution potential.

Meteorological parameters play a significant role in influencing the concentration, dispersion, and transport of different air pollutants in the atmosphere. These parameters can affect how pollutants are emitted, dispersed, and eventually removed from the air. Here are some examples of how various meteorological parameters can impact different air pollutants:

2.2.2 Impact of Meteorological Parameters on Air Pollutants Dispersion

2.2.2.1. Wind Speed and Direction: Wind speed and direction determine how pollutants disperse in the atmosphere. Higher wind speeds can help disperse pollutants more effectively, reducing their local concentrations. **Wind direction** is crucial in understanding the potential impact of pollution on specific areas, especially downwind of pollution sources. Since the **wind directs** the travel of the pollutants, the expected persistence of the wind direction, as related to the topographic features and the locations of the receptors, must be considered both in forecasting the air pollution potential as well as in selecting sites for plants. The effect of an increase in **wind speed** on the concentrations resulting from low-level sources of emissions is to dilute the pollutants - the concentration of pollutants in a downwind location from a ground-level source is inversely proportional to the wind speed. High air pollution potential forecasts for most large urban areas where low-level emissions are the principal sources of pollution include light wind speed as one of the criteria. In contrast, with high-stack sources of hot emissions, an increase in the wind speed will lower the plume rise, and tend to increase ground level concentrations. There is a critical wind speed for each stack design at which concentrations downstream reach a maximum. These values can be calculated via different empirical formulae Such as by Holland (1953) Plume Rise equation, and by the Pasquill (1962) – Gifford (1961) Dispersion formula. Although it might be noted that various **Atmosphere Stability Class** affect the Plume behavior greatly which can be seen in the FIG 5 below:

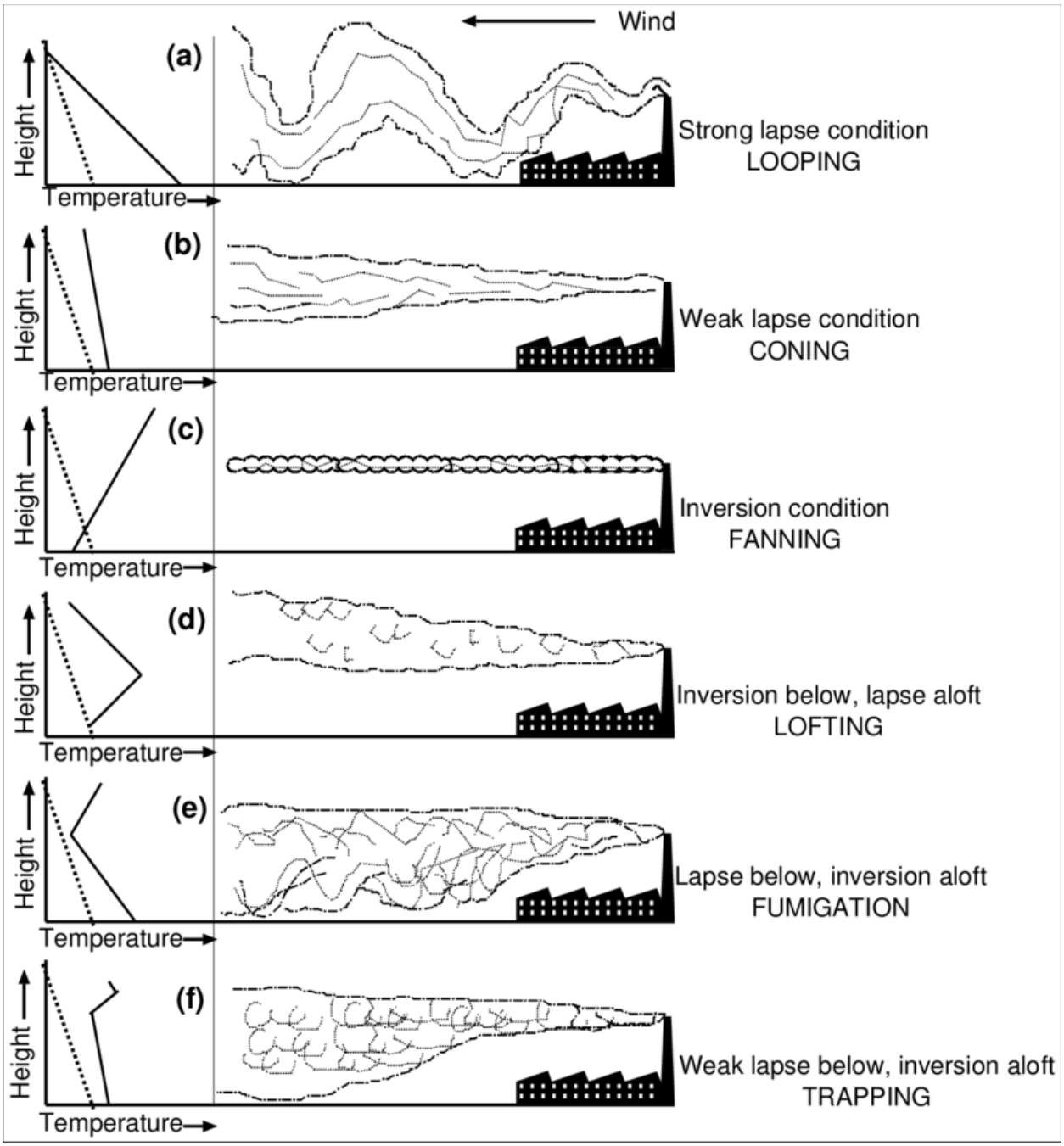

FIG 5: Plume behavior for various Atmosphere Stability Class.

2.2.2.2 Temperature and Inversions: Temperature influences the vertical mixing of air [4]. Inversions, where a layer of warmer air traps cooler air beneath it, can lead to the accumulation of pollutants near the surface. Cold temperatures can also enhance the formation of ground-level ozone in certain conditions.

2.2.2.3. Atmospheric Stability: Atmospheric stability refers to the resistance of air to vertical mixing. Stable conditions (when warm air overlies cooler air) can lead to poor dispersion and the accumulation of pollutants near the ground, while unstable conditions enhance vertical mixing and pollutant dispersion. Detailed views of how different Atmospheric Stability class affect the plume rise or movement of pollutants from a high-rise emission source is given in the FIG 5.

2.2.2.4. Relative Humidity: Relative humidity affects the formation of secondary pollutants such as particulate matter ($PM_{2.5}$) and ground-level ozone. Higher humidity can lead to the condensation of water vapor around particulate matter, increasing its size and mass, which affects its behavior in the atmosphere. Humidity can affect air pollution in several ways, including the dispersion of pollutants, reactions between chemicals, movement of pollutants, impacting visibility, precipitation, etc. Humidity can affect pollution dispersion. If humidity is high, pollutants can stick to water droplets and other particles in the air, causing them to be removed from the atmosphere. In turn, this reduces pollutant concentrations and improves air quality. But it can also cause pollution to accumulate on surfaces, which can harm the environment.

Humidity can speed up the chemical reactions that produce air pollutants, like ozone and particulate matter. Basically, water molecules can react with pollutants and other chemicals in the air to create new compounds. In the presence of sunlight, nitrogen oxides and volatile organic compounds may react to form ground-level ozone, which is harmful to the environment.

2.2.2.5. Precipitation: Rain can effectively "wash out" pollutants from the atmosphere by carrying them to the ground. It can help remove particulate matter and some gaseous pollutants, contributing to improved air quality. Rain eases this problem by forcing down the most common air pollutants, like particulate matter and pollen down. Thereby, the quality of air becomes drastically better. This phenomenon is called **wet deposition**. It is the primary natural process that eliminates the air pollutants through atmospheric hydrometeors, like rain, hail, and snow. It delivers and deposits the contaminants to the ground. The process is also known as precipitation *scavenging, rainout, wet removal*, or *simply washout*.

2.2.2.6. Solar Radiation: Solar radiation, specifically ultraviolet (UV) radiation, can drive photochemical reactions in the atmosphere, leading to the formation of ground-level ozone and other secondary pollutants. UV radiation can also influence the degradation of pollutants. Particulate matter can reduce the amount of solar radiation that reaches the earth's surface, affecting the rate at which water evaporates and moves into the atmosphere. They also affect clouds' formation and water-carrying capacity. Although Solar Radiation directly doesn't affect the air pollutants but some pollutants may undergo chemical reaction to be toxic substances under UV radiation. After the pollutants in the atmosphere absorb the energy of solar radiation, photochemical reactions may occur to produce toxic substances. Most previous studies analyzed the influence mechanism of AQI on solar radiation. However, this cannot completely reveal the

influence mechanism of air pollutants on solar radiation. Therefore, in this study. AQI and six pollutants (**$PM_{2.5}$, PM_{10}, SO_2, NO_2, CO, and O_3**) were considered for mechanism and prediction analyses; subsequently, the mechanism analysis based on pollutants was verified. The comprehensive evaluation index AQI was negatively correlated with solar radiation, while some pollution components (such as O_3) were positively correlated with the daily total solar radiation.

2.2.2.7. Topography: The local terrain can influence how pollutants disperse. Valleys and urban canyons can trap pollutants and create stagnant conditions, leading to higher concentrations in these areas. Pollution levels can be greater in valleys than for areas of higher ground due to the interaction between air flow (winds) and the Earth's surface. On hill tops and exposed areas, moderate wind will typically cause the pollutant to be dispersed (blown and spread out) but in low-lying areas like valleys, it is harder for the wind to penetrate, causing air pollutants to become trapped and levels of air pollution to rise.

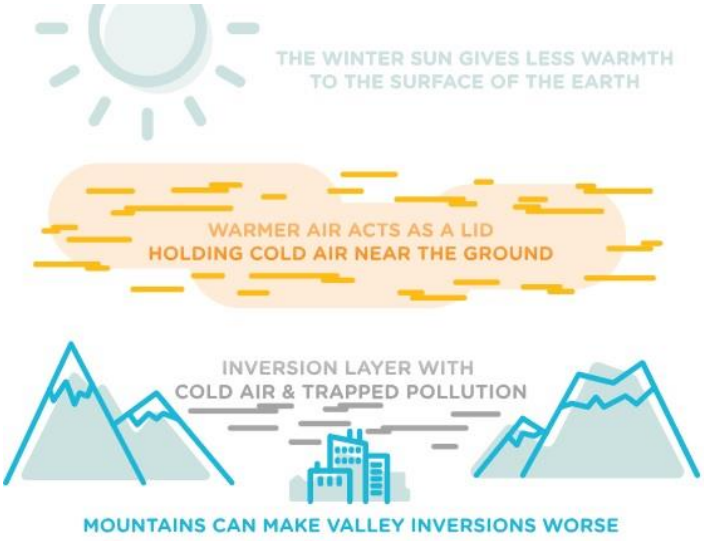

FIG 6: Inversion in mountainous region during colder climate.

2.2.2.8. Mixing Height: The mixing height is the vertical height to which pollutants can be dispersed in the atmosphere. A higher mixing height allows for greater dispersion and dilution of pollutants. "Mixing Height" or "Mixing Depth" (ft or m) signifies the height above the surface throughout which a pollutant such as smoke can be dispersed. During times of surface temperature inversions (typically nighttime with clear skies), the mixing height goes to zero and smoke dispersion is minimal.

"Ventilation Rate" (VR) equals the product of the two (m*m/s) and represents the ability of the boundary layer to get rid of the smoke. When VR values are low, there is not much mixing potential and surface air quality suffers. When VR values are consistently low (day and night), it is possible to "smoke in" large areas for several days.

Ventilation Rate (m*m /s) = Mixing Height (m) x Transport Wind (m/s). [20]

2.2.2.9. Air Pressure: Changes in atmospheric pressure can influence wind patterns and affect the movement of air masses, which in turn can impact the transport of pollutants over larger distances. In a high-pressure system, air tends to be more still, allowing greater concentrations of air pollutants to build up. In low-pressure systems, wet and windy conditions cause air pollutants to be dispersed or washed out of the atmosphere by rain. In low-pressure systems Wind disperses the air pollution formed from both natural and anthropogenic activities. Air pollutants that travel higher up into the air can also react to form other types of pollutants. For example, sulfur dioxide and nitrous oxides emitted from upwind sources can undergo chemical reactions in the atmosphere to form particulate matter, and nitrous oxides may also react to form ground-level ozone, or smog. Even though wind may move air pollutants to another geographic location, these pollutants still threaten human and environmental health wherever they settle.

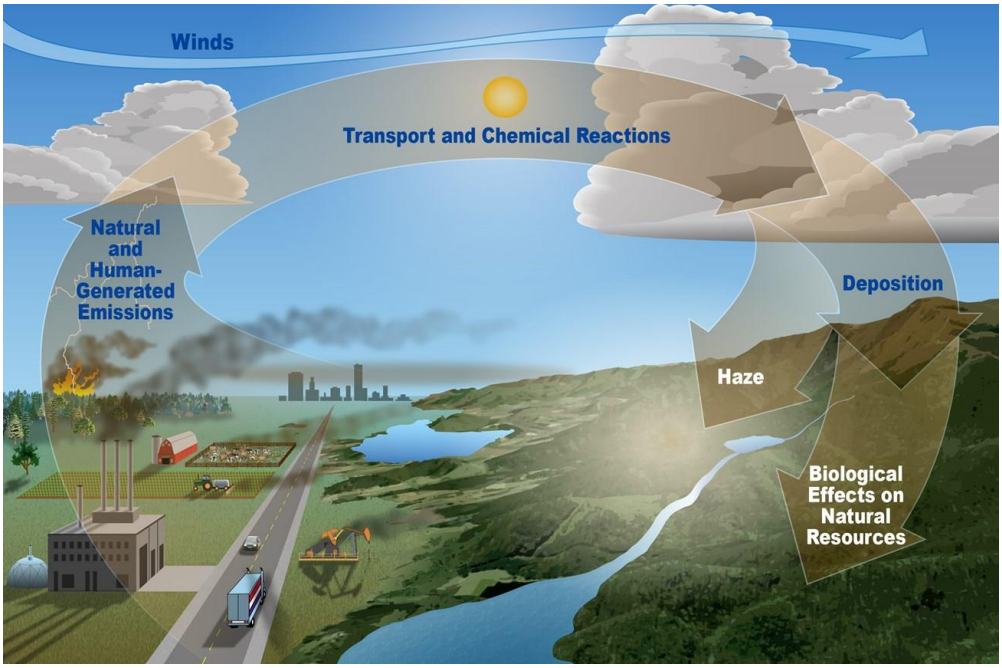

FIG 7: Wind can move air pollutants short or very long distances before they cause harmful impacts.

10. Seasonal Variations: Seasonal changes in meteorological conditions, such as temperature inversions in winter, can lead to variations in pollutant concentrations. For instance, winter months might see higher levels of pollutants due to poor dispersion.

It's important to note that the interactions between meteorological parameters and pollutants are complex and can vary depending on the specific pollutants involved and the local atmospheric conditions. Understanding these interactions is crucial for predicting and managing air quality and pollution-related environmental impacts.

2.3 Major Air Pollutants

The terms **"Air pollutants"** and **"Major Air Pollutants"** are closely related but have distinct meanings when discussing environmental and atmospheric issues. "Air pollutants" is a general term that refers to substances released into the atmosphere that can have harmful effects on human health, the environment, and ecosystems. Air pollutants can include a wide range of gases, particles, and volatile organic compounds (VOCs) that are emitted from various sources, both natural and human-made. These pollutants can originate from sources such as vehicles, industrial processes, power plants, construction activities, agricultural operations, and natural events like wildfires and volcanic eruptions. Air pollutants can have short-term and long-term impacts, causing respiratory diseases, cardiovascular problems, damage to vegetation, acid rain, smog formation, and other adverse effects.

"Major air pollutants," also known as **"criteria pollutants**," refer to a specific set of common and widespread pollutants that are regulated by environmental agencies due to their significant impact on human health and the environment. The term "criteria pollutants" was coined by the United States Environmental Protection Agency **(USEPA)** to refer to pollutants for which National Ambient Air Quality Standards **(NAAQS)** have been established to protect public health and welfare.

In summary, "air pollutants" is a broad term encompassing a wide range of substances released into the atmosphere, while "major air pollutants" or "criteria pollutants" refer to a specific subset of these pollutants that have significant health and environmental impacts and are subject to regulatory controls to maintain air quality standards.

Air pollutants are substances that are released into the atmosphere and have the potential to degrade air quality, harm human health, damage ecosystems, and contribute to various environmental problems. These pollutants can come from natural sources, such as volcanic eruptions and wildfires, but a significant portion of air pollution is generated by human activities, including industrial processes, transportation, and energy production. Some major types of air pollutants include:

2.3.1. Particulate Matter (PM): Particulate matter consists of tiny solid particles and liquid droplets suspended in the air. They vary in size and can be categorized as PM_{10} (particles with a diameter of 10 micrometers or smaller) and $PM_{2.5}$ (particles with a diameter of 2.5 micrometers or smaller). PM can originate from combustion processes (such as vehicle emissions and industrial activities), construction activities, and natural sources like dust and pollen. The IARC and WHO designate airborne particulates as a Group 1 carcinogen.Particulates are the most harmful form (other than ultra-fines) of air pollution due to their ability to penetrate deep into the lungs

and brain from blood streams, causing health problems such as heart disease, lung disease, and premature death.

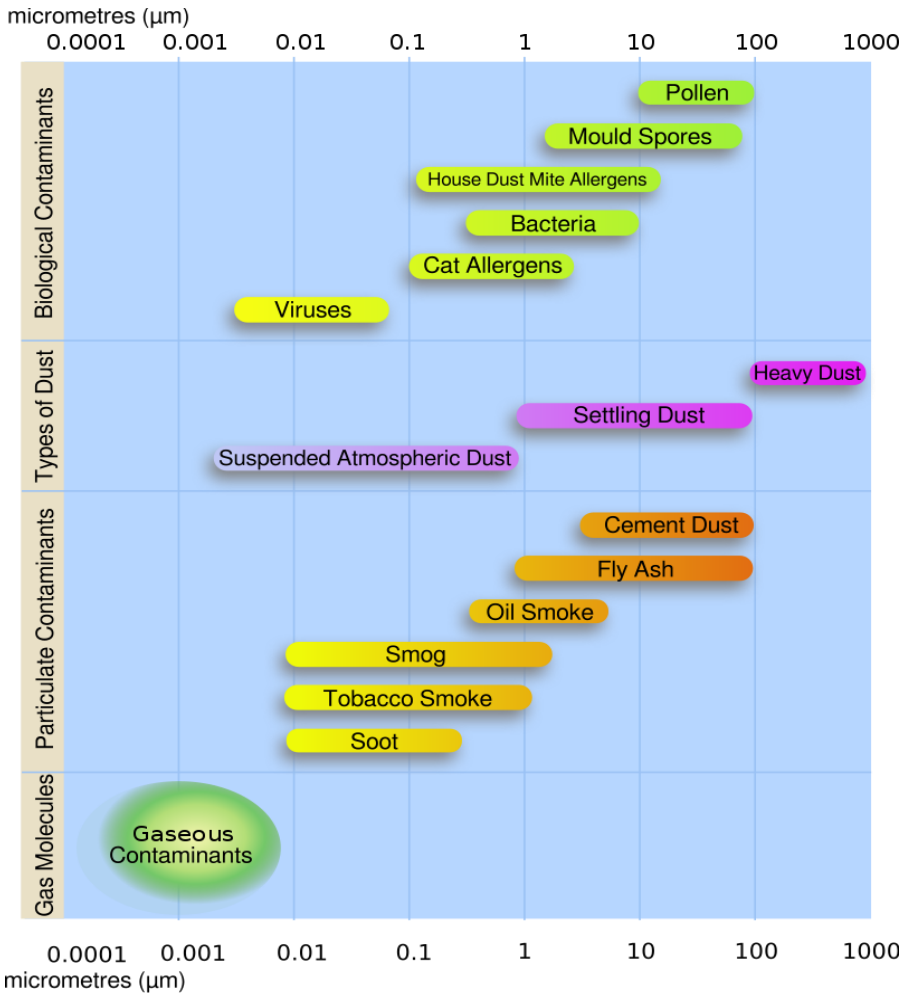

FIG 8: This diagram shows types, and size distribution in micrometers (µm), of atmospheric particulate matter.

2.3.2. Ground Level Ozone (O_3): Ground-level ozone is not emitted directly into the air but forms through complex chemical reactions involving precursor pollutants, such as nitrogen oxides (NOx) and volatile organic compounds (VOCs). Ozone is a major component of smog and can cause respiratory problems in humans and damage crops and ecosystems. Ground-level ozone (O_3), also known as surface-level ozone and tropospheric ozone, is a trace gas in the troposphere (the lowest level of the Earth's atmosphere), with an average concentration of 20–30 parts per billion by volume (ppbv), with close to 100 ppbv in polluted areas.[21]

Photolysis of ozone occurs at wavelengths below approximately 310–320 nanometers.This reaction initiates a chain of chemical reactions that remove carbon monoxide, methane, and

other hydrocarbons from the atmosphere via oxidation. Therefore, the concentration of tropospheric ozone affects how long these compounds remain in the air. If the oxidation of carbon monoxide or methane occur in the presence of nitrogen monoxide (NO), this chain of reactions has a net product of ozone added to the system. Ozone in atmosphere can be measured by remote sensing technology, or by in-situ monitoring technology. One of the latest ozone measuring device by remote sensing is **Total ozone mapping spectrometer-earth probe (TOMS-EP)** aboard a satellite from NASA is an example of an ozone layer measuring satellite.

2.3.3. Nitrogen Oxides (NOx): NOx includes nitrogen dioxide (NO_2) and nitrogen monoxide (NO). They are primarily emitted from combustion processes, such as those in vehicles and power plants. In areas of high motor vehicle traffic, such as in large cities, the nitrogen oxides emitted can be a significant source of air pollution. NO_x gases are also produced naturally by lightning. NOx can contribute to the formation of smog, acid rain, and ground-level ozone, and can also have negative health impacts.

NO_y is defined as the sum of **NO_x** plus the **NO_z** compounds produced from the oxidation of **NO_x** which include nitric acid **(HONO),** dinitrogen pentoxide (**N_2O_5**), peroxyacetyl nitrate **(PAN**), alkyl nitrates **($RONO_2$)**, peroxyalkyl nitrates **($ROONO_2$),** the nitrate radical **(NO_3),** and peroxynitric acid **(HNO_4).**

2.3.4. Sulfur Dioxide (SO_2): Sulfur dioxide is produced mainly by burning fossil fuels containing sulfur, such as coal and oil. It can lead to the formation of acid rain, which can harm aquatic ecosystems, forests, and buildings. SO_2 can also irritate the respiratory system in humans. Emissions that lead to high concentrations of SO_2 generally also lead to the formation of other SO_x. The largest sources of SO_2 emissions are from fossil fuel combustion at power plants and other industrial facilities. SO_2 and other sulfur oxides can react with other compounds in the atmosphere to form fine particles that reduce visibility (haze). At high concentrations, gaseous SO_x can harm trees and plants by damaging foliage and decreasing growth.

2.3.5. Volatile Organic Compounds (VOCs): VOCs are a group of organic chemicals that can easily evaporate into the air. They are emitted from a variety of sources, including vehicle exhaust, industrial processes, and the use of solvents in products like paints and cleaners. VOCs can contribute to the formation of ground-level ozone and smog and have health and environmental impacts.

2.3.6. Carbon Monoxide (CO): Carbon monoxide is a colorless, odorless gas produced by incomplete combustion of carbon-containing fuels. It's primarily emitted from vehicle exhaust and can interfere with the body's ability to transport oxygen, leading to health problems.

2.3.7. Lead (Pb): While lead emissions have significantly decreased due to regulations, lead can still be present in the air, particularly in areas near certain industrial activities or from the use of leaded gasoline. Lead exposure can have serious neurological and developmental effects, especially in children.

2.3.8. Mercury (Hg): Mercury is a toxic heavy metal released into the air from natural sources and human activities such as coal combustion. It can accumulate in the food chain, posing health risks to humans, particularly through consumption of contaminated fish.

2.3.9. Hazardous Air Pollutants (HAPs): These are a group of pollutants that pose significant health risks due to their toxicity and potential for causing cancer, reproductive issues, and other serious health problems. Examples include benzene, formaldehyde, and certain heavy metals.

Efforts to reduce air pollution involve regulations, technological advancements, and shifts toward cleaner energy sources and transportation systems. Managing and controlling air pollutants is essential for safeguarding public health and protecting the environment

2.4 Noteworthy Works done in this Field

2.4.1 The Paper titled **Quantifying the relationship between extreme air pollution events and extreme weather events** authored **by Henian Zhang, Yuhang Wang, Tae-Won Park and Yi Deng** did a quantitative study to establish a correlation between the air pollutants ($PM_{2.5}$ and Ozone). and with extreme weather events, the location-specific 95th or 5th percentile threshold derived from historical reanalysis data (30 years for ozone and 10 years for PM2.5) and the relationship between extreme ozone and PM2.5 (particular matter with an aerodynamic diameter less than 2.5 μm) events and the representative meteorological parameters such as daily maximum temperature (Tmax), minimum relative humidity (RHmin), and minimum wind speed (Vmin).They observed that the ozone and PM2.5 datapoint extremes were getting smaller over time, that was indicative of the EPA's more stringent rules and efforts to lower the emissions of the related precursor. Particularly in the eastern United States, annual ozone and PM2.5 severe days showed a strong correlation with Tmax and RHmin. They were positively (negatively) correlated with Vmin in urban (rural and suburban) stations. The overlapping ratios of ozone extreme days with Tmax were fairly constant, about 32%, and tended to be high in fall and low in winter. Ozone extreme days were most sensitive to Tmax, then RHmin, and least sensitive to Vmin. The majority of ozone extremes occurred when Tmax was between 300 K and 320 K, RHmin was less than 40%, and Vmin was less than 3 m/s. The number of annual extreme PM2.5 days was highly positively correlated with the extreme RHmin/Tmax days, with correlation coefficient between PM2.5/RHmin highest in urban and suburban regions and the correlation coefficient between PM2.5/Tmax highest in rural area. Tmax has more impact on PM2.5 extreme over the eastern U.S. Extreme PM2.5 days were more likely to occur at low RH conditions in the central and southeastern U.S., especially during spring time, and at high RH conditions in the northern U.S. and the Great Plains. Most extreme PM2.5 events occurred when Tmax was between 300 K and 320 K and RHmin was between 10% and 50%. Extreme PM2.5 days usually occurred when Vmin was under 2 m/s. *Although multiple readings and a data collection for a longer period would have given a more satisfactory correlation.*

2.4.2 The paper titled **Intercomparison of MODIS, MISR, OMI, and CALIPSO aerosol optical depth retrievals for four locations on the Indo-Gangetic plains and validation against AERONET data** authored by **Humera Bibi and others (2015)** computed figures for root mean square error (RMSE), mean absolute error (MAE) and root mean bias (RMB). Using AERONET data to validate $MODIS_{STD}$, $MODIS_{DB}$, MISR, OMI, and CALIPSO data revealed that $MODIS_{STD}$ While MISR data was more accurate over places near the water bodies than over other areas, it was more accurate over vegetated locations than over unvegetated locations. Compared to the other instruments, the MISR instrument outperformed them over Karachi and Kanpur. while the $MODIS_{STD}$ AOD retrievals were better than those from the other instruments over Lahore and Jaipur. They also computed the expected error bounds (EEBs) for both MODIS retrievals and found that MODISSTD consistently outperformed MODISDB in all of the investigated areas. High AOD values were

observed by the $MODIS_{STD}$, $MODIS_{DB}$, MISR, and OMI instruments during the summer months (April to August); these ranged from 0.32 to 0.78, possibly due to human activity and biomass burning. In contrast, high AOD values were observed by the CALIPSO instrument between September and December, due to high concentrations of smoke and soot aerosols.

2.4.3 The paper titled **Correlation between air pollution and weather data in urban areas: Assessment of the city of Rome (Italy) as spatially and temporally independent regarding pollutants** authored by **Gabriele Battista and others (2017**) examined and analyzed many types of pollutants in Rome between 2006 and 2015, using various post-elaboration approaches. Techniques related to statistics and cross-statistics in space and time received special attention. Rome was described as being independent of pollutants both temporally and spatially based on the findings. Pollution and even variations in the weather were researched together. With the exception of one specific matter, cross-correlation analyses focusing on air temperature, solar radiation, wind direction, and velocity revealed a strong coupling in the majority of cases. The pollutants that were taken into were NO, NO_2, C_6H_6, PM_{10}, $PM_{2.5}$ and O_3 were taken into account.

2.4.4 The paper titled **Spatiotemporal variability of the PM2.5 distribution and weather anomalies during severe pollution events: Observations from 462 air quality monitoring stations across South Korea** authored by **Subin Han and others (2023)** investigated the nationwide spatiotemporal variability of PM2.5 during 49 severe PM2.5 pollution events based on observations from 462 air quality monitoring stations (AQMSs) across South Korea during 2015–2020. Regarding the time series of average PM2.5 in the Seoul area, the coefficient of divergence (COD) and Pearson correlation coefficient (R) were computed for the complete countrywide AQMS network. Out of 49 pollution occurrences, three unique spatial COD and R distribution patterns (Cases I–III) were chosen that can be used to pinpoint the locations of further AQMSs. The inter-district movement of PM2.5 is made clear by the spatial distributions of time lags associated with PM2.5 pollution incidents at each monitoring station in relation to the Seoul region. When the time lag was adjusted, the average R values at all AQMSs were greater than 0.74 for all cases (compared to 0.52–0.57 before adjustment), suggesting that characteristic weather patterns over East Asia drive nationwide severe PM2.5 pollution. Analyses of composite anomalies of meteorological variables (compared to climatology for 1991–2020) suggest that weakened surface winds accompanied by strong positive temperature anomalies in East Asia play an important role in the onset of severe PM2.5 pollution in Korea (for all classified cases). The findings have elucidated the weather patterns that lead to severe PM2.5 pollution, variations of spatiotemporal PM2.5 pollution patterns over Korea on the regional scale with weather patterns, and pollution transport across air quality districts (inter-air-quality-district transport patterns).

2.4.5 The paper titled **Distinct responses of PM2.5 and O3 extremes to persistence of weather conditions in eastern China** authored by **Shanshan Liu and others (2023)** explored that the meteorological reanalysis dataset and ground-level air pollution datasets to investigate the impact of weather persistence on China's summers O_3 and winters $PM_{2.5}$ extremes. Alongside differing weather circumstances, related variations in the distributions' morphologies were also explored. With 0.07, 0.12, and 0.19 standard deviation per day (or roughly 1.97, 3.12, and 4.63 ppb per day) for the Beijing-Tianjin-Hebei (BTH), Yangtze River Delta (YRD), and Pearl River Delta (PRD) regions, respectively, the median summertime O_3 increases significantly as air stagnation days continue. Only the YRD region experiences significant increases in the median (about 0.31 ppb per day) and 90th percentile (about 0.78 ppb per day) of summertime O_3, as high temperature days persist. However, the final day of four-day high temperature events for both the BTH and YRD regions shows the highest probability of O_3 extreme (90th percentile). On the other hand, rather than increasing the median PM2.5 concentration, prolonged stagnation results in a notable rise in the 90th percentile, which is approximately 17.87 and 10.88 $\mu g/m^3$ daily for the BTH and YRD regions. The best markers for PM2.5 extreme (90th percentile) in the BTH, YRD, and PRD regions, respectively, are stagnation occurrences that persist for five, four, and five days.

Analysis of opposing monthly weather conditions indicates that the wintertime $PM_{2.5}$ extreme is significantly amplified by stronger stagnation, whereas the summertime O_3 extreme is amplified by higher mean daily maximum air temperature (T) in the BTH region and co-occurrences of high T and stagnation in the YRD region. These findings imply that megacities are more susceptible to future heat waves and instability if they have relatively high emissions.

2.5. Research Objective and Scope of Work

As we all know that air pollution is expected to rise in upcoming years from various sectors such as the power generation, transportation, natural calamities etc. although alternative technologies are being explored it will not replace the fossil fuels completely as countries are planning to go net zero by 2035 (for most European countries) and 2070 (for India), it is evident that air pollutants will be released in the atmosphere for a long period to come. So, it will further aggravate the problem of Climate change and lead to extreme weather events which will directly or indirectly affect all of us. So, a correlation between the Extreme Weather events and air pollution concentration will become an important tool to predict the upcoming weather events in advance if we know the background air pollution concentration and prediction-based modelling for future emission of a particular area of interest.

2.5.1 Objective of the Work

The main objective of this work is to establish a correlation between *Extreme weather events and air pollution concentration*.

2.5.2 Scope of the work

2.5.2.1 Data collection in the area of interest of different kind of air pollutants via the Copernicus Atmosphere Monitoring Service (CAMS) satellite and other satellites as required during the scope of the work.

2.5.2.2 Data collection of various Meteorological parameters via the NASA / POWER CERES / MERRA2 SHELL (The Modern-Era Retrospective analysis for Research and Applications, version 2)

2.5.2.3 Analysis of the data via statistical model, **Pearson Correlation Coefficient** The coefficient is a number between -1 and 1 and determines the strength and direction of the relationship between two variables.

2.5.2.4 Regression analysis of probable correlation from PCC into Excel for *linear and polynomial of higher degrees* for satisfactory value of R^2

2.5.2.5 Modelling for Prediction values via *Random Forest Regression* for least mean squared error and least mean absolute error

3. Overview of the Study area

A total of 9 (nine) locations were chosen as the study area, the reason being weather anomalies being reported specially in these regions, unpredictable heatwaves in the east to sudden cloudburst and heavy rainfall in the northern regions of India has been reported in last few years also the northern regions chosen are prone to stubble burning and eastern part has relatively higher pollutant concentration due to wind pattern.

The 9 locations are as follows:

1. Manali 32.2396,77.1887
2. Shimla 31.0886,77.1797
3. Dehradun 30.3164,78.0321
4. Haridwar 29.9456,78.1642
5. Durgapur 23.5334,87.3219
6. Burdwan 23.2325,87.8634
7. Kolkata 22.5784,88.3645
8. Delhi 28.6448,77.2167
9. Mohali 30.7001,76.6990

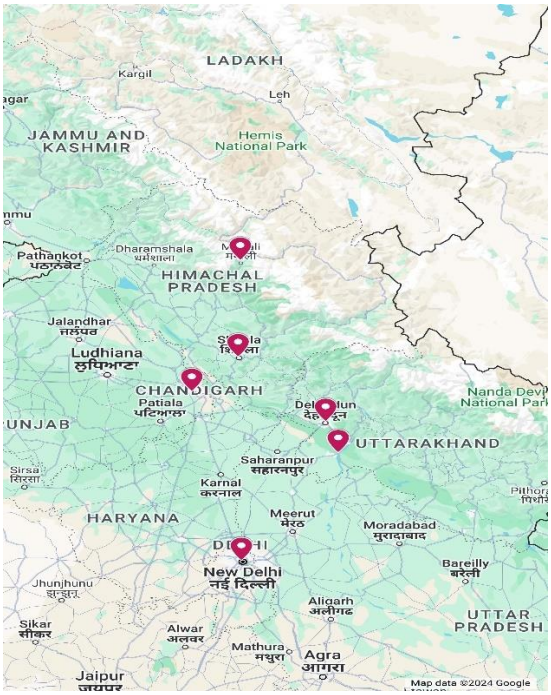

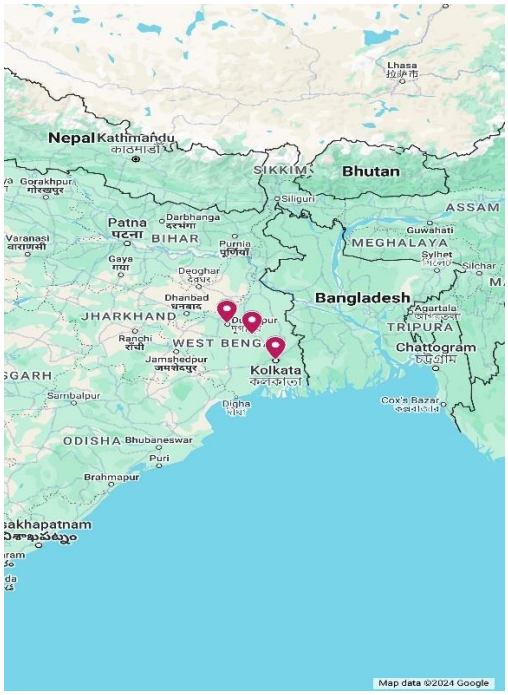

FIG 9 and FIG 10 shows the area of study marked in the northern and eastern sector of the Indian map.

4. Data Collection and Methodology

4.1 Satellites

Satellites over the last few decades has heavily influenced the way we gather data regarding our environment, the trend and future works in this field is heavily influenced by Remote Sensing where a particular satellite revolves around a fixed orbit around the Earth, collecting various input data by the various instruments equipped onboard and relaying that information back to earth for further analysis.

Remote sensing means observing something from a large distance. Satellites in space observe the Earth from a large distance and help scientists study large tracts of land and how that land changes over time. Optical remote sensing satellites use reflected light to detect electromagnetic energy on the Earth's surface. The level of energy is represented by the electromagnetic spectrum, which is the range of energy that comes from the Sun. The light from the Sun that we can see is only a small part of the electromagnetic spectrum and includes the colors of the rainbow. Satellite sensors can detect light that we can't see. The electromagnetic energy reflects off the Earth's surface and up to the satellite sensor, which collects and records information about that energy. That information is transmitted to a receiving station in the form of data that are processed into an image with different colour gradient for ease in identification of a particular parameter.

The data that is mainly received as electromagnetic energy is then captured by the receiver onboard the satellite and useful data is taken out of the raw data via various calibration instruments.

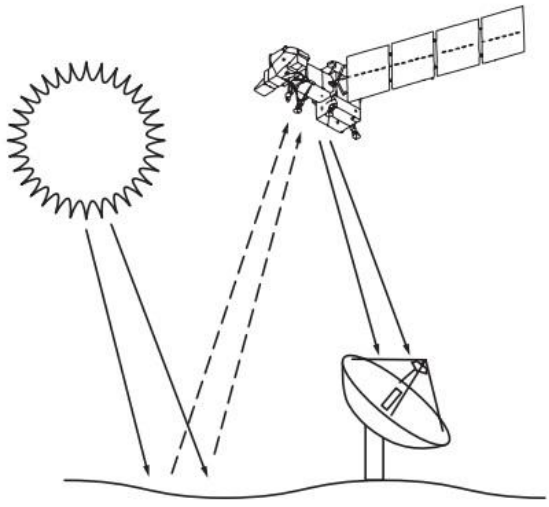

FIG 11: Basic sequence of satellite data collection.

In the scope of data collection of this thesis, data was mainly collected via two satellites namely **Sentinel-5P** and **NASA MERRA-2**.

4.1.1 Sentinel-5P

The Sentinel-5P (P for precursor) mission aims at providing information and services on air quality and climate between 2017 and at least 2023. With the TROPOMI sensor installed on board it takes daily global observations of key atmospheric constituents, including ozone, nitrogen dioxide, sulfur dioxide, carbon monoxide, methane, formaldehyde as well as cloud and aerosol properties.

Properties:

Table 5: Properties of the Sentinel-5P satellite

Property	**Info**
Spatial resolution	Up to 5.5* km x 3.5 km.
Sensor	Tropospheric Monitoring Instrument (TROPOMI), a spectrometer measuring ultraviolet and visible (270–495 nm), near infrared (675–775 nm) and shortwave infrared (2305–2385 nm) light.
Revisit time	Less than one day.
Spatial coverage	Global coverage.
Data availability	Since April 2018.
Common usage/purpose	To provide global information on a multitude of atmospheric trace gases, aerosols and cloud distributions affecting air quality and climate.

The Data availability can also be forced into three different modes namely NRTI (for near Realtime), OFFL (for offline) and RPRO (for reprocessing).

The Units that most of the Pollutant concentration is calculated is by default set to kg/m^3, we have to convert it into the microgram unit as per our needs.

The main Sentinel-5P products relevant for Ozone monitoring are the O3 family (O3, O3_TCL and O3_PR),

4.1.2 MERRA-2

The Modern-Era Retrospective analysis for Research and Applications, Version 2 (MERRA-2) provides data collection, beginning in 1980 with a few major parameters and gradually to all present constituents. It was introduced to replace the original MERRA dataset because of the advances made in the assimilation system that enable assimilation of modern hyperspectral radiance and microwave observations, along with GPS-Radio Occultation datasets. It also uses NASA's ozone profile observations that began in late 2004. Additional advances in both the GEOS model and the GSI assimilation data systema that are included in MERRA-2. Spatial resolution remains about the same (about 50 km in the latitudinal direction) as in MERRA.

MERRA-2 (Gelaro et al. 2017) is composed calibrated with the Goddard Earth Observing System Atmospheric Data Assimilation System (GEOS ADAS), which incorporates another reanalysis parameter known as Global Statistical Interpolation (GSI) analysis scheme of Wu et al. (2002). The system utilizes a revised version of the GEOS global atmospheric model (Molod et al., 2014). A fundamental motive for replacing MERRA with MERRA-2 is that MERRA (decommissioned 2008) is not capable of including important new data types which maybe in need in the future, and the aging and failure of older satellite instruments greatly reduced the data set available for combination and merging for the earlier reanalysis. MERRA-2's GEOS system (version 5.12.4) is able to assimilate data from the newer microwave instruments and from hyperspectral infrared radiance instruments.

Highlights of the new MERRA-2 combined with GEOS ADAS

1. Hourly data recordings doubling from previous iterations.
2. More consistent time series.
3. Inclusion of stratospheric ozone products
4. Use of daily sea ice monitoring and SST fields (rather than weekly in the original MERRA)
5. High spatial resolution of ½ degree latitude by 5/8-degree longitude by 72 modal levels and temporal hourly resolution
6. Improved observations and data gathering as a result of more advanced instruments and optimization in calibration software.

4.2 DATA ANALYSIS

For the data analysis part I have used Microsoft excel 2019, for checking the trend line in normal as well as in Polynomial trendline of higher degree for higher R^2 values. The average trendline for each pollutant in all the 9 locations mentioned in the study area was plotted in graphs along with their standard deviation as error bars, same process was repeated during the analysis part of the meteorological parameters of all the locations.

For the plotting of Scatter Plot matrices and Pearson correlation coefficient I have used the software OriginPro 2024 version 10.1.0.178. The data from excel files were simplified in a four column for the 4X4 matrix that was then used in Pearson correlation coefficient, Descriptive statistics part in the origin pro software.

For the modelling in Random Forest regression, Python was used in google colab. Main goal here was to train an artificial neural node on vast iteration to come up with a model that would give the least mean standard and absolute error.

4.2 JAVASCRIPT API

4.2.1 JAVASCRIPT API FOR COLLECTION OF BLACK CARBON DATA IN GOOGLE EARTH ENGINE

```
var dataset = ee.ImageCollection('NASA/GSFC/MERRA/aer/2')
                .filter(ee.Filter.date('2019-12-01', '2019-12-31'));
var black_carbon = dataset.select('BCSMASS');
var bcsmass = {
  min: -0.0000116,
  max: 0.0000165,
  palette: ['001137', '01abab', 'e7eb05', '620500']
};
Map.setCenter(88.3578, 22.574, 8);
Map.addLayer(black_carbon, bcsmass);
```

4.2.2 JAVASCRIPT API FOR COLLECTION OF CARBON MONOXIDE(CO) DATA IN GOOGLE EARTH ENGINE

```
var collection = ee.ImageCollection('COPERNICUS/S5P/NRTI/L3_CO')
  .select('CO_column_number_density')
  .filterDate('2018-11-22', '2018-11-30');

var band_viz = {
  min: 0,
  max: 0.05,
  palette: ['black', 'blue', 'purple', 'cyan', 'green', 'yellow', 'red']
};

Map.addLayer(collection.mean(), band_viz, 'S5P CO');
Map.setCenter(88.3578, 22.574, 8);
```

4.2.3 JAVASCRIPT API FOR COLLECTION OF OZONE(O_3) DATA IN GOOGLE EARTH ENGINE

```
var collection = ee.ImageCollection('COPERNICUS/S5P/OFFL/L3_O3_TCL')
  .select('ozone_tropospheric_vertical_column')
  .filterDate('2019-06-01', '2019-07-01');


var band_viz = {
  min: 0,
  max: 0.02,
  palette: ['black', 'blue', 'purple', 'cyan', 'green', 'yellow', 'red']
};


Map.addLayer(collection.mean(), band_viz, 'S5P O3');
Map.setCenter(88.3578, 22.574, 8);
```

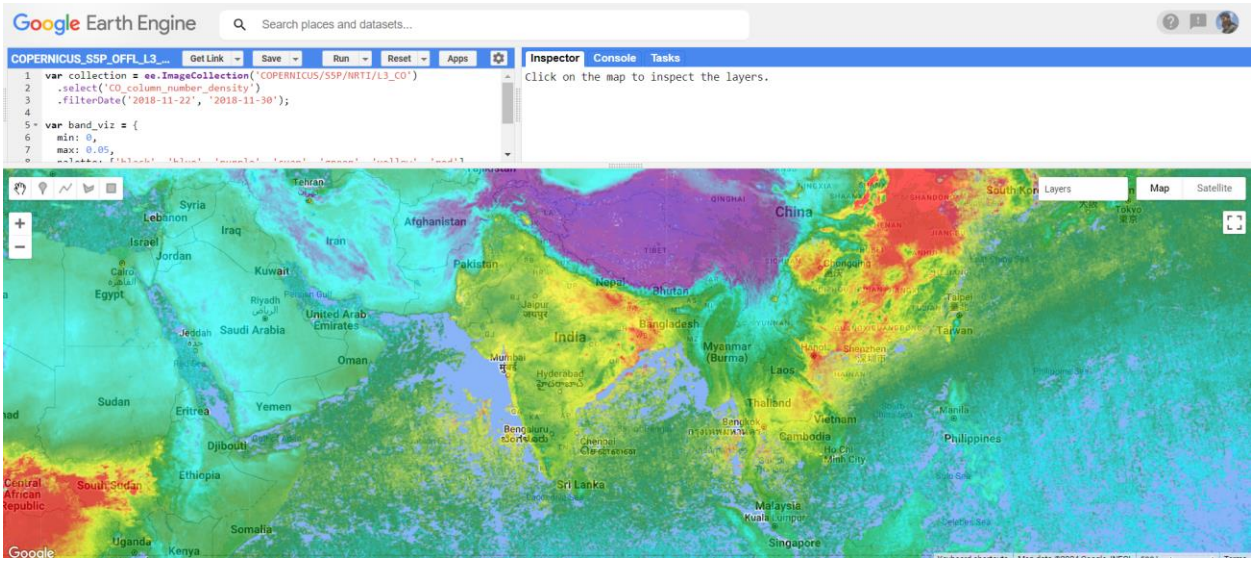

FIG 12: Screengrab of a code running for COPERNICUS showing gradient variation of CO variations in the Indian subcontinent (unit in kg/m^3)

5. RESULTS AND DISCUSSION

5.1 Monthly average trend for Black Carbon concentration 2015 – 2022

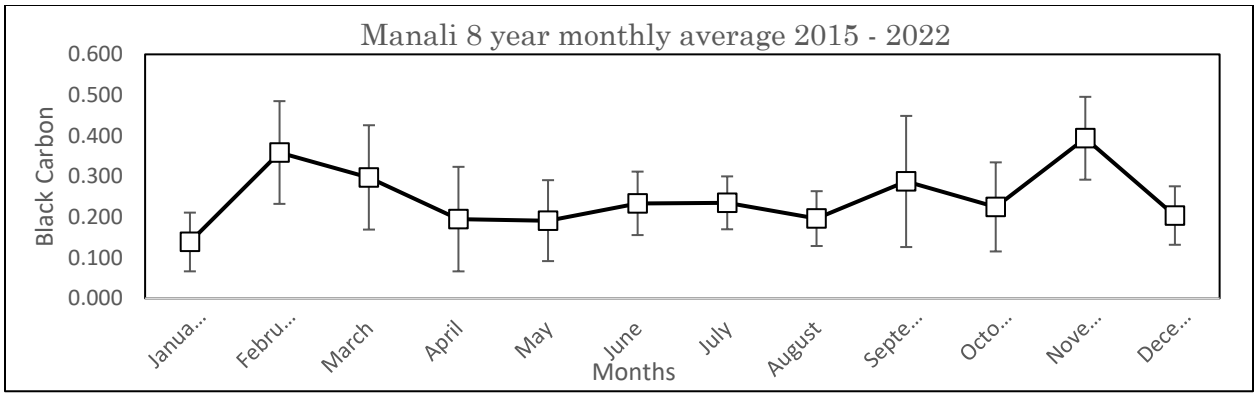

FIG 13(a)

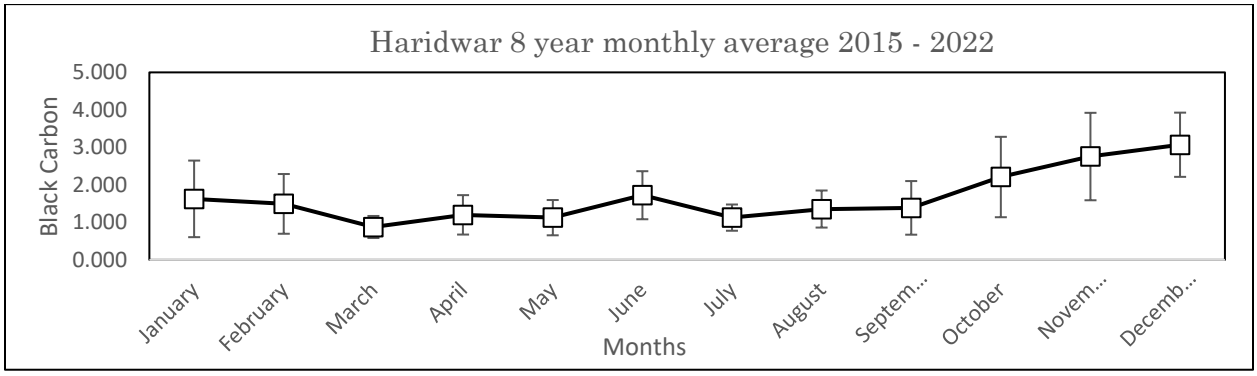

FIG 13(b)

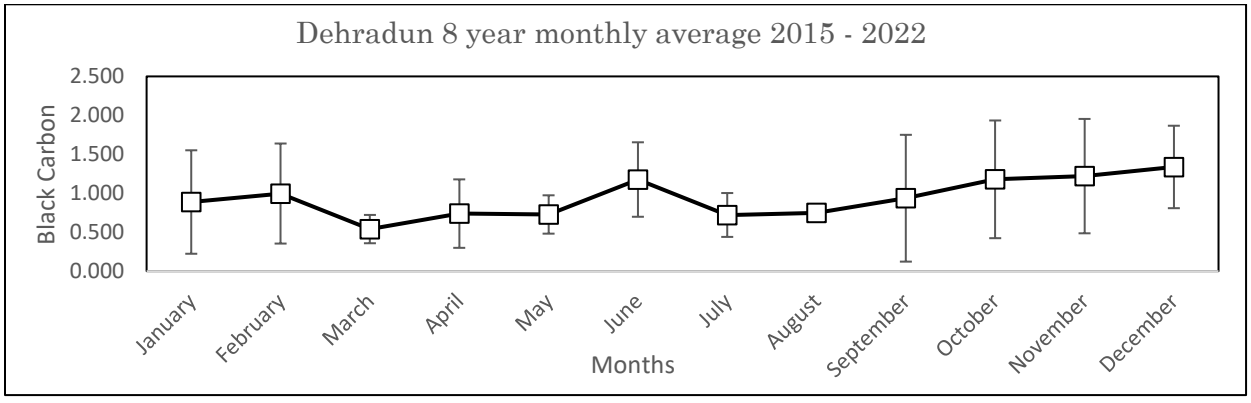

FIG 13(c)

FIG 13(a),13(b),13(c) depicting the average annual trend line for Black Carbon concentration from 2015 to 2022 in Manali, Haridwar and Dehradun respectively. Both Manali and Dehradun showed higher standard deviation in the month of September.

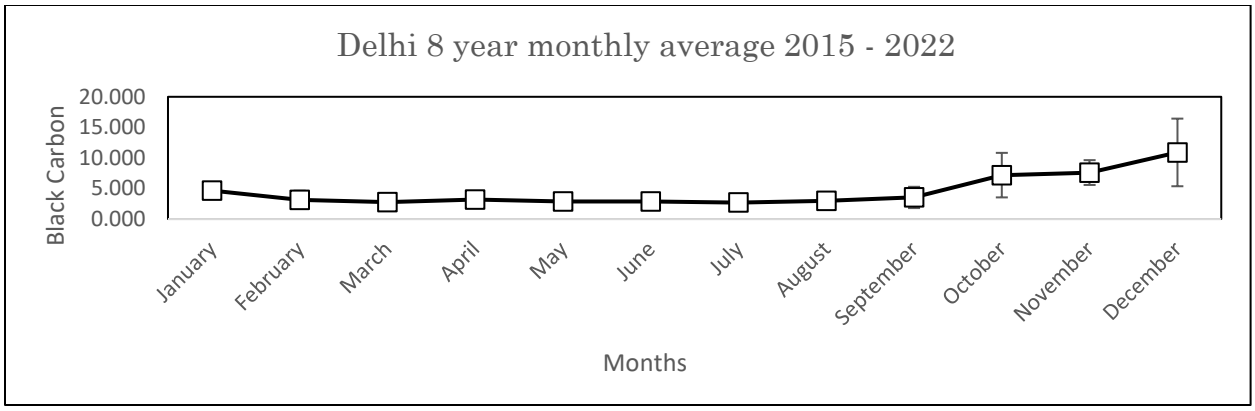

FIG 13(d)

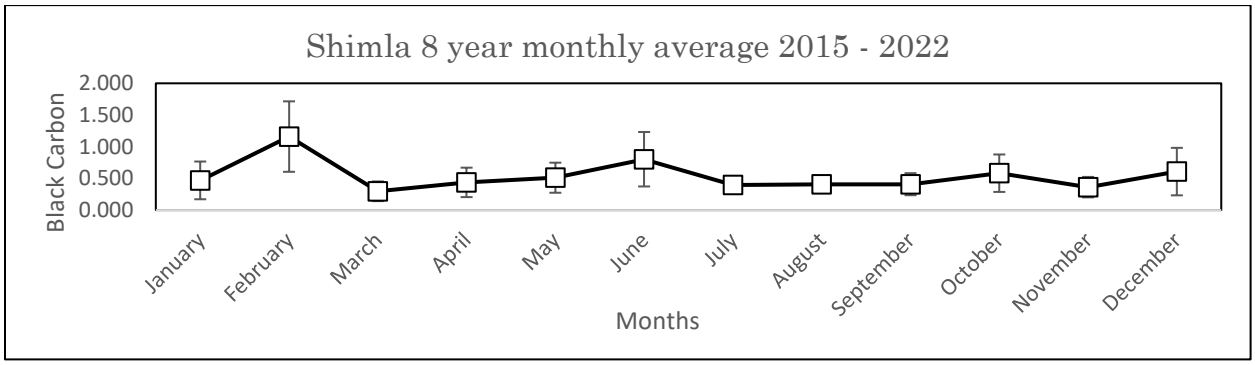

FIG 13*(e)*

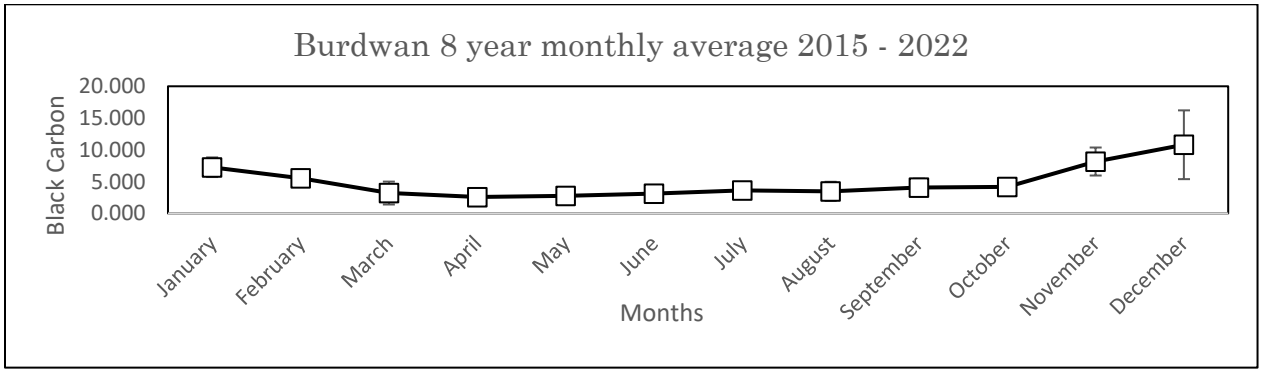

FIG 13 (f)

FIG 13(d),13(e),13(f) depicting the average annual trend line for Black Carbon concentration from 2015 to 2022 in Delhi, Shimla and Burdwan respectively. Both Delhi and Burdwan showed higher concentration and deviation in the month of September, while Shimla showed relatively concentration in February.

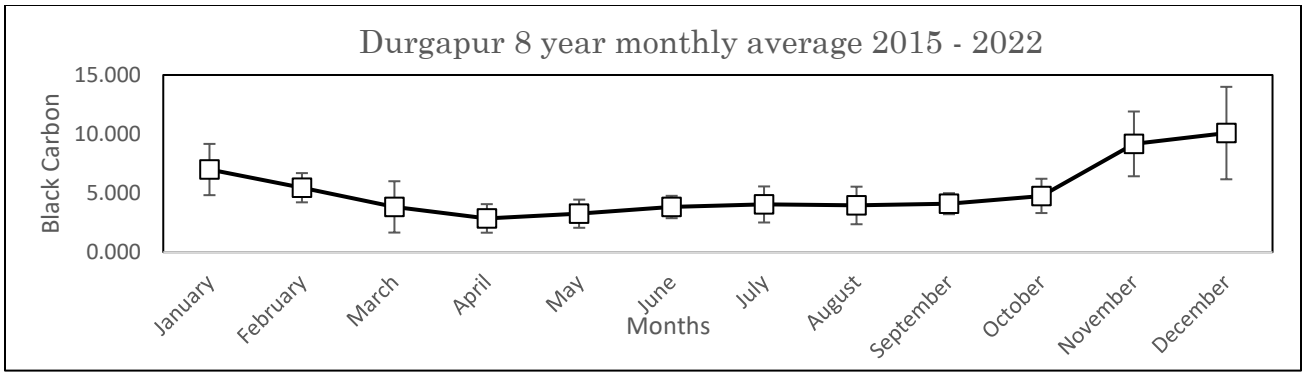

FIG 13 (g)

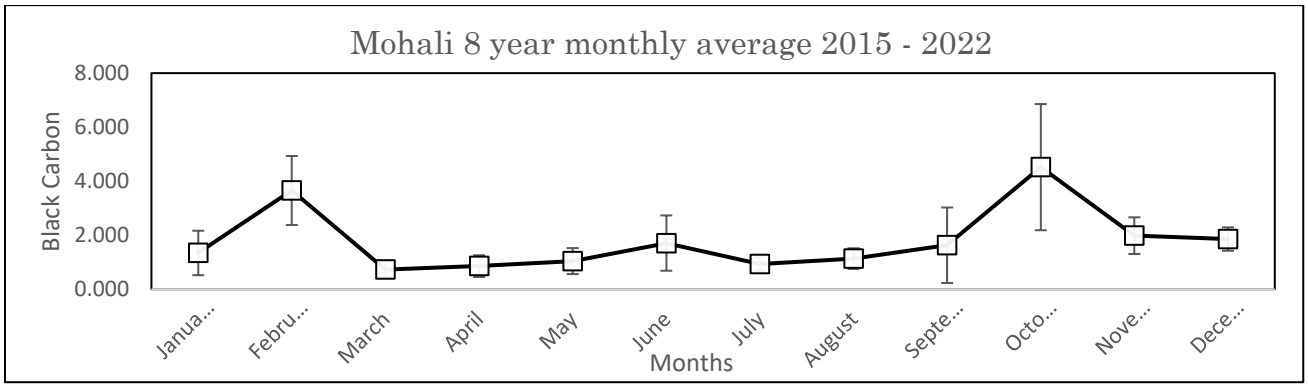

FIG 13 (h)

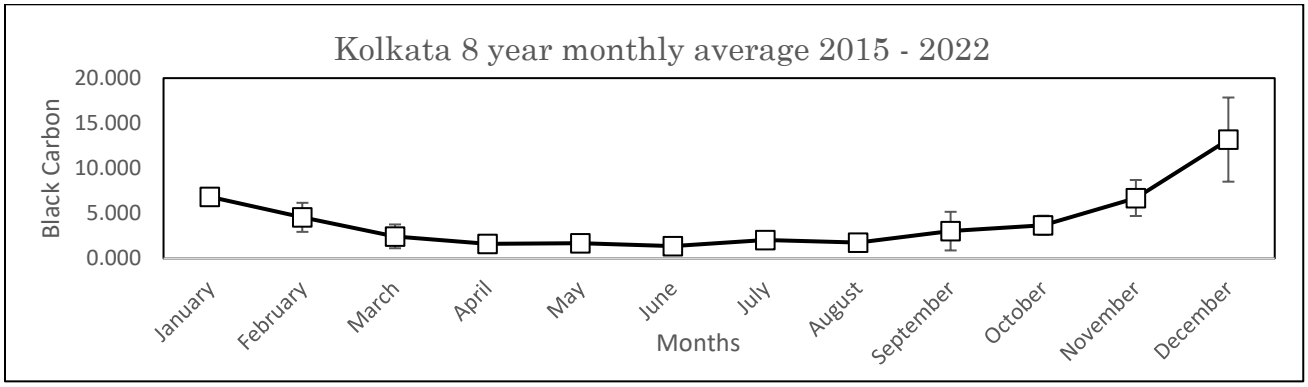

FIG 13 (i)

FIG 13(g),13(h),13(i) depicting the average annual trend line for Black Carbon concentration from 2015 to 2022 in Durgapur, Mohali and Kolkata respectively. Both Durgapur and Kolkata showed higher concentration standard deviation in the month of December, while Mohali showed maximum concentration and deviation in the month of October.

5.2 Monthly average trend for Carbon Monoxide concentration 2015 – 2022

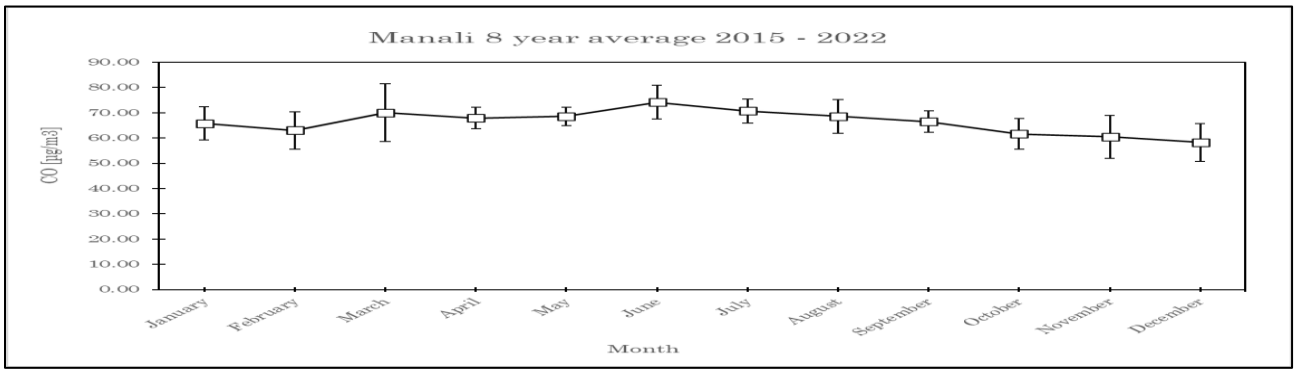

FIG 14 (a)

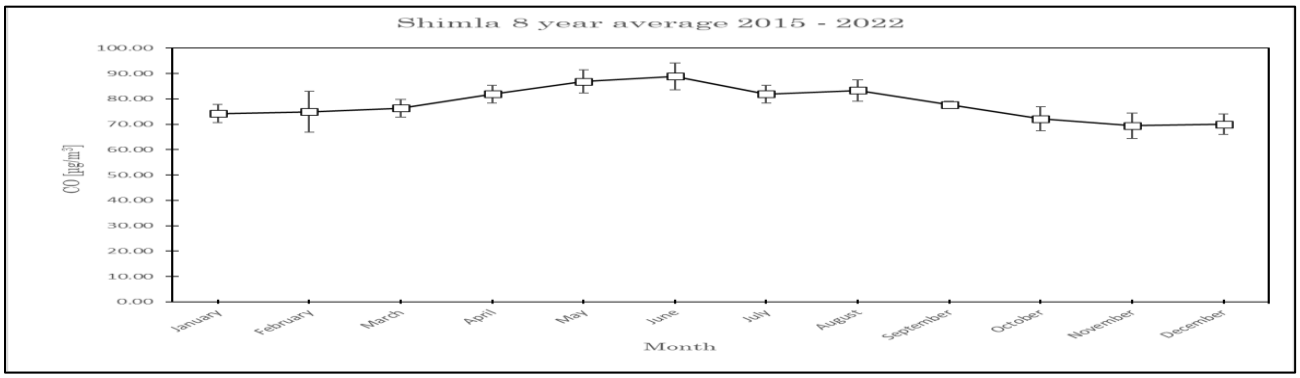

FIG 14 (b)

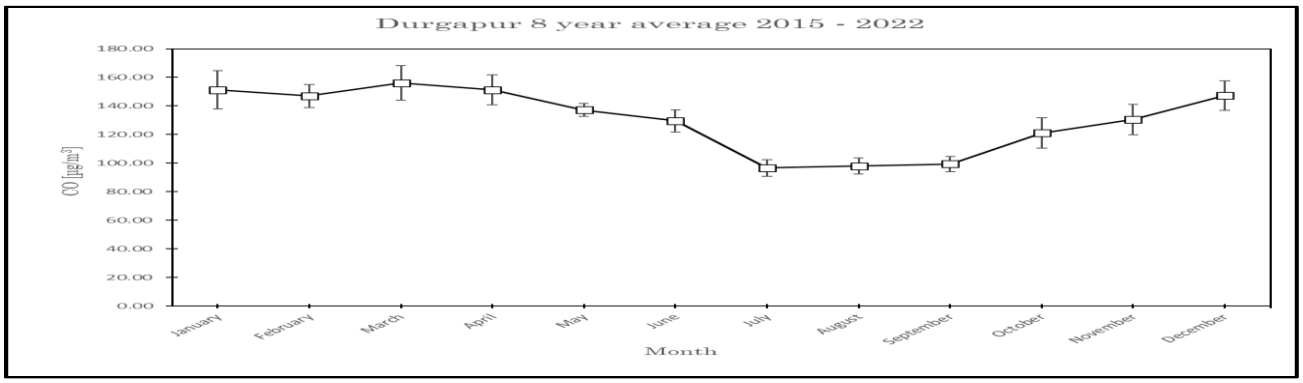

FIG 14 (c)

FIG 14(a),14(b),14(c) depicting the average annual trend line for Carbon Monoxide concentration from 2015 to 2022 in Manali, Shimla and Durgapur respectively. Both Manali and Shimla showed relatively same concentration throughout the year whereas Durgapur had a sudden drop in concentration in the month of June and July most likely due to the arrival of monsoon.

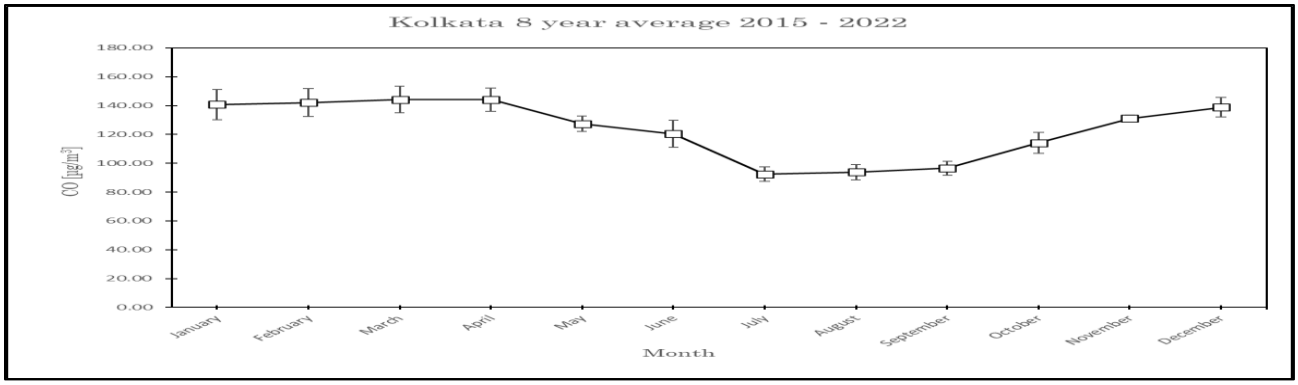

FIG 14 (d)

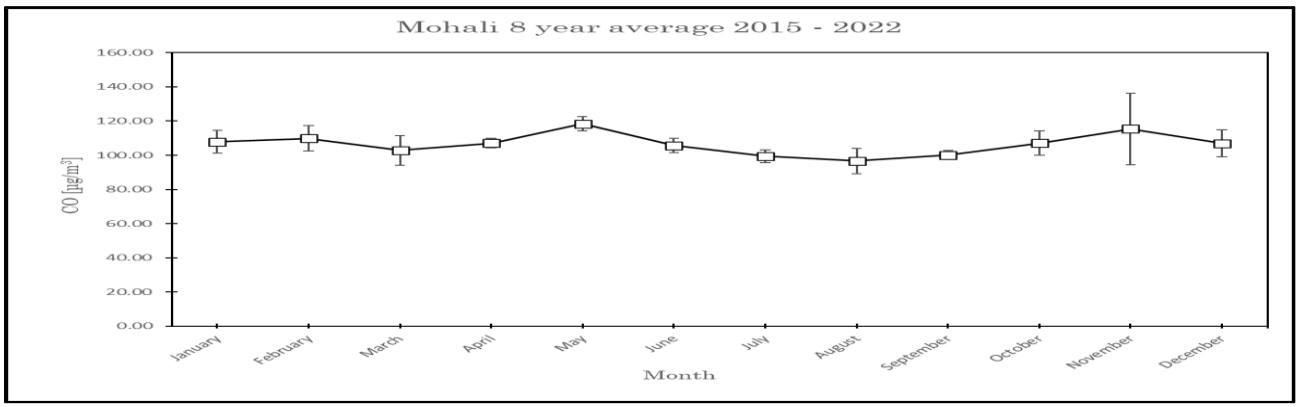

FIG 14 (e)

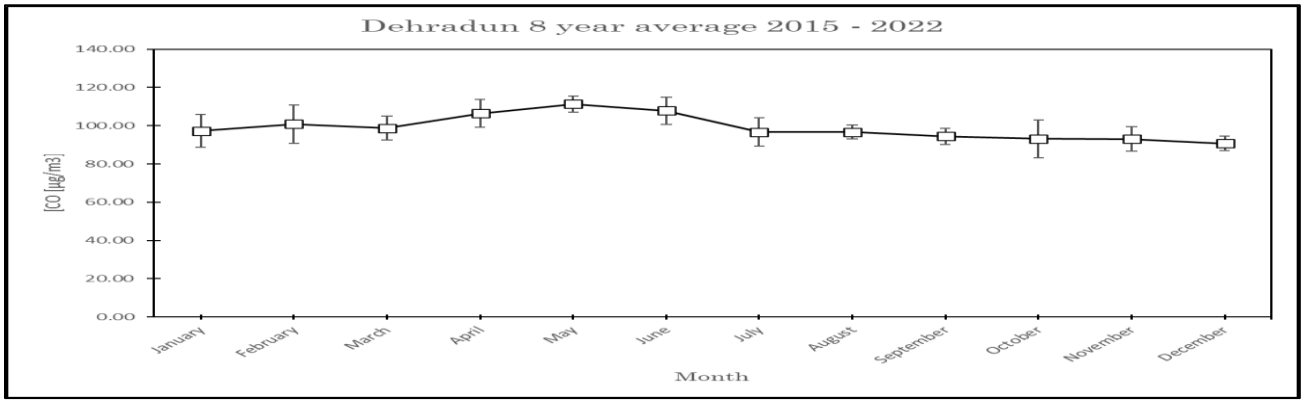

FIG 14 (f)

FIG 14(d),14(e),14(f) depicting the average annual trend line for Carbon Monoxide concentration from 2015 to 2022 in Kolkata, Mohali and Dehradun respectively. Both Dehradun and Mohali showed relatively same concentration throughout the year with Mohali showing a higher deviation in the month of November whereas Kolkata had a sudden drop in concentration in the month from May, most likely due to the arrival of monsoon.

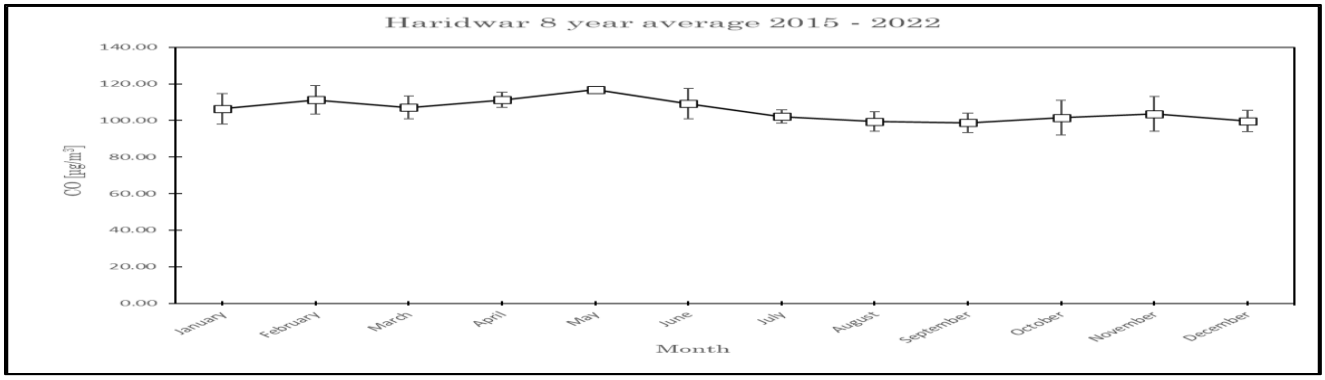

FIG 14 (g)

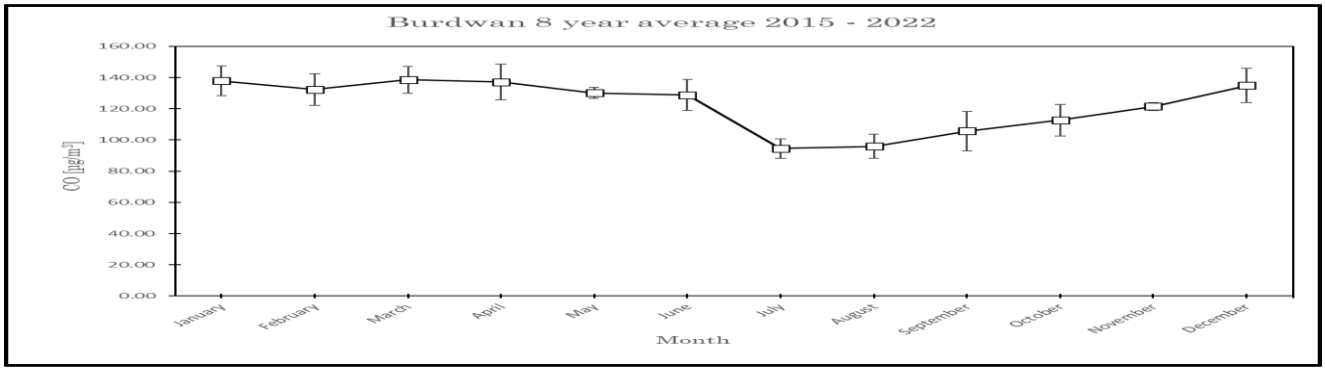

FIG 14 (h)

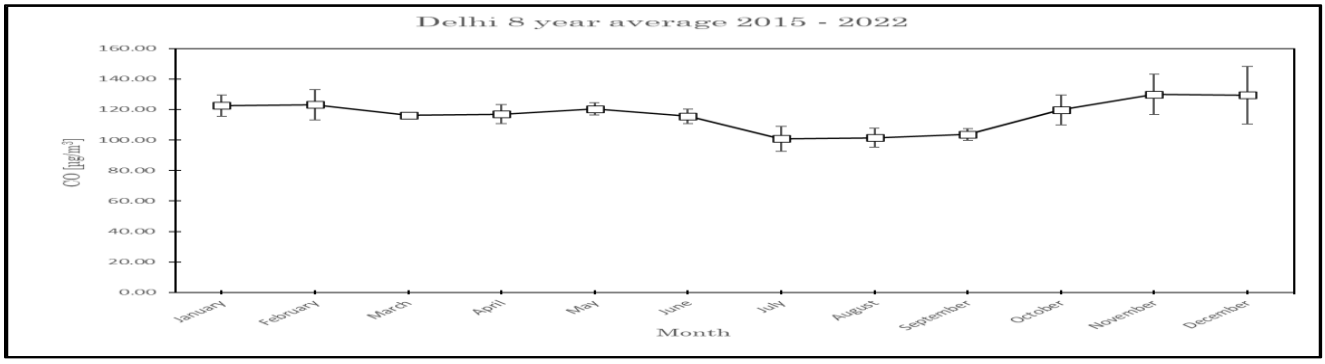

FIG 14 (i)

FIG 14(g),14(h),14(i) depicting the average annual trend line for Carbon Monoxide concentration from 2015 to 2022 in Haridwar, Burdwan and Delhi respectively. Both Haridwar and Delhi showed relatively same concentration throughout the year except in November and December where Delhi Concentration increased whereas Burdwan had a sudden drop in concentration in the month of June, likely due to the arrival of monsoon.

5.3 Monthly average trend for Ozone concentration 2015 – 2022

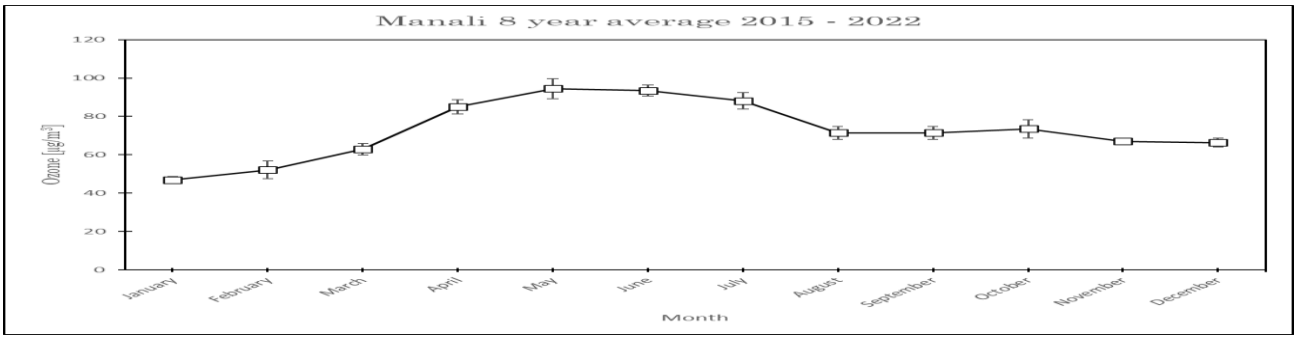

FIG 15 (a)

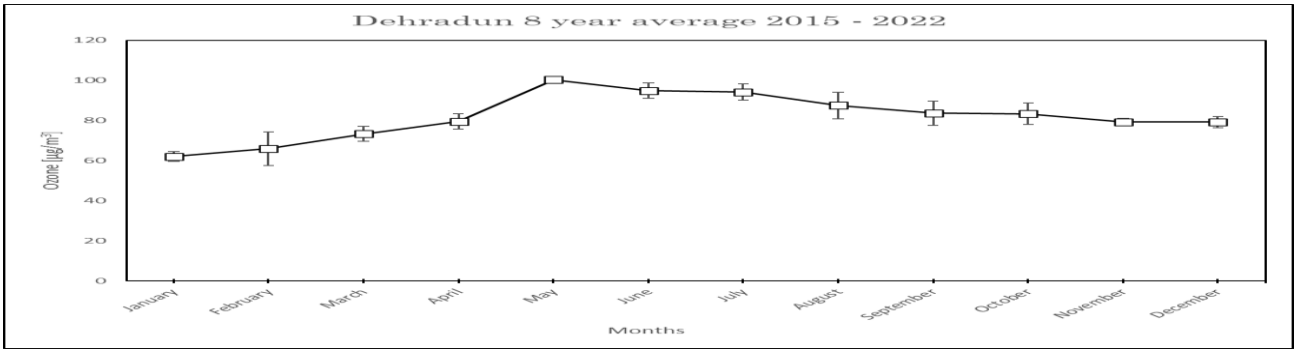

FIG 15 (b)

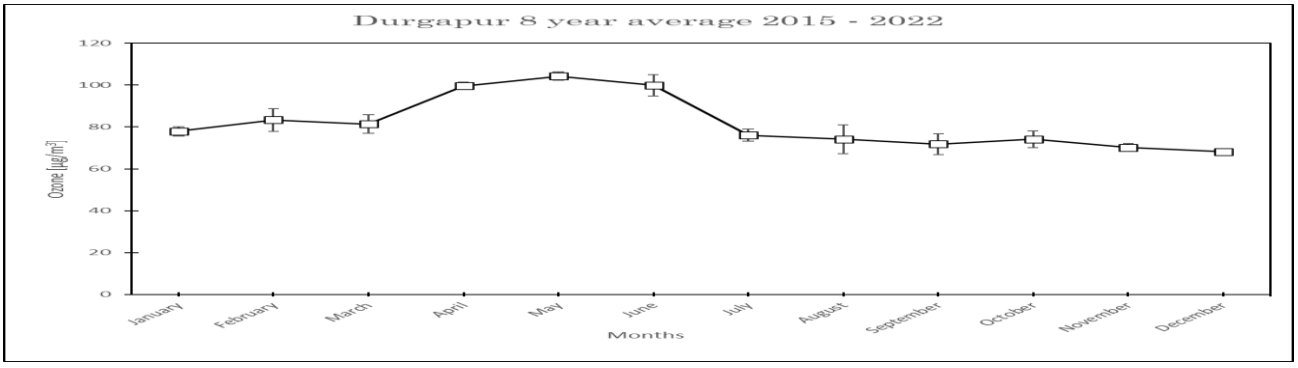

FIG 15 (c)

FIG 15(a),15(b),15(c) depicting the average annual trend line for Ozone concentration (tropospheric) from 2015 to 2022 in Manali, Dehradun and Durgapur respectively. All three locations showed an increase in ambient Ozone concentration in the summer months. While Manali and Durgapur showing a drop during the month of June and July.

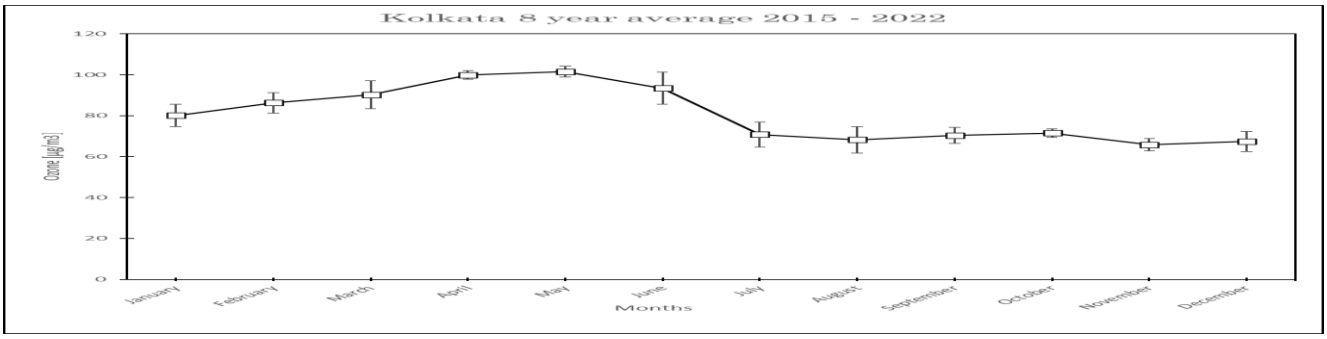

FIG 15 (d)

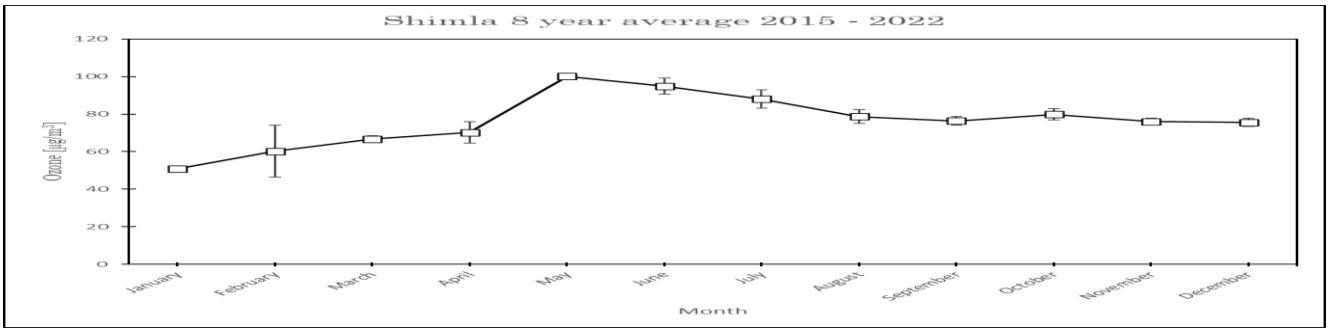

FIG 15 (e)

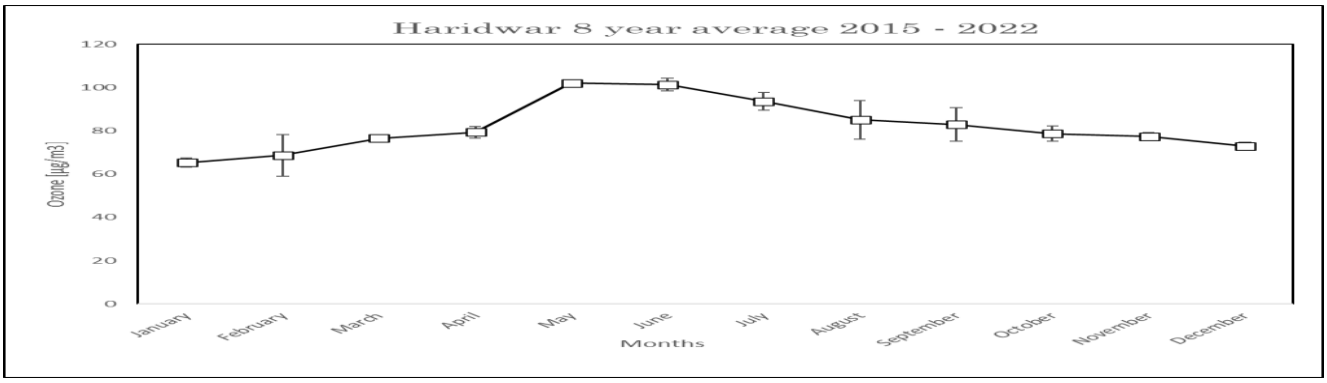

FIG 15 (f)

FIG 15(d),15(e),15(f) depicting the average annual trend line for Ozone concentration (tropospheric) from 2015 to 2022 in Kolkata, Shimla and Haridwar respectively. All three locations showed an increase in ambient Ozone concentration in the summer months, especially Shimla and Haridwar which had sudden increase while Kolkata showing a drop during the month of June and July.

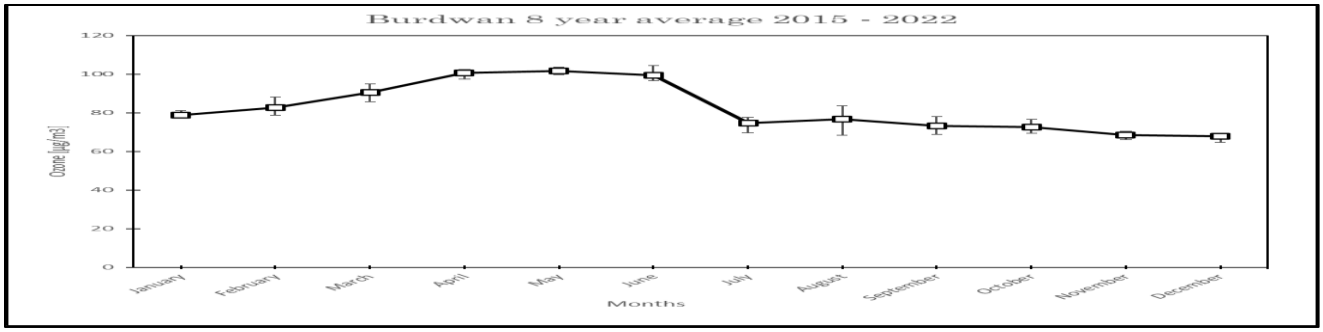

FIG 15 (g)

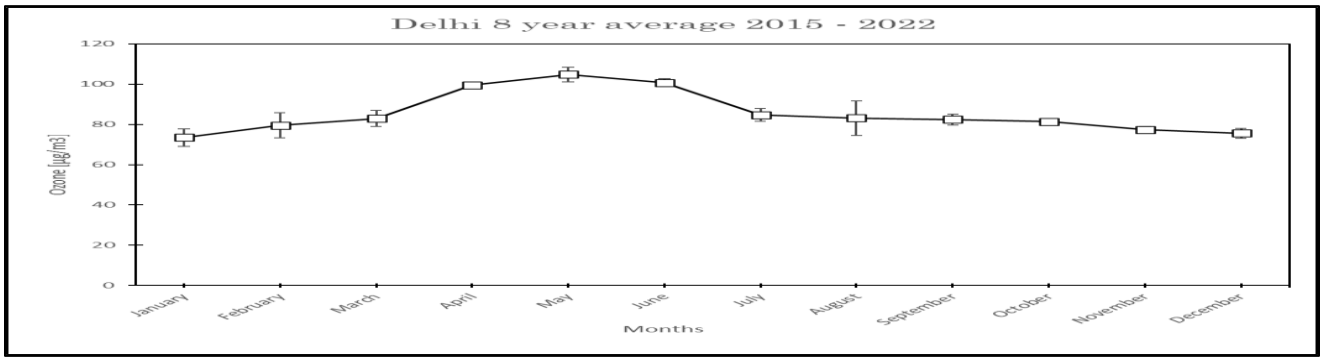

FIG 15 (h)

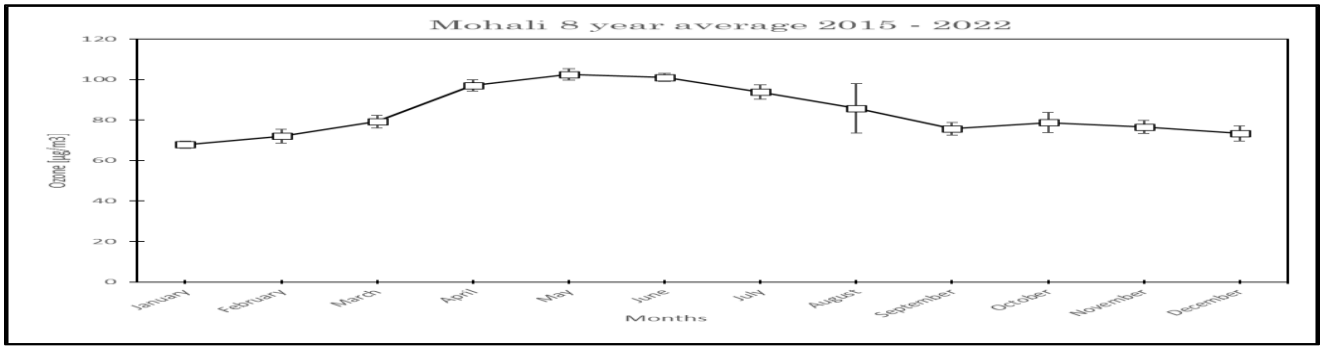

FIG 15 (i)

FIG 15(g),15(h),15(i) depicting the average annual trend line for Ozone concentration (tropospheric) from 2015 to 2022 in Burdwan, Delhi and Mohali respectively. All three locations showed an increase in ambient Ozone concentration in the summer months, while Burdwan showed a sharp decrease in June, all three locations also showed higher deviation in the month of August.

6. Statistical Analysis (Pearson Correlation Coefficient) via Scatter Plot Matrix

6.1 To find patterns, trends, connections, and insights, *statistical analysis* entails gathering, processing, interpreting, and presenting data. It is employed in many different disciplines, including sociology, psychology, business, economics, and medicine. There are various kinds of statistical analysis methods, such as multivariate, inferential, and descriptive statistics. While inferential statistics make assumptions or predictions about a population based on sample data, **descriptive statistics** summaries and characterize the features of a dataset. The simultaneous examination of data comprising several variables is the focus of multivariate statistics. Statistical software like R, Python (with libraries like NumPy, SciPy, and pandas), Origin Pro, ANOVA, SPSS, Excel, and R are commonly used in statistical analysis.

The Pearson correlation coefficient, often denoted as r, is a measure of the linear relationship between two variables. It ranges from -1 to 1, where:

Range of r	Degree of Relationship
$-1.0 \leq r \leq -0.7$	A strong negative linear relationship
$-0.7 \leq r \leq -0.3$	A distinct negative linear relationship
$-0.3 \leq r \leq -0.1$	A weak negative linear relationship
$-0.1 \leq r \leq +0.1$	Not a linear relationship
$+0.1 \leq r \leq +0.3$	A weak positive linear relationship
$+0.3 \leq r \leq +0.7$	A distinct positive linear relationship
$+0.7 \leq r \leq +1.0$	A strong positive linear relationship

FIG 16: Pearson correlation coefficient [r]

It's calculated as the covariance of the two variables divided by the product of their standard deviations. Mathematically, for two variables X and Y with observations (x_i, y_i) the Pearson correlation coefficient is:

$$r_{xy} = \frac{\sum_{i=1}^{n}(x_i - \bar{x})(y_i - \bar{y})}{\sqrt{\sum_{i=1}^{n}(x_i - \bar{x})^2}\sqrt{\sum_{i=1}^{n}(y_i - \bar{y})^2}}$$

FIG 17: Formula for calculating value of r.

- *Where* $\bar{x}$ and $\bar{y}$ are the means of X and Y respectively, and
- n is the number of observations.

6.2 Scatter Plot Matrix

MANALI MONTHLY BLACK CARBON VS METEROLOGICAL PARAMETERS SCATTER PLOT MATRIX

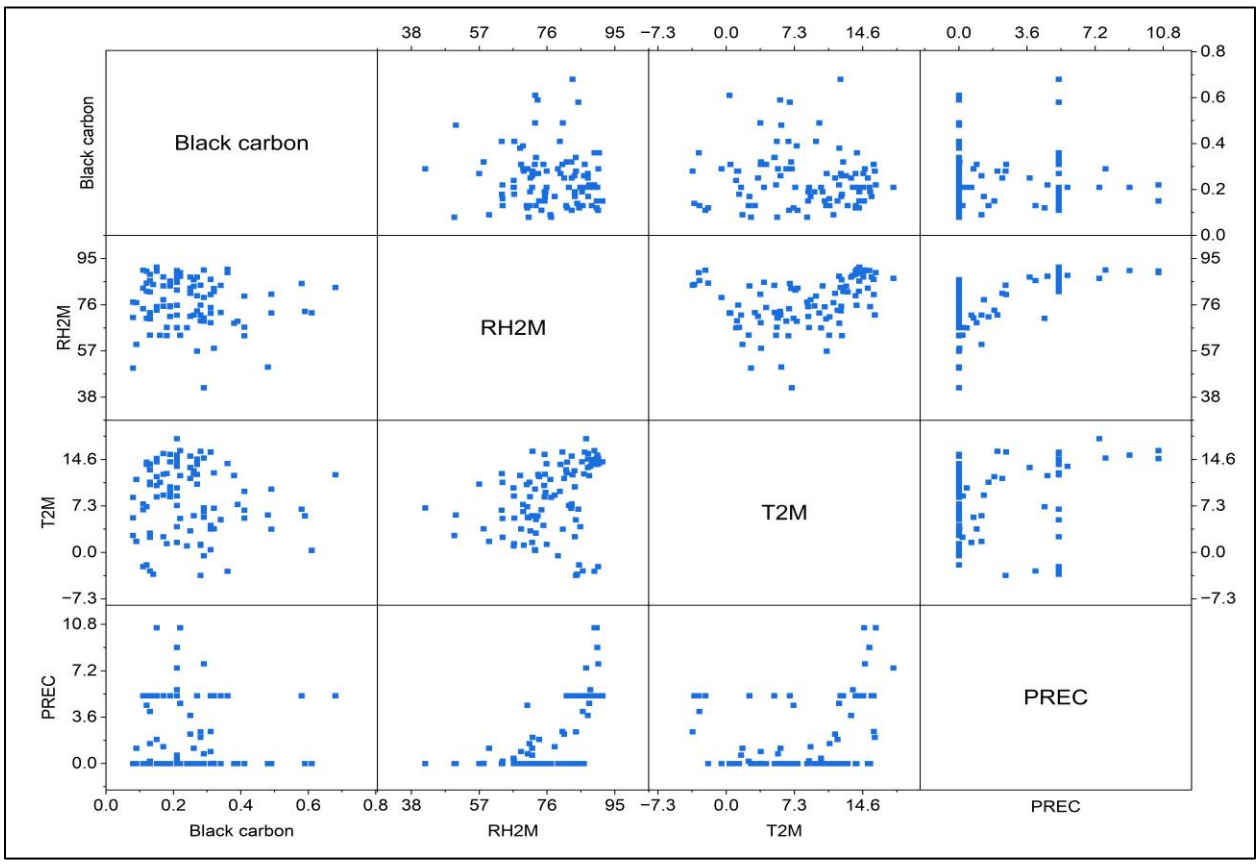

FIG 18: 4X4 Scatter Plot Matrix of Pearson Correlation for Black Carbon, RH2M, T2M and Precipitation in MANALI

Table 6: Pearson Correlation coefficients for the FIG 18.

Pearson Correlations	Black carbon	RH2M	T2M	PREC
Black carbon	1			
RH2M	**-0.07105**	1		
T2M	**-0.07440**	0.30356	1	
PREC	**-0.05754**	0.6475	0.35155	1

It is evident from the Table 6, that there is no linear relationship between the parameters.

MANALI MONTHLY CARBON MONOXIDE VS METEROLOGICAL PARAMETERS SCATTER PLOT MATRIX

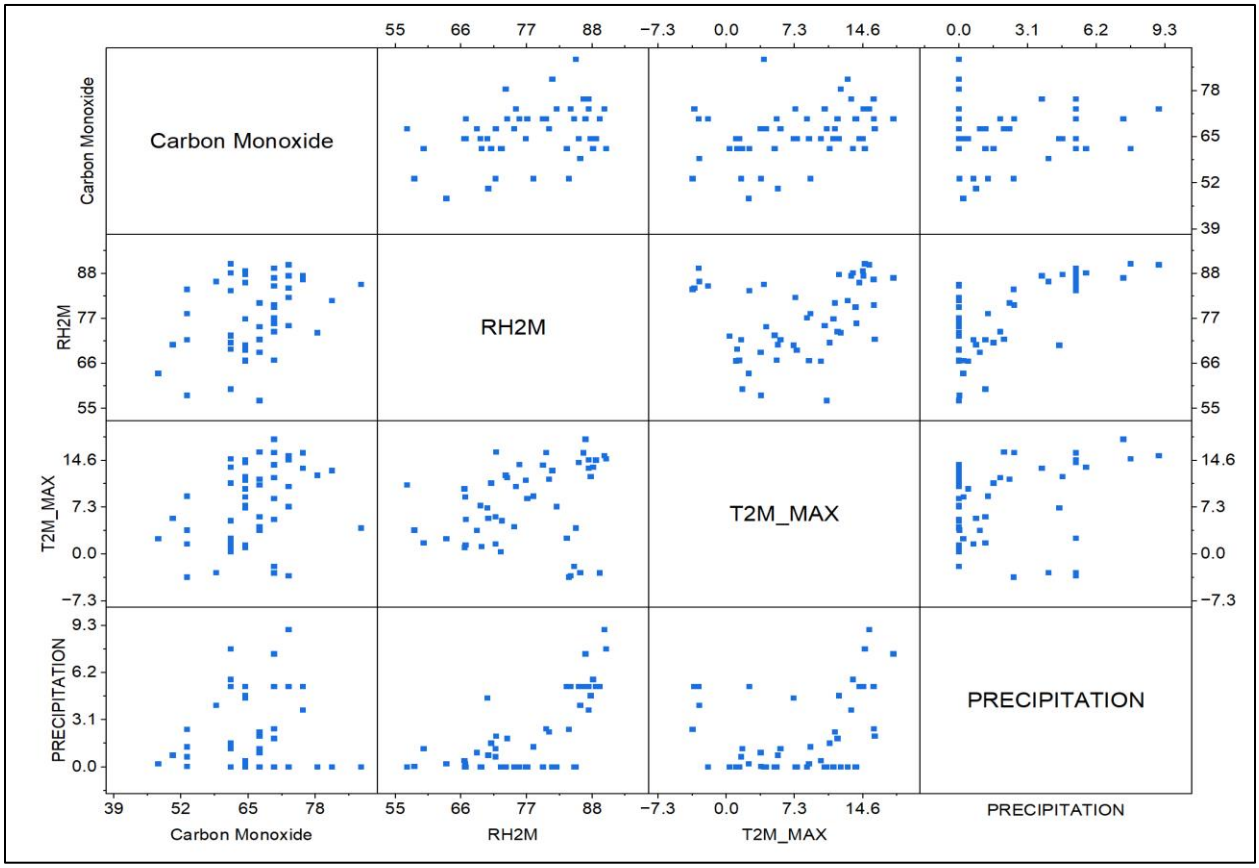

FIG 19: 4X4 Scatter Plot Matrix of Pearson Correlation for Carbon Monoxide, RH2M, T2M_MAX and Precipitation in MANALI

Table 7: Pearson Correlation coefficients for the FIG 19.

Pearson Correlations	Carbon Monoxide	RH2M	T2M_MAX	PRECIPITATION
Carbon Monoxide	1			
RH2M	**0.36019**	1		
T2M_MAX	**0.34775**	0.26043	1	
PRECIPITATION	0.06745	0.6981	0.31351	1

Here, in Table 7, Carbon Monoxide shows a distinct positive linear relationship with RH2M and T2M_MAX.

MANALI MONTHLY OZONE(O_3) VS METEROLOGICAL PARAMETERS SCATTER PLOT MATRIX

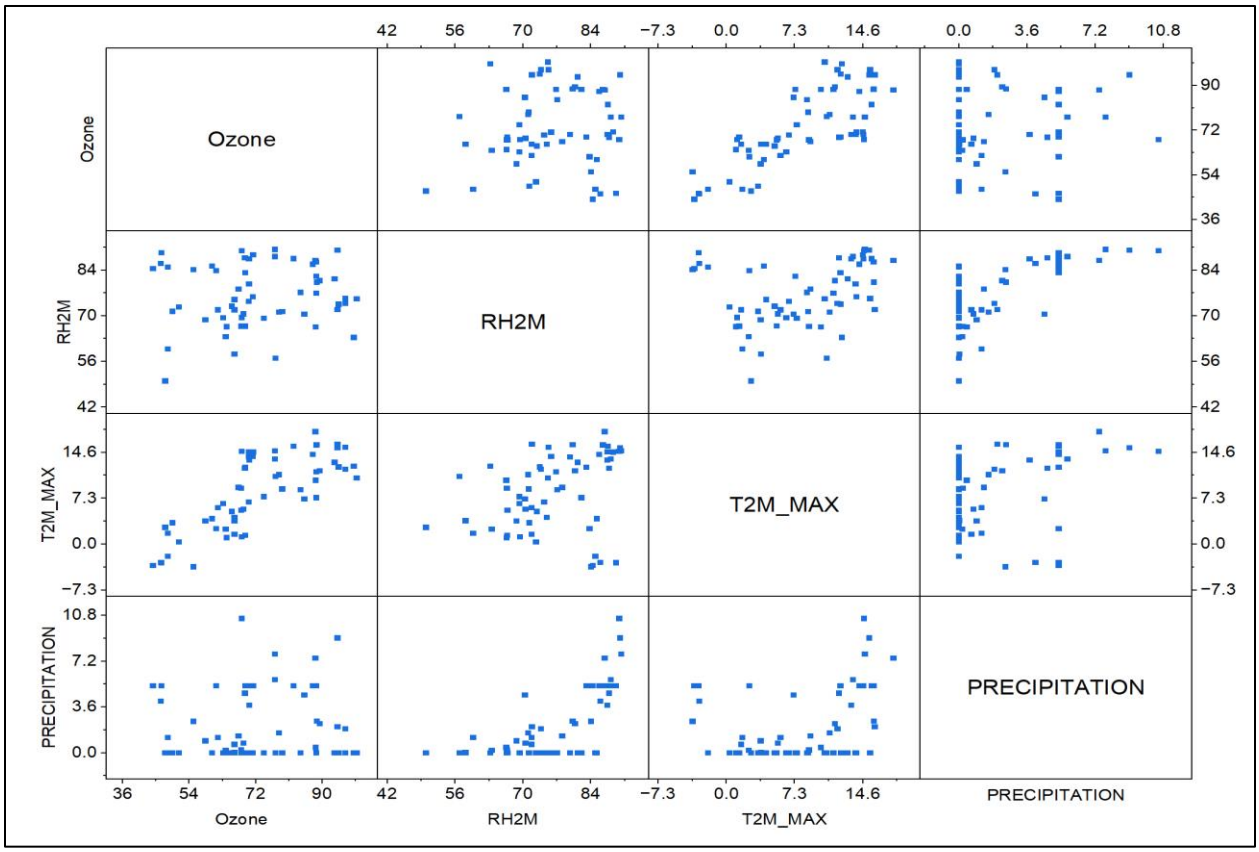

FIG 20: 4X4 Scatter Plot Matrix of Pearson Correlation for Ozone, RH2M, T2M_MAX and Precipitation in MANALI

Table 8: Pearson Correlation coefficients for the FIG 20.

Pearson Correlations	Ozone	RH2M	T2M_MAX	PRECIPITATION
Ozone	1			
RH2M	0.09345	1		
T2M_MAX	**0.77324**	0.30532	1	
PRECIPITATION	0.05492	0.70673	0.35012	1

Here, In Table 8, Ozone shows a strong Positive linear relationship with T2M_MAX.

SHIMLA MONTHLY BLACK CARBON VS METEROLOGICAL PARAMETERS SCATTER PLOT MATRIX

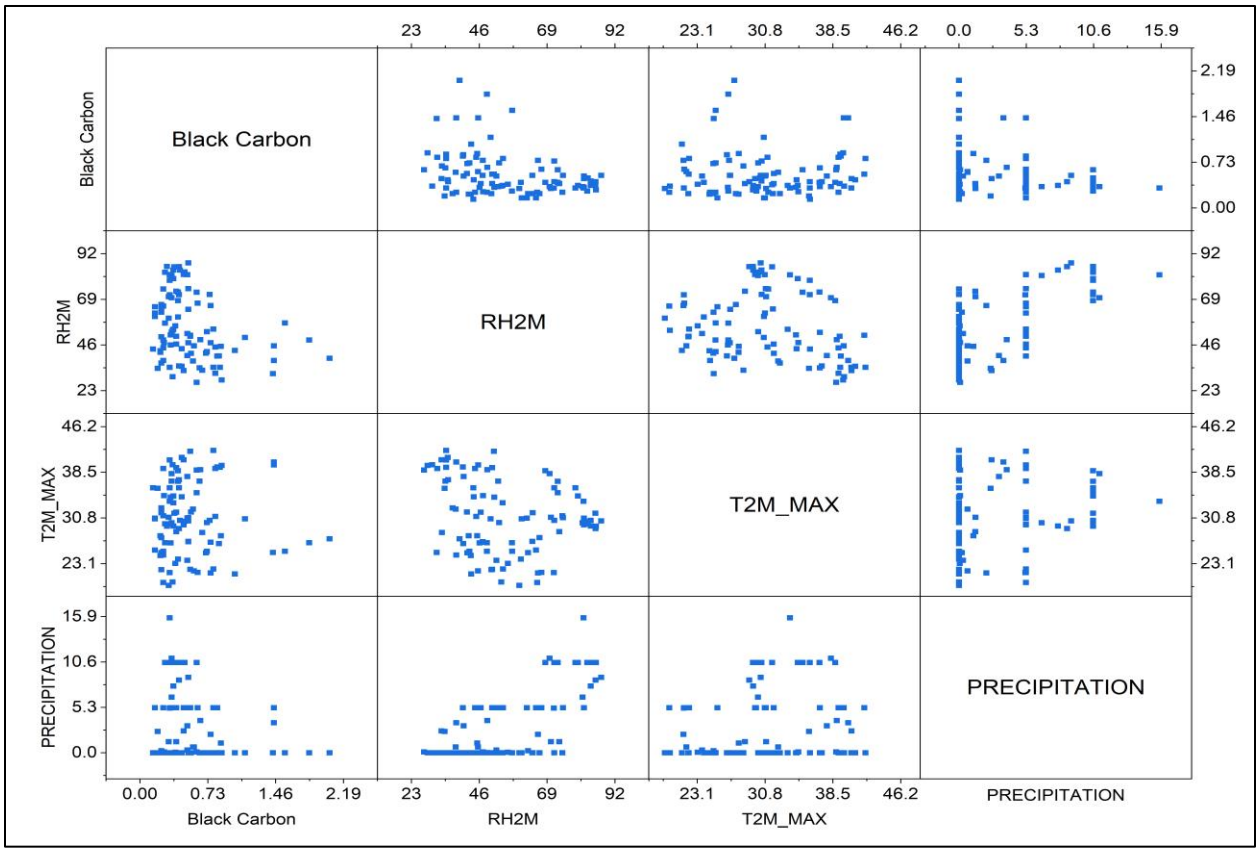

FIG 21: 4X4 Scatter Plot Matrix of Pearson Correlation for Black Carbon, RH2M, T2M_MAX and Precipitation in SHIMLA

Table 9: Pearson Correlation coefficients for FIG 21.

Pearson Correlations	Black Carbon	RH2M	T2M_MAX	PRECIPITATION
Black Carbon	1			
RH2M	**-0.31799**	1		
T2M_MAX	0.00162	-0.2322	1	
PRECIPITATION	**-0.20088**	0.70047	0.21727	1

Here, In Table 9, Black Carbon shows a distinct negative linear relationship with RH2M and weak negative linear relationship with Precipitation.

SHIMLA MONTHLY CARBON MONOXIDE(CO) VS METEROLOGICAL PARAMETERS SCATTER PLOT MATRIX

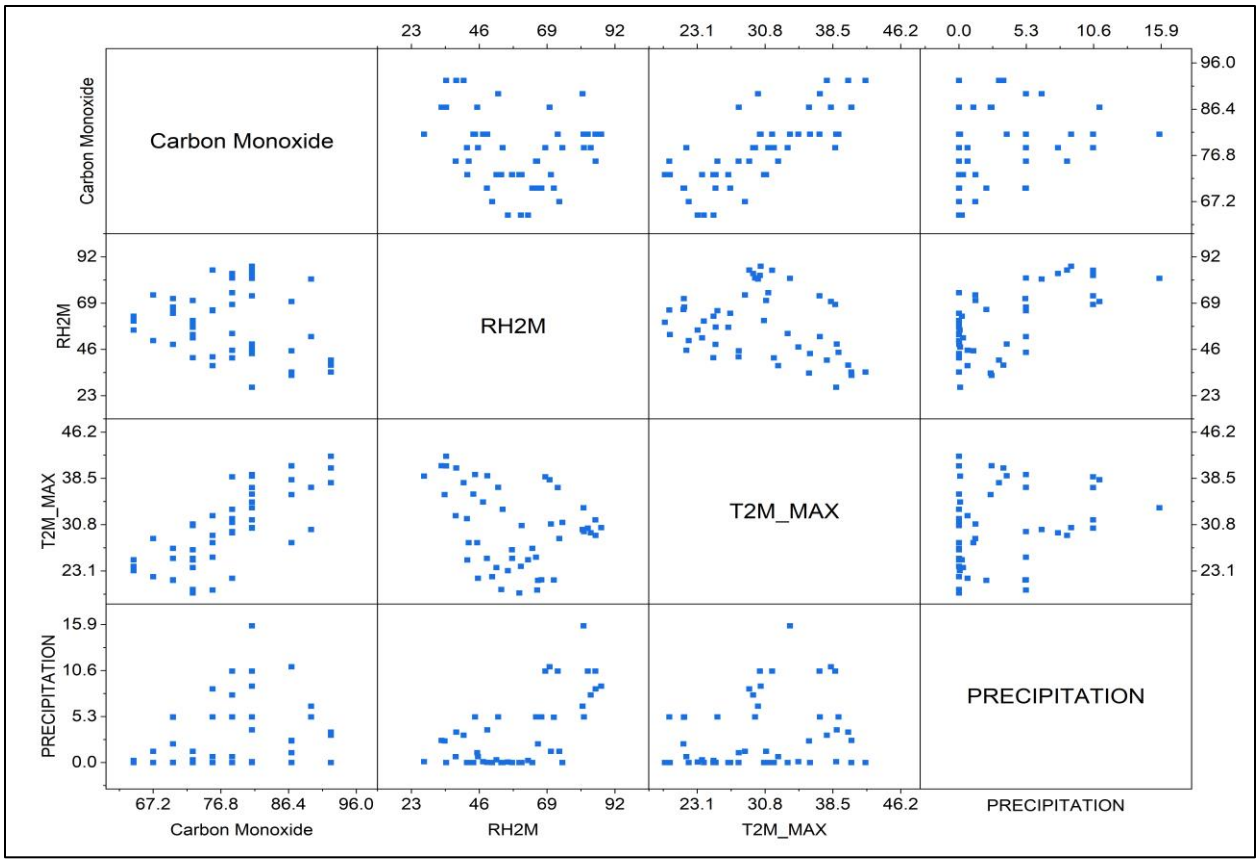

FIG 22: 4X4 Scatter Plot Matrix of Pearson Correlation for Carbon Monoxide, RH2M, T2M_MAX and Precipitation in SHIMLA

Table 10: Pearson Correlation coefficients for the FIG 22.

Pearson Correlations	Carbon Monoxide	RH2M	T2M_MAX	PRECIPITATION
Carbon Monoxide	1			
RH2M	**-0.24458**	1		
T2M_MAX	**0.76461**	-0.3049	1	
PRECIPITATION	**0.31233**	0.64663	0.24094	1

Here in Table 10, CO shows a weak negative, strong positive and distinct positive linear relationship with RH2M, T2M_MAX and PRECIPITATION respectively.

SHIMLA MONTHLY OZONE(O_3) VS METEROLOGICAL PARAMETERS SCATTER PLOT MATRIX

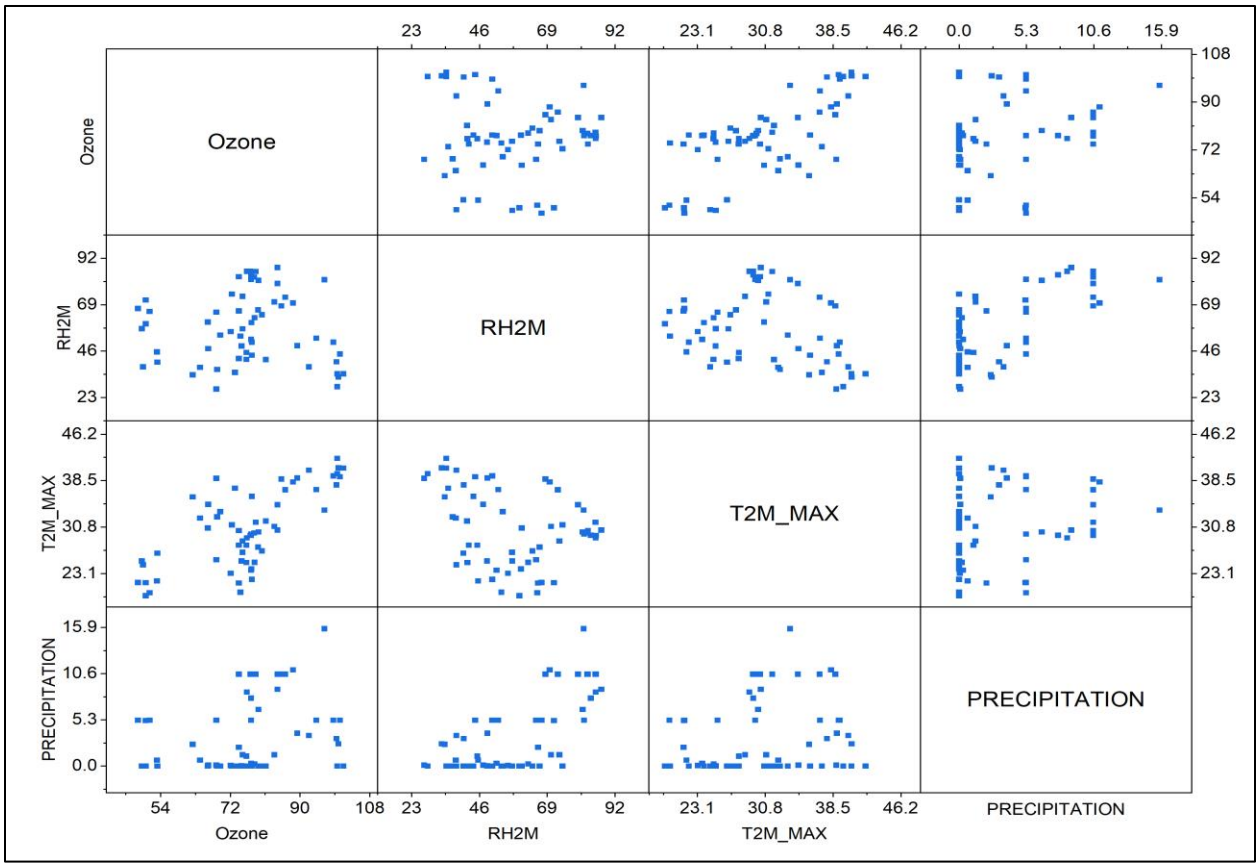

FIG 23: 4X4 Scatter Plot Matrix of Pearson Correlation for Ozone, RH2M, T2M_MAX and Precipitation in SHIMLA

Table 11: Pearson Correlation coefficients for the FIG 23.

Pearson Correlations	Ozone	RH2M	T2M_MAX	PRECIPITATION
Ozone	1			
RH2M	-0.05912	1		
T2M_MAX	**0.70187**	-0.29752	1	
PRECIPITATION	**0.25771**	0.69422	0.21104	1

Here in Table 11, Ozone shows a strong positive and weak positive linear relationship with T2M_MAX and PRECIPITATION respectively.

DEHRADUN MONTHLY BLACK CARBON VS METEROLOGICAL PARAMETERS SCATTER PLOT MATRIX

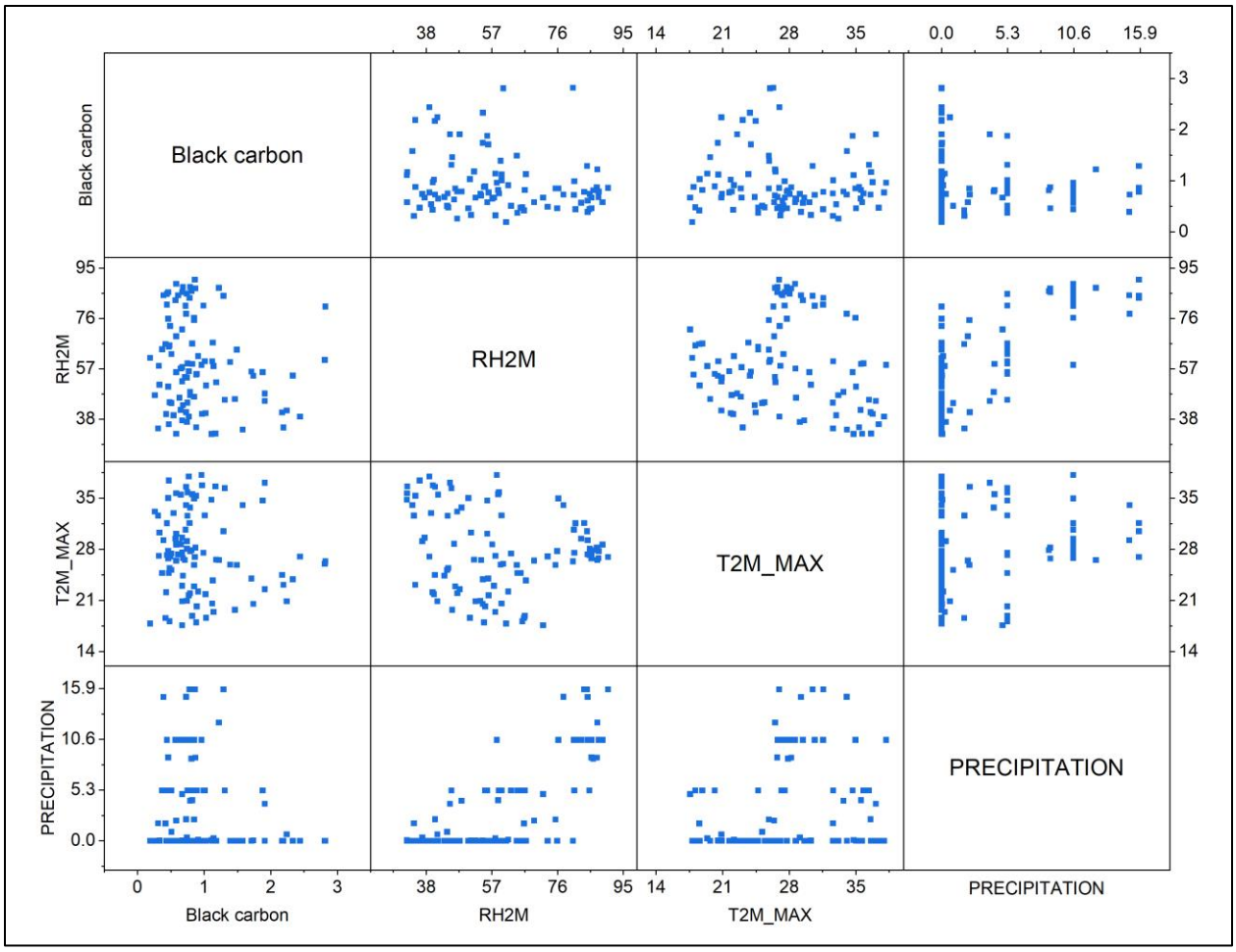

FIG 24: 4X4 Scatter Plot Matrix of Pearson Correlation for Black Carbon, RH2M, T2M_MAX and Precipitation in DEHRADUN

Table 12: Pearson Correlation coefficients for FIG 24.

Pearson Correlations	Black carbon	RH2M	T2M_MAX	PRECIPITATION
Black carbon	1			
RH2M	**-0.17319**	1		
T2M_MAX	-0.09812	-0.15838	1	
PRECIPITATION	**-0.17945**	0.75569	0.20656	1

Here in Table 12, Black Carbon shows weak negative linear relationship with both RH2M and PRECIPITATION.

DEHRADUN MONTHLY CARBON MONOXIDE(CO) VS METEROLOGICAL PARAMETERS SCATTER PLOT MATRIX

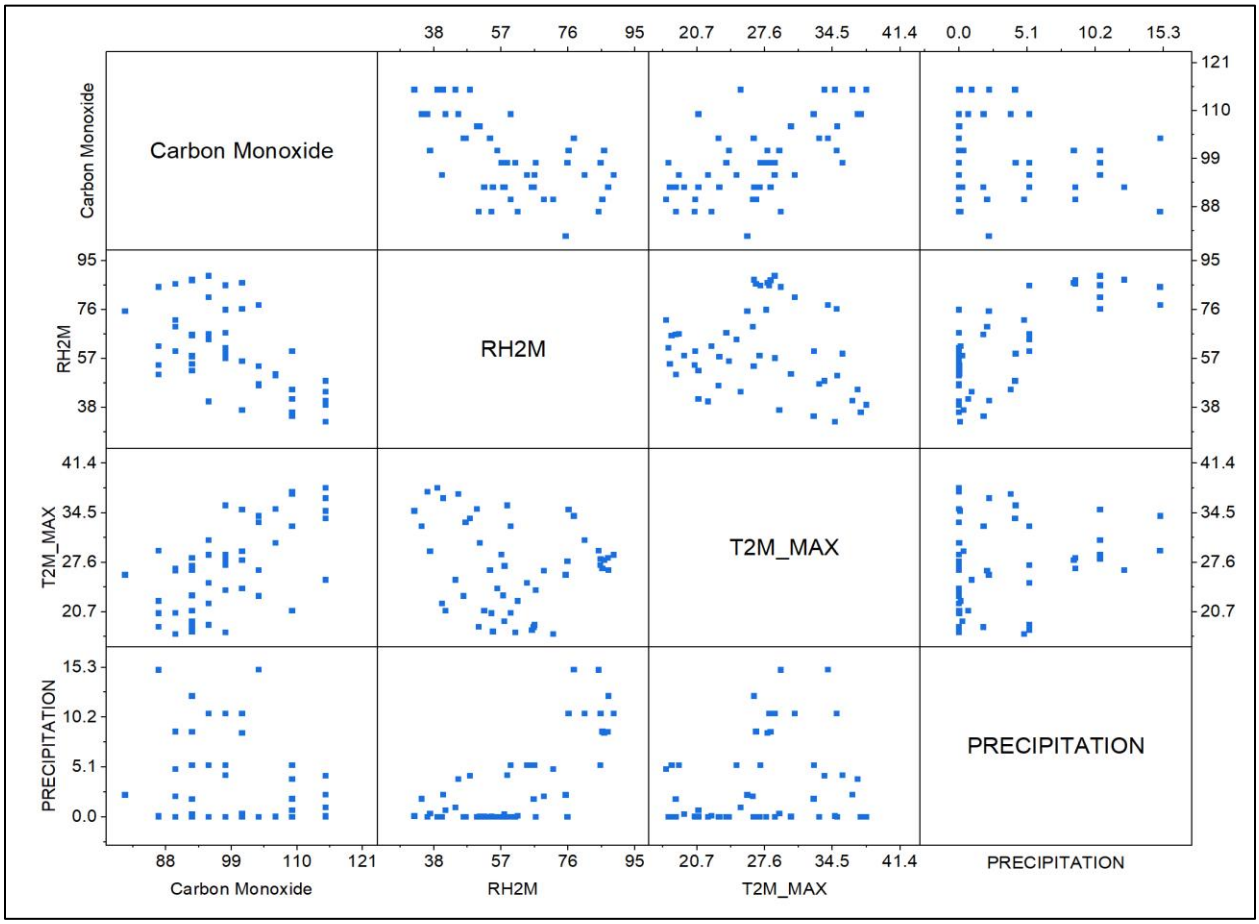

FIG 25: 4X4 Scatter Plot Matrix of Pearson Correlation for Carbon Monoxide, RH2M, T2M_MAX and Precipitation in DEHRADUN

Table 13: Pearson Correlation coefficients for FIG 25.

Pearson Correlations	Carbon Monoxide	RH2M	T2M_MAX	PRECIPITATION
Carbon Monoxide	1			
RH2M	**-0.56575**	1		
T2M_MAX	**0.63498**	-0.16207	1	
PRECIPITATION	**-0.15692**	0.74241	0.23006	1

Here in Table 13, Carbon Monoxide shows distinct negative, distinct positive and weak negative linear relationship with RH2M, T2M_MAX and PRECIPITATION respectively.

DEHRADUN MONTHLY OZONE(O_3) VS METEROLOGICAL PARAMETERS SCATTER PLOT MATRIX

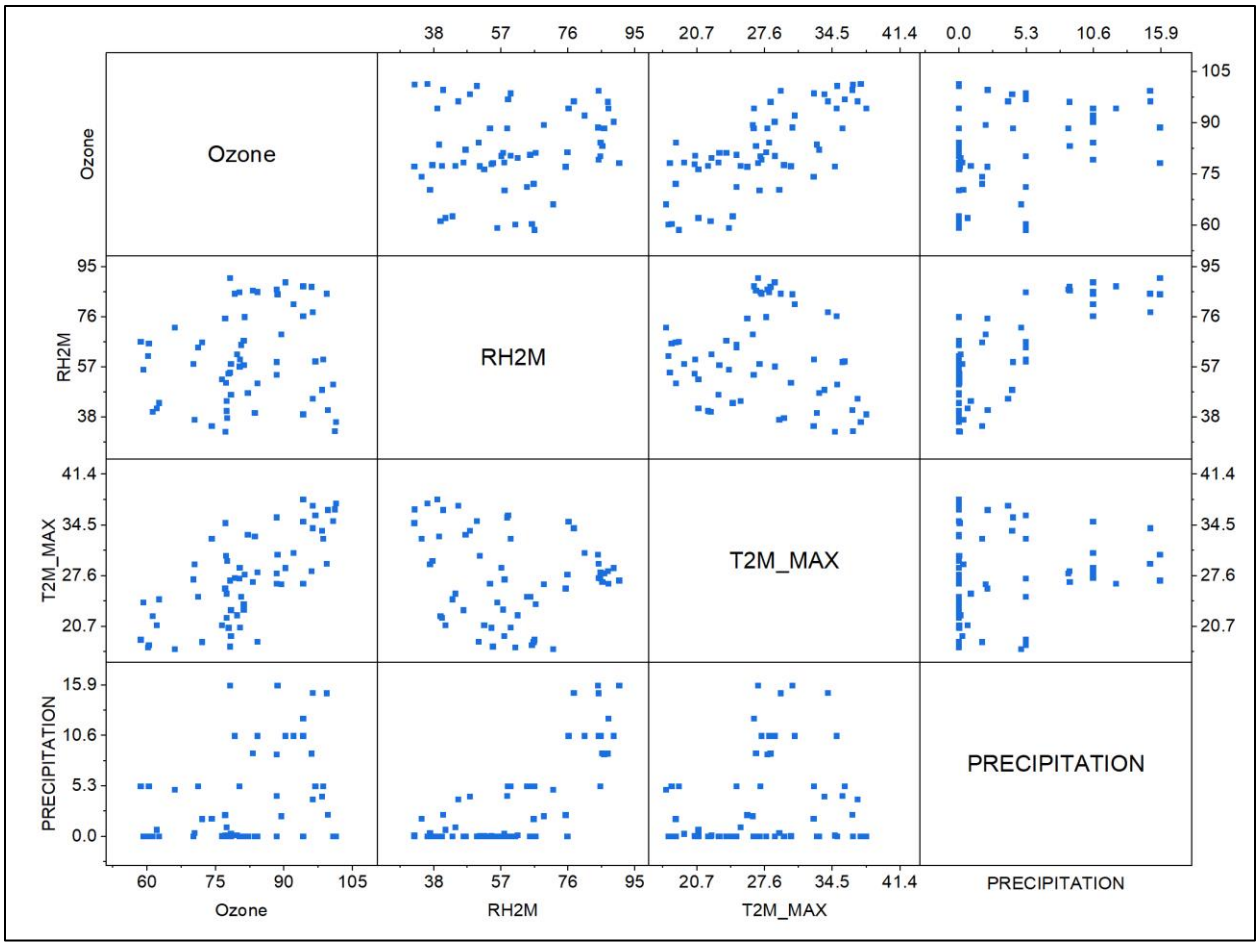

FIG 26: 4X4 Scatter Plot Matrix of Pearson Correlation for OZONE, RH2M, T2M_MAX and Precipitation in DEHRADUN

Table 14: Pearson Correlation Coefficients for FIG 26.

Pearson Correlations	Ozone	RH2M	T2M_MAX	PRECIPITATION
Ozone	1			
RH2M	**0.13258**	1		
T2M_MAX	**0.71684**	-0.16998	1	
PRECIPITATION	**0.33199**	0.77382	0.19619	1

Here in Table 14, Ozone shows a weak positive, strong positive and distinct positive linear relationship with RH2M, T2M_MAX and PRECIPITATION respectively.

HARIDWAR MONTHLY BLACK CARBON VS METEROLOGICAL PARAMETERS SCATTER PLOT MATRIX

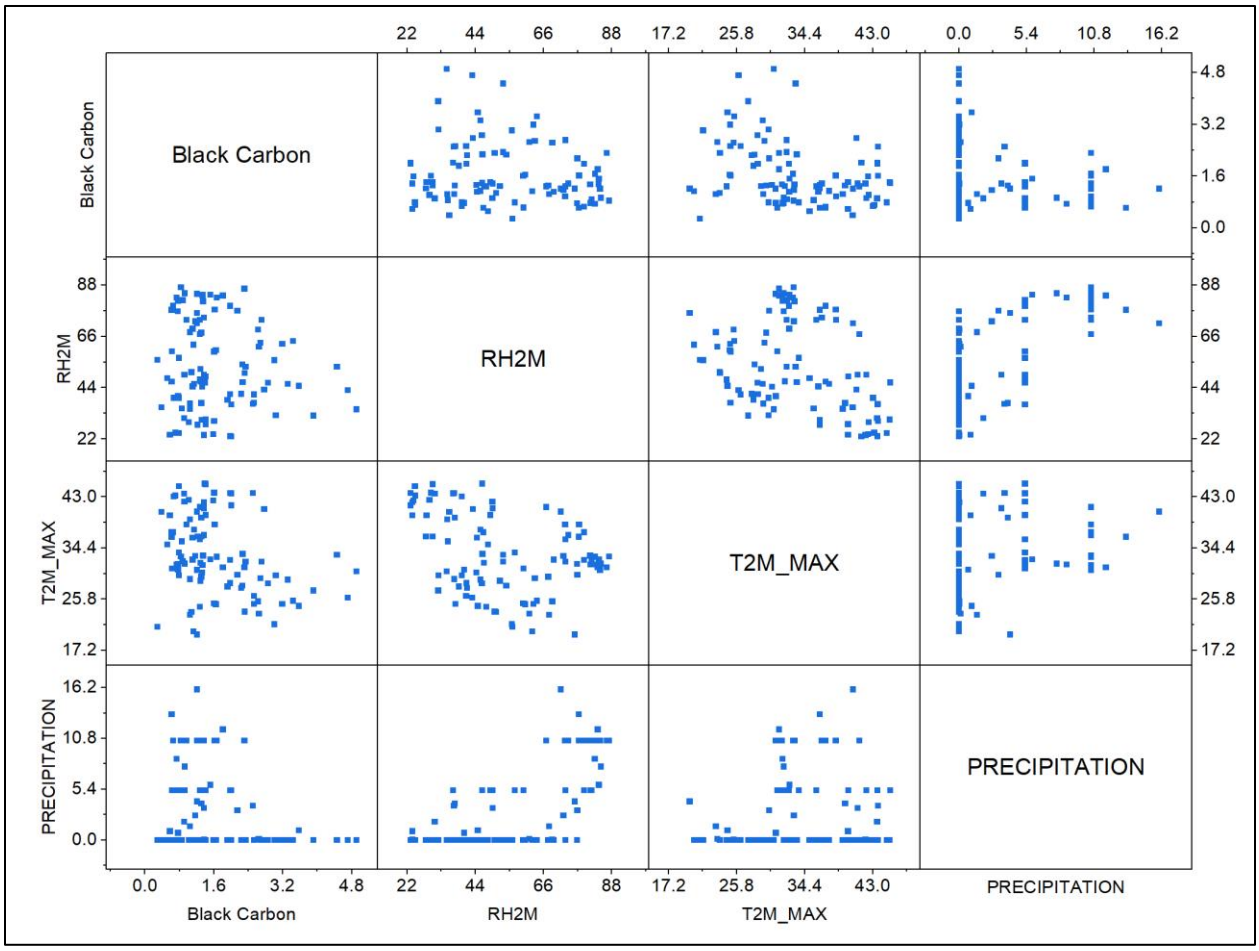

FIG 27: 4X4 Scatter Plot Matrix of Pearson Correlation for Black Carbon, RH2M, T2M_MAX and Precipitation in HARIDWAR

Table 15: Pearson Correlation Coefficients for FIG 27.

Pearson Correlations	Black Carbon	RH2M	T2M_MAX	PRECIPITATION
Black Carbon	1			
RH2M	**-0.11595**	1		
T2M_MAX	**-0.32991**	-0.35746	1	
PRECIPITATION	**-0.26224**	0.67776	0.19012	1

Here in Table 15, Black Carbon shows a weak negative, distinct negative and weak negative linear relationship with RH2M, T2M_MAX and PRECIPITATION respectively.

HARIDWAR MONTHLY CARBON MONOXIDE(CO) VS METEROLOGICAL PARAMETERS SCATTER PLOT MATRIX

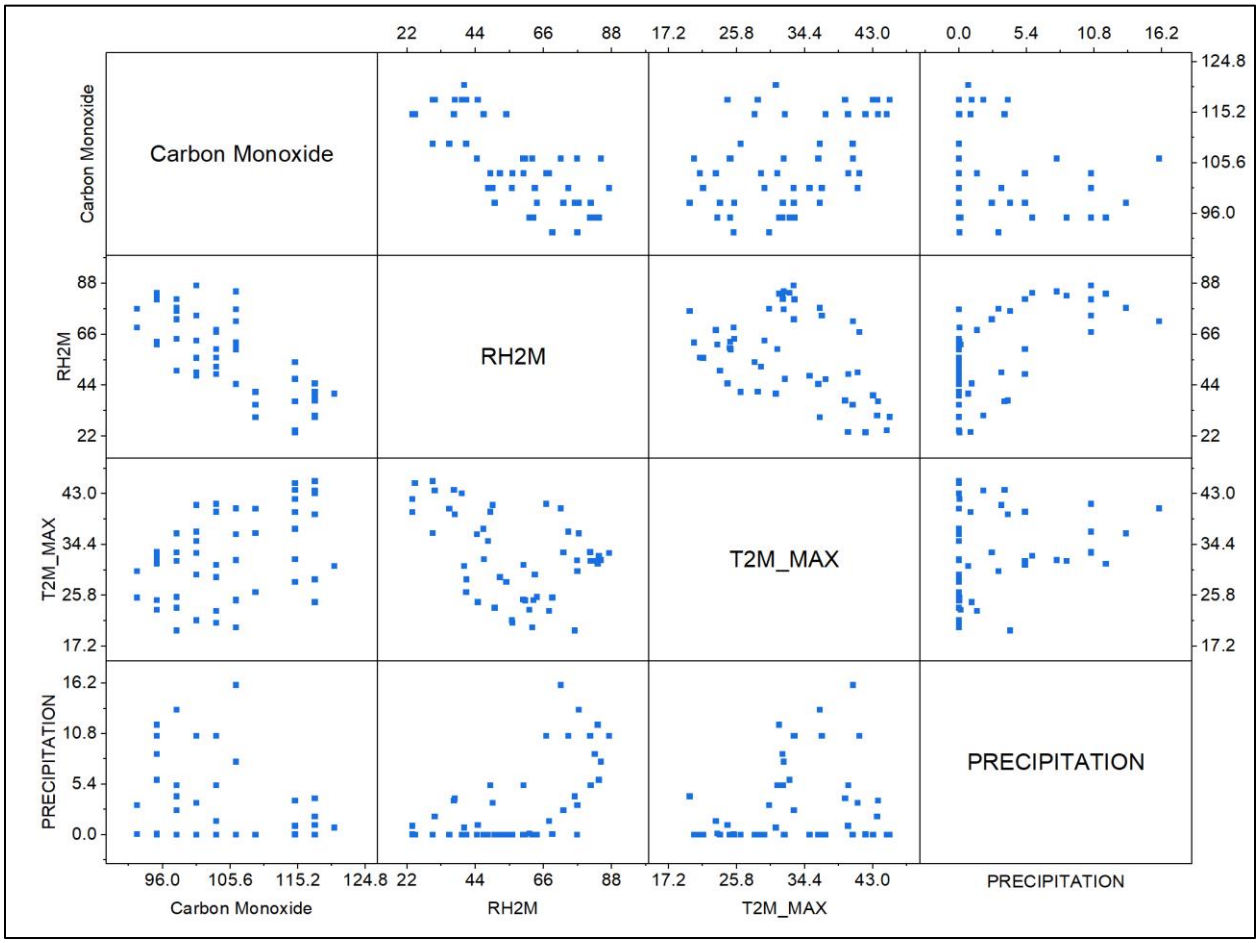

FIG 28: 4X4 Scatter Plot Matrix of Pearson Correlation for Carbon Monoxide, RH2M, T2M_MAX and Precipitation in HARIDWAR

Table 16: Pearson Correlation Coefficients for FIG 28.

Pearson Correlations	Carbon Monoxide	RH2M	T2M_MAX	PRECIPITATION
Carbon Monoxide	1			
RH2M	**-0.76595**	1		
T2M_MAX	**0.42702**	-0.42173	1	
PRECIPITATION	**-0.3522**	0.60095	0.25029	1

Here in Table 16, Carbon Monoxide shows strong negative, distinct positive and distinct negative linear relationship with RH2M, T2M_MAX and PRECIPITATION respectively.

HARIDWAR MONTHLY OZONE(O_3) VS METEROLOGICAL PARAMETERS SCATTER PLOT MATRIX

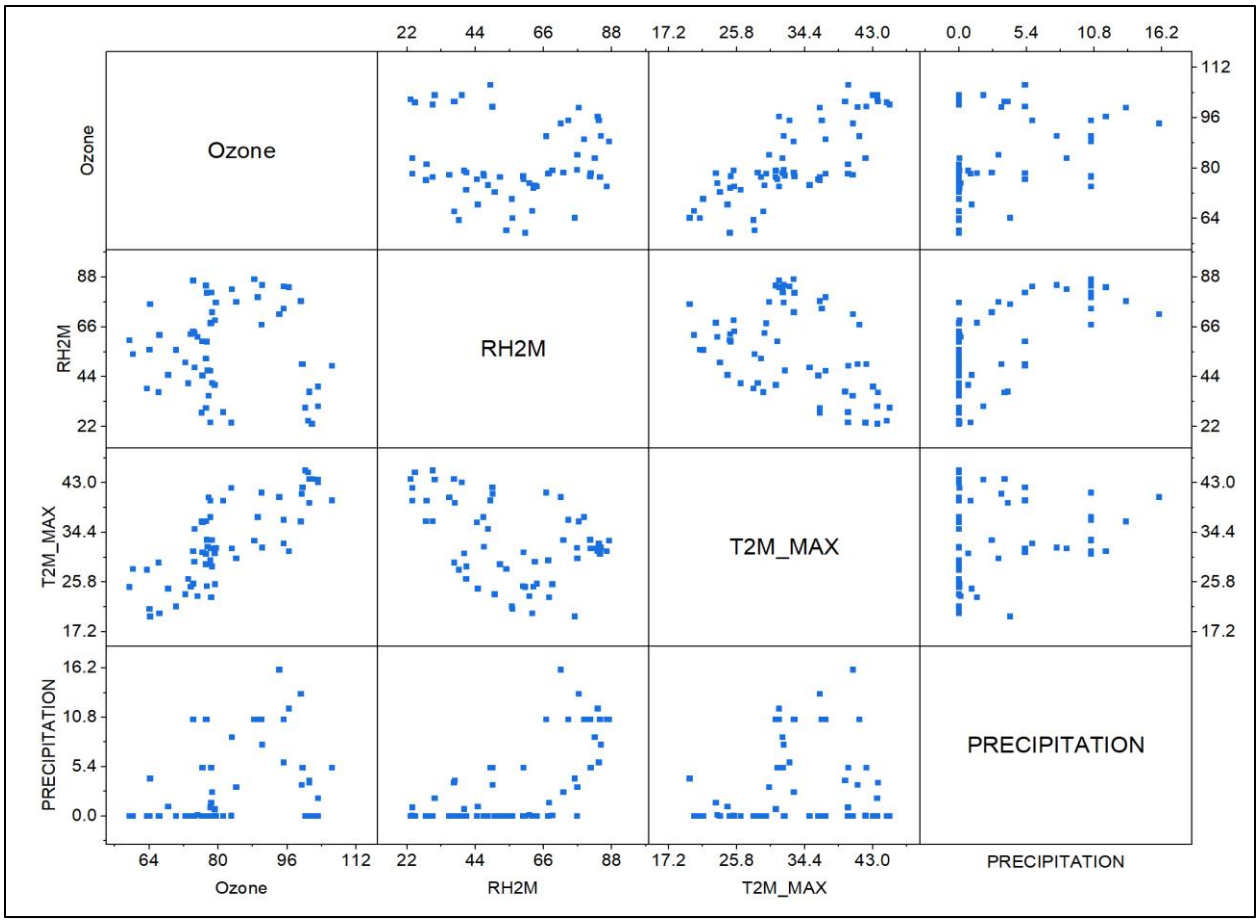

FIG 29: 4X4 Scatter Plot Matrix of Pearson Correlation for Ozone, RH2M, T2M_MAX and Precipitation in HARIDWAR

Table 17: Pearson Correlation Coefficient for FIG 29.

Pearson Correlations	Ozone	RH2M	T2M_MAX	PRECIPITATION
Ozone	1			
RH2M	-0.08567	1		
T2M_MAX	**0.77264**	-0.41808	1	
PRECIPITATION	**0.39509**	0.64937	0.20801	1

Here in Table 17, Ozone shows a strong positive and distinct positive linear relationship with T2M_MAX and PRECIPITATION respectively.

DURGAPUR MONTHLY BLACK CARBON VS METEROLOGICAL PARAMETERS SCATTER PLOT MATRIX

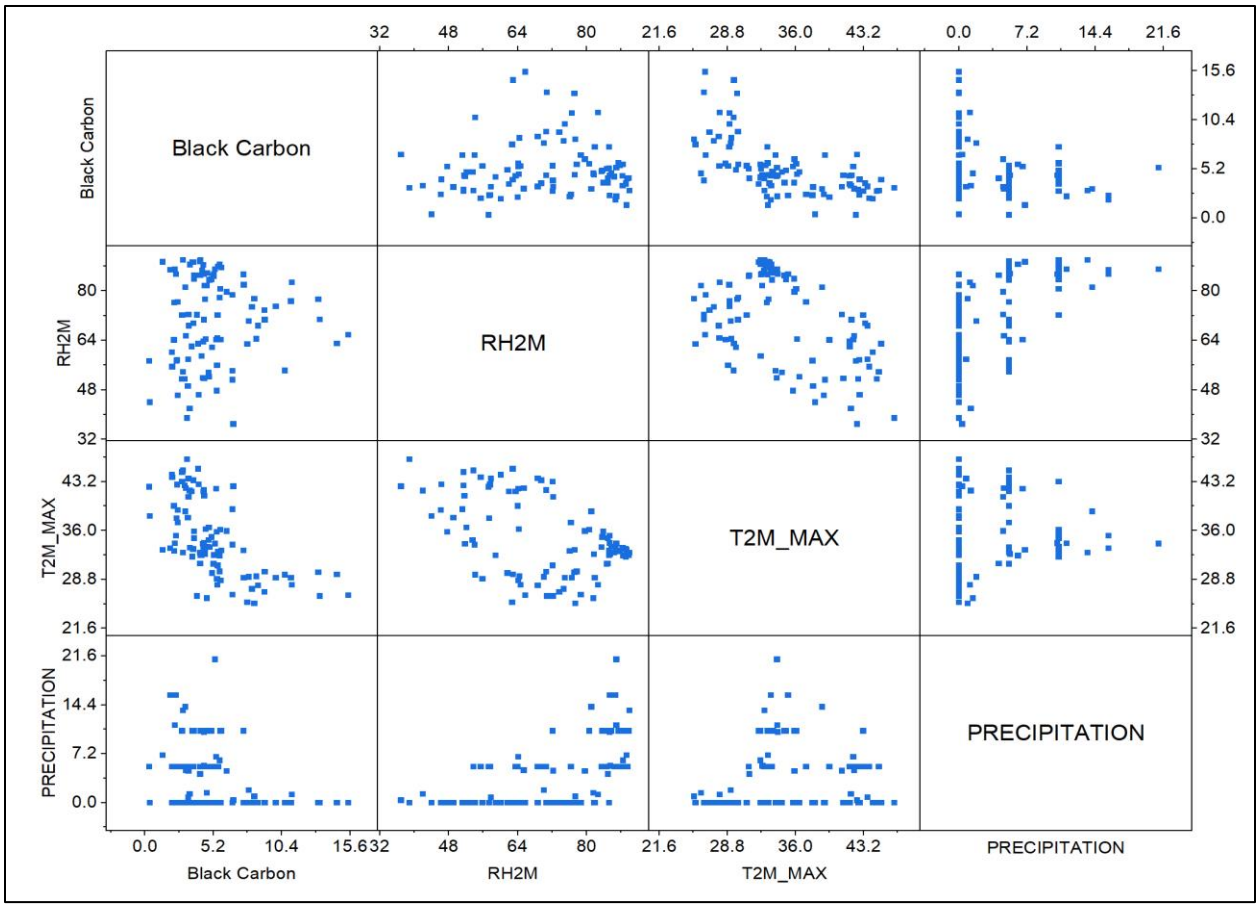

FIG 30: 4X4 Scatter Plot Matrix of Pearson Correlation for Black Carbon, RH2M, T2M_MAX and Precipitation in DURGAPUR

Table 18: Pearson Correlation Coefficients for FIG 30.

Pearson Correlations	Black Carbon	RH2M	T2M_MAX	PRECIPITATION
Black Carbon	1			
RH2M	0.06356	1		
T2M_MAX	**-0.60751**	-0.47091	1	
PRECIPITATION	**-0.33062**	0.59299	0.1289	1

Here in Table 18, Black carbon shows a distinct negative linear relationship with both T2M_MAX and PRECIPITATION.

DURGAPUR MONTHLY CARBON MONOXIDE(CO) VS METEROLOGICAL PARAMETERS SCATTER PLOT MATRIX

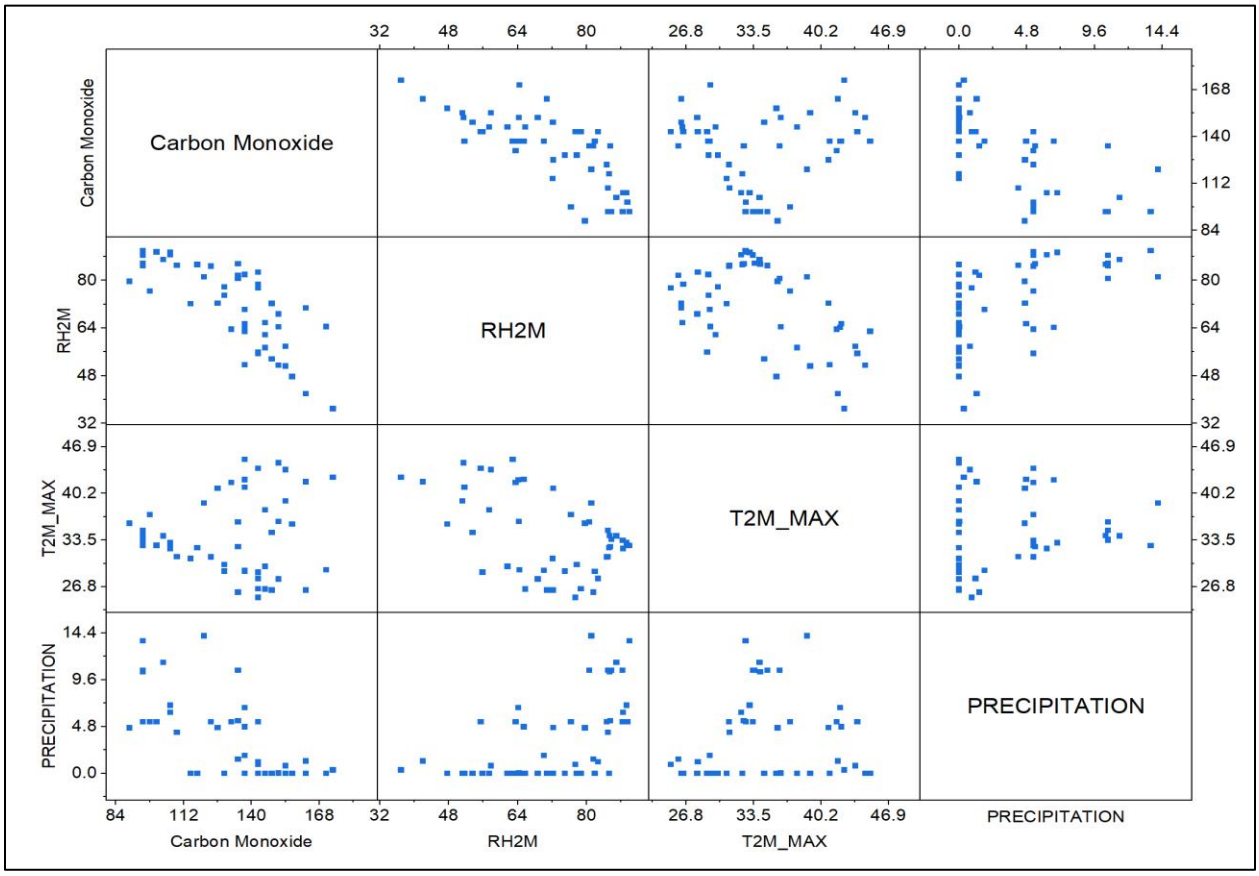

FIG 31: 4X4 Scatter Plot Matrix of Pearson Correlation for Carbon Monoxide, RH2M, T2M_MAX and Precipitation in DURGAPUR

Table 19: Pearson Correlation Coefficients for FIG 31

Pearson Correlations	Carbon Monoxide	RH2M	T2M_MAX	PRECIPITATION
Carbon Monoxide	1			
RH2M	**-0.77322**	1		
T2M_MAX	0.07329	-0.48942	1	
PRECIPITATION	**-0.70469**	0.57387	0.17159	1

Here in Table 19, Carbon Monoxide shows a strong negative linear relationship with both RH2M and PRECIPITATION.

DURGAPUR MONTHLY OZONE(O_3) VS METEROLOGICAL PARAMETERS SCATTER PLOT MATRIX

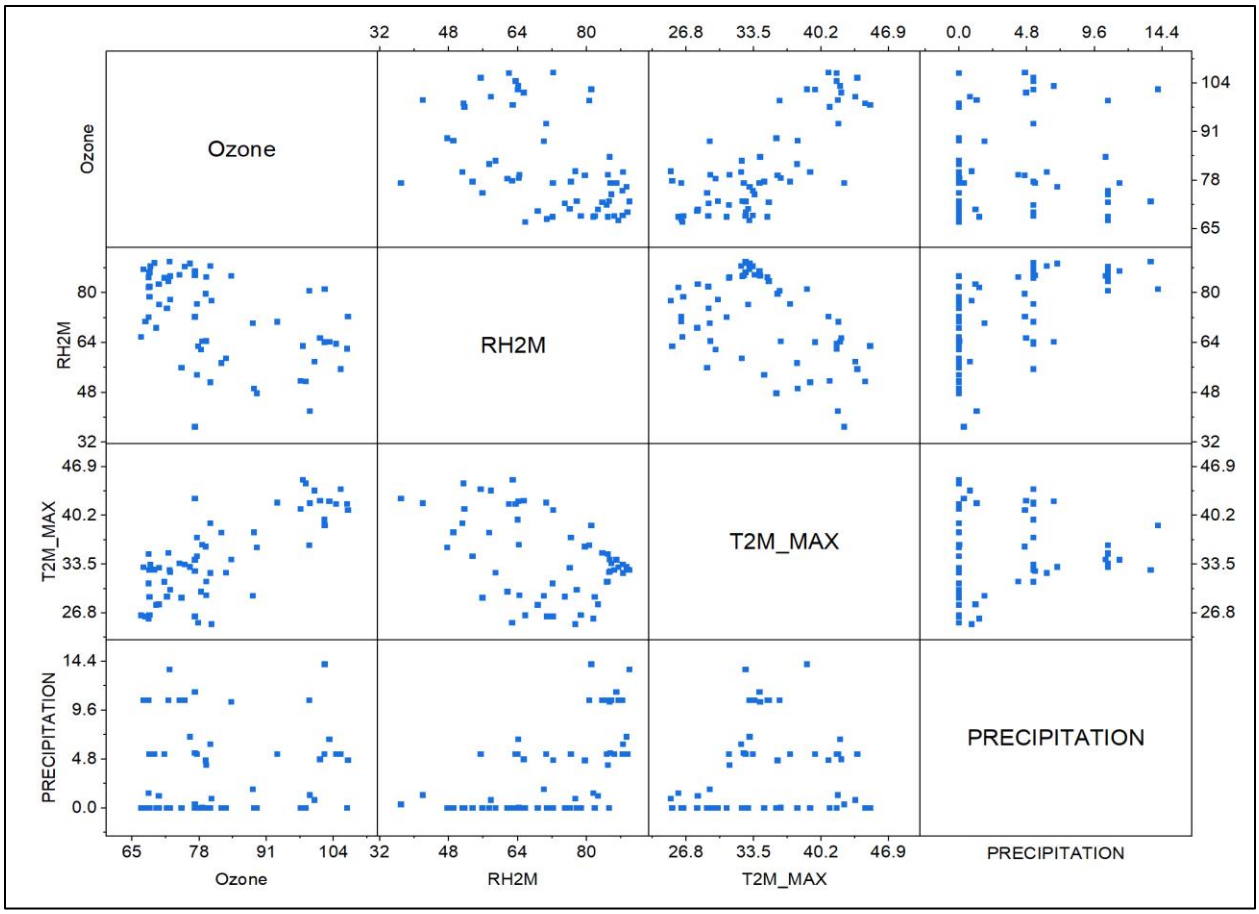

FIG 32: 4X4 Scatter Plot Matrix of Pearson Correlation for Ozone, RH2M, T2M_MAX and Precipitation in DURGAPUR

Table 20: Pearson correlation coefficients for FIG 32.

Pearson Correlations	Ozone	RH2M	T2M_MAX	PRECIPITATION
Ozone	1			
RH2M	**-0.48444**	1		
T2M_MAX	**0.77522**	-0.45347	1	
PRECIPITATION	0.05681	0.59887	0.16089	1

Here in Table 20, Ozone shows a distinct negative and strong positive linear relationship with RH2M and T2M_MAX respectively.

BURDWAN MONTHLY BLACK CARBON VS METEROLOGICAL PARAMETERS SCATTER PLOT MATRIX

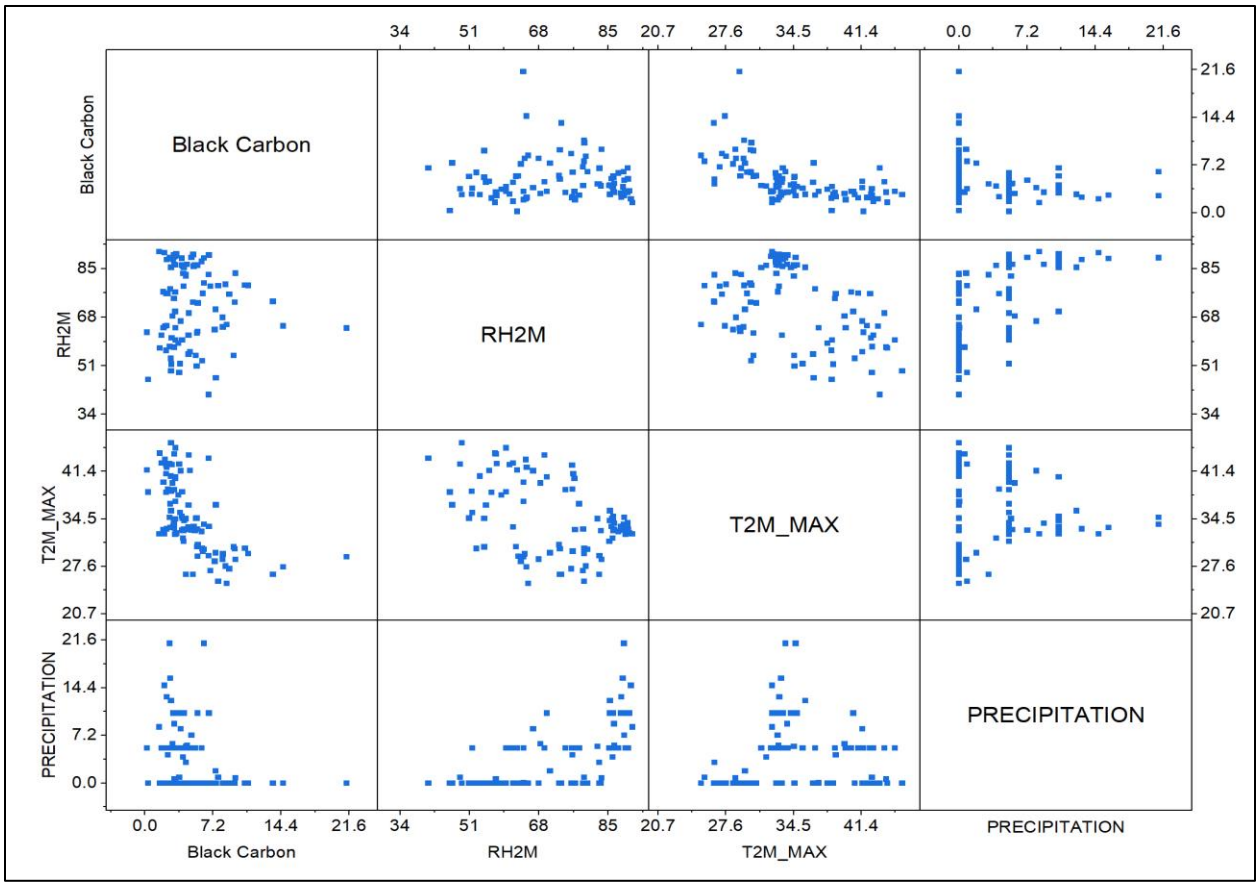

FIG 33: 4X4 Scatter Plot Matrix of Pearson Correlation for Black Carbon, RH2M, T2M_MAX and Precipitation in BURDWAN

Table 21: Pearson correlation coefficients for FIG 33.

Pearson Correlations	Black Carbon	RH2M	T2M_MAX	PRECIPITATION
Black Carbon	1			
RH2M	-0.03722	1		
T2M_MAX	**-0.59844**	-0.43837	1	
PRECIPITATION	**-0.34149**	0.62499	0.07518	1

Here in Table 21, Black Carbon shows distinct negative linear relationship with both T2M_MAX and PRECIPITATION.

BURDWAN MONTHLY CARBON MONOXIDE(CO) VS METEROLOGICAL PARAMETERS SCATTER PLOT MATRIX

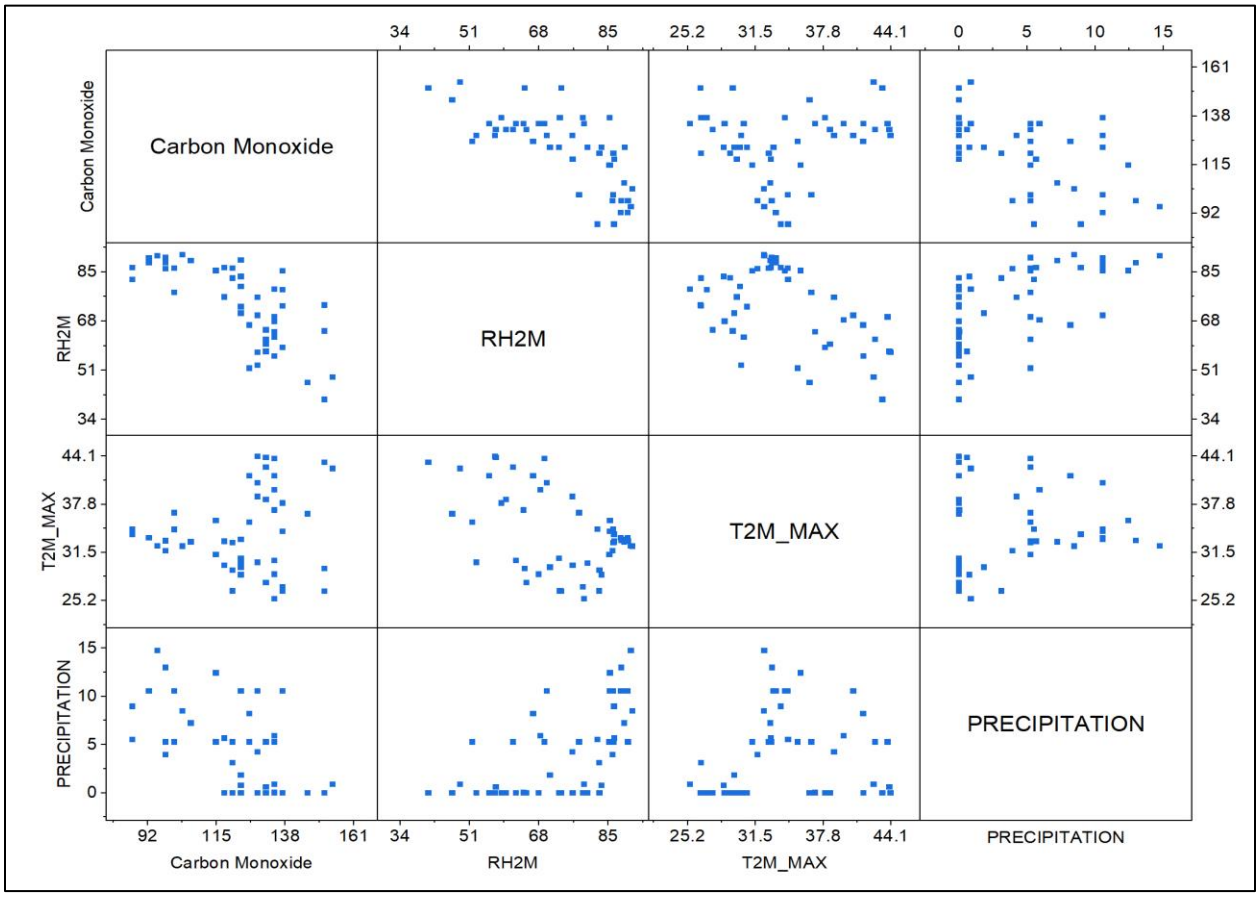

FIG 34: 4X4 Scatter Plot Matrix of Pearson Correlation for Carbon Monoxide, RH2M, T2M_MAX and Precipitation in BURDWAN

Table 22: Pearson correlation coefficients for FIG 34.

Pearson Correlations	Carbon Monoxide	RH2M	T2M_MAX	PRECIPITATION
Carbon Monoxide	1			
RH2M	**-0.72653**	1		
T2M_MAX	**0.15166**	-0.47646	1	
PRECIPITATION	**-0.63565**	0.60723	0.1403	1

Here in Table 22, Carbon Monoxide shows strong negative, weak positive and distinct negative linear relationship with RH2M, T2M_MAX and PRECIPITATION respectively.

BURDWAN MONTHLY OZONE(O_3) VS METEROLOGICAL PARAMETERS SCATTER PLOT MATRIX

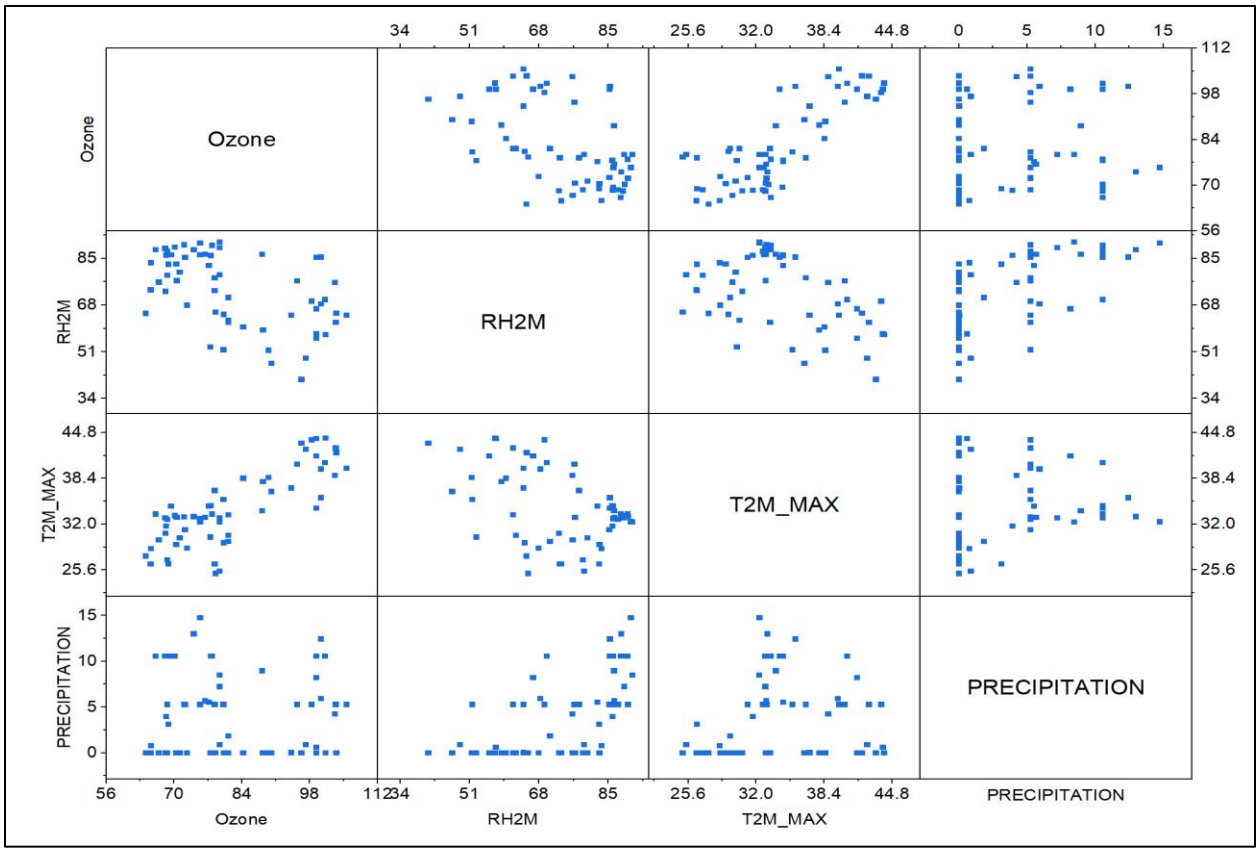

FIG 35: 4X4 Scatter Plot Matrix of Pearson Correlation for Ozone, RH2M, T2M_MAX and Precipitation in BURDWAN

Table 23: Pearson correlation coefficients for FIG 35.

Pearson Correlations	Ozone	RH2M	T2M_MAX	PRECIPITATION
Ozone	1			
RH2M	**-0.50764**	1		
T2M_MAX	**0.81177**	-0.44463	1	
PRECIPITATION	0.01788	0.62977	0.12107	1

Here in Table 23, Ozone shows a distinct negative and strong positive linear relationship with RH2M and T2M_MAX respectively.

KOLKATA MONTHLY BLACK CARBON VS METEROLOGICAL PARAMETERS SCATTER PLOT MATRIX.

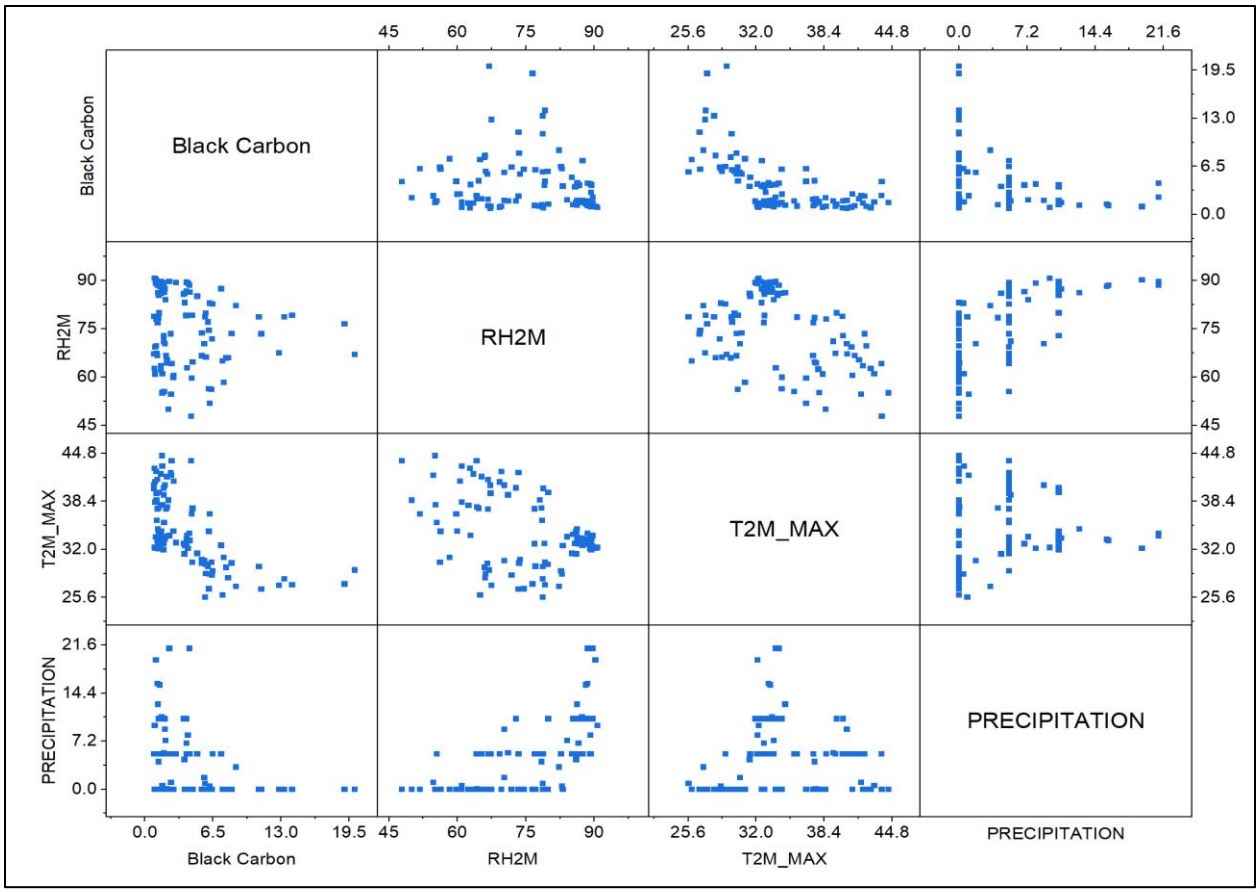

FIG 36: 4X4 Scatter Plot Matrix of Pearson Correlation for Black Carbon, RH2M, T2M_MAX and Precipitation in KOLKATA

Table 24: Pearson correlation coefficients for FIG 36.

Pearson Correlations	Black Carbon	RH2M	T2M_MAX	PRECIPITATION
Black Carbon	1			
RH2M	-0.09278	1		
T2M_MAX	**-0.62601**	-0.40914	1	
PRECIPITATION	**-0.41407**	0.65988	0.06773	1

Here in Table 24, Black Carbon shows distinct negative linear relationship with both T2M_MAX and PRECIPITATION.

KOLKATA MONTHLY CARBON MONOXIDE(CO) VS METEROLOGICAL PARAMETERS SCATTER PLOT MATRIX

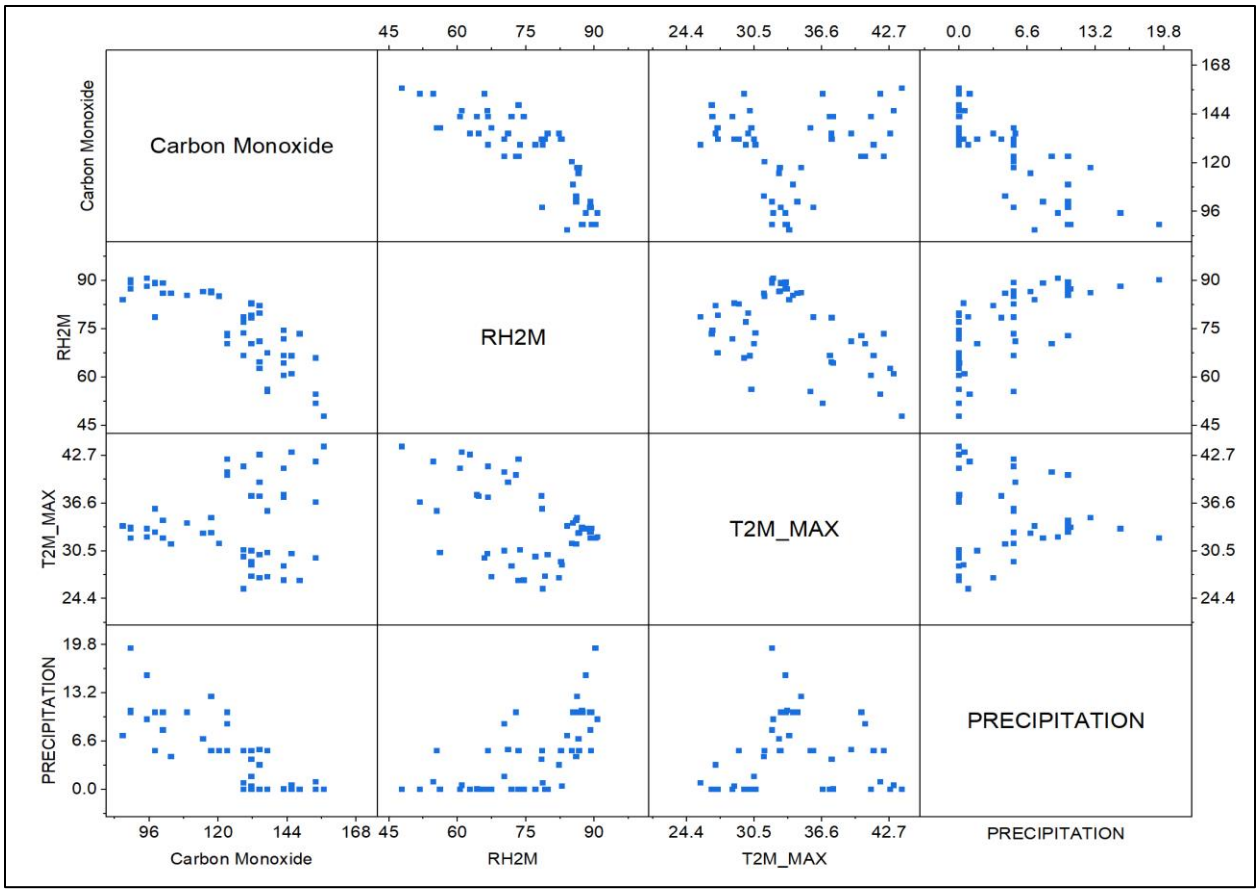

FIG 37: 4X4 Scatter Plot Matrix of Pearson Correlation for Carbon Monoxide, RH2M, T2M_MAX and Precipitation in KOLKATA

Table 25: Pearson correlation coefficients for FIG 37.

Pearson Correlations	Carbon Monoxide	RH2M	T2M_MAX	PRECIPITATION
Carbon Monoxide	1			
RH2M	**-0.81881**	1		
T2M_MAX	**0.11431**	-0.45244	1	
PRECIPITATION	**-0.80803**	0.65225	0.08617	1

Here in Table 25, Carbon Monoxide shows strong negative, weak positive and strong negative linear relationship with RH2M, T2M_MAX and PRECIPITATION respectively.

KOLKATA MONTHLY OZONE(O_3) VS METEROLOGICAL PARAMETERS SCATTER PLOT MATRIX

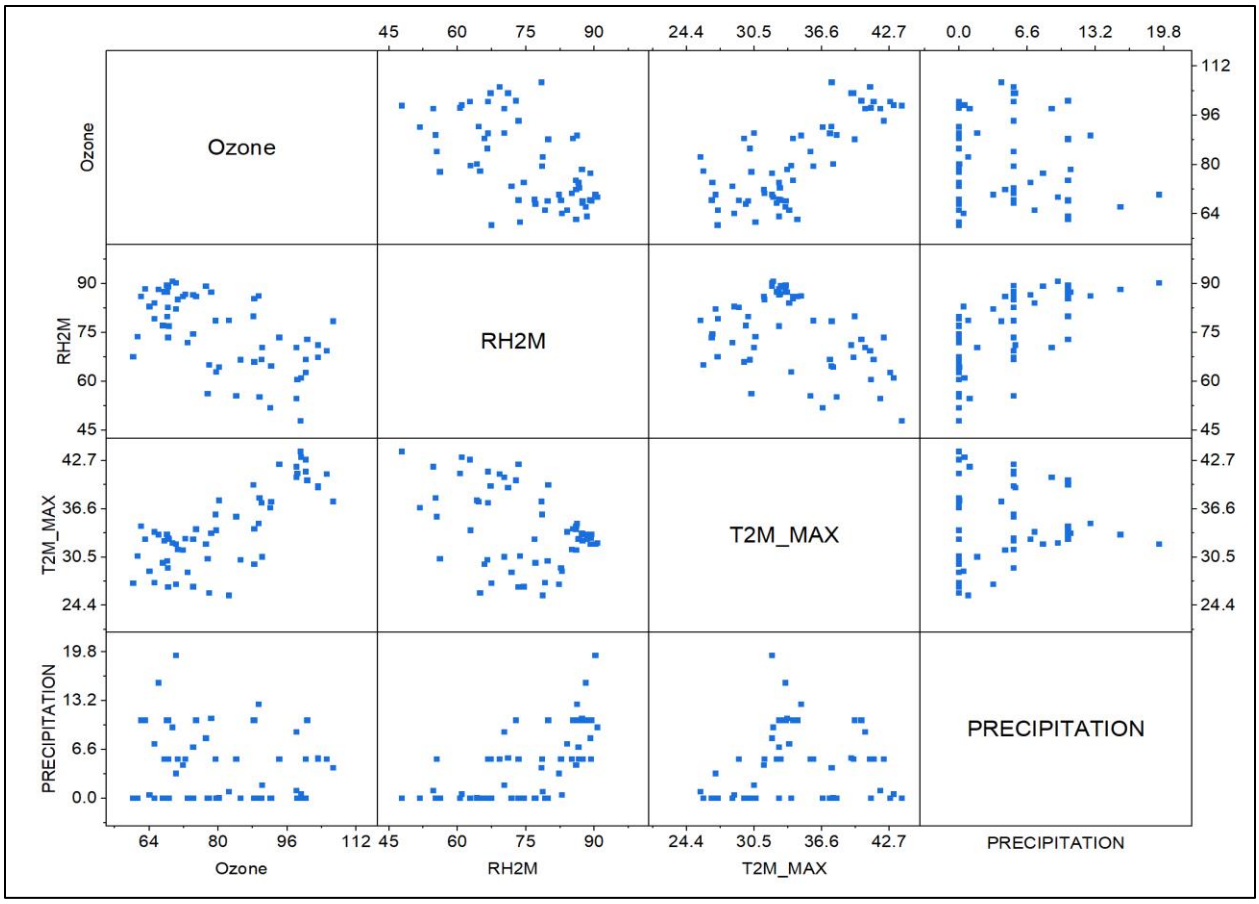

FIG 38: 4X4 Scatter Plot Matrix of Pearson Correlation for Ozone, RH2M, T2M_MAX and Precipitation in KOLKATA

Table 26: Pearson correlation coefficients for FIG 38.

Pearson Correlations	Ozone	RH2M	T2M_MAX	PRECIPITATION
Ozone	1			
RH2M	**-0.59726**	1		
T2M_MAX	**0.75711**	-0.41253	1	
PRECIPITATION	**-0.14268**	0.6645	0.11684	1

Here in Table 26, Ozone shows distinct negative, strong positive and weak negative linear relationship with RH2M, T2M_MAX and PRECIPITATION respectively.

DELHI MONTHLY BLACK CARBON VS METEROLOGICAL PARAMETERS SCATTER PLOT MATRIX.

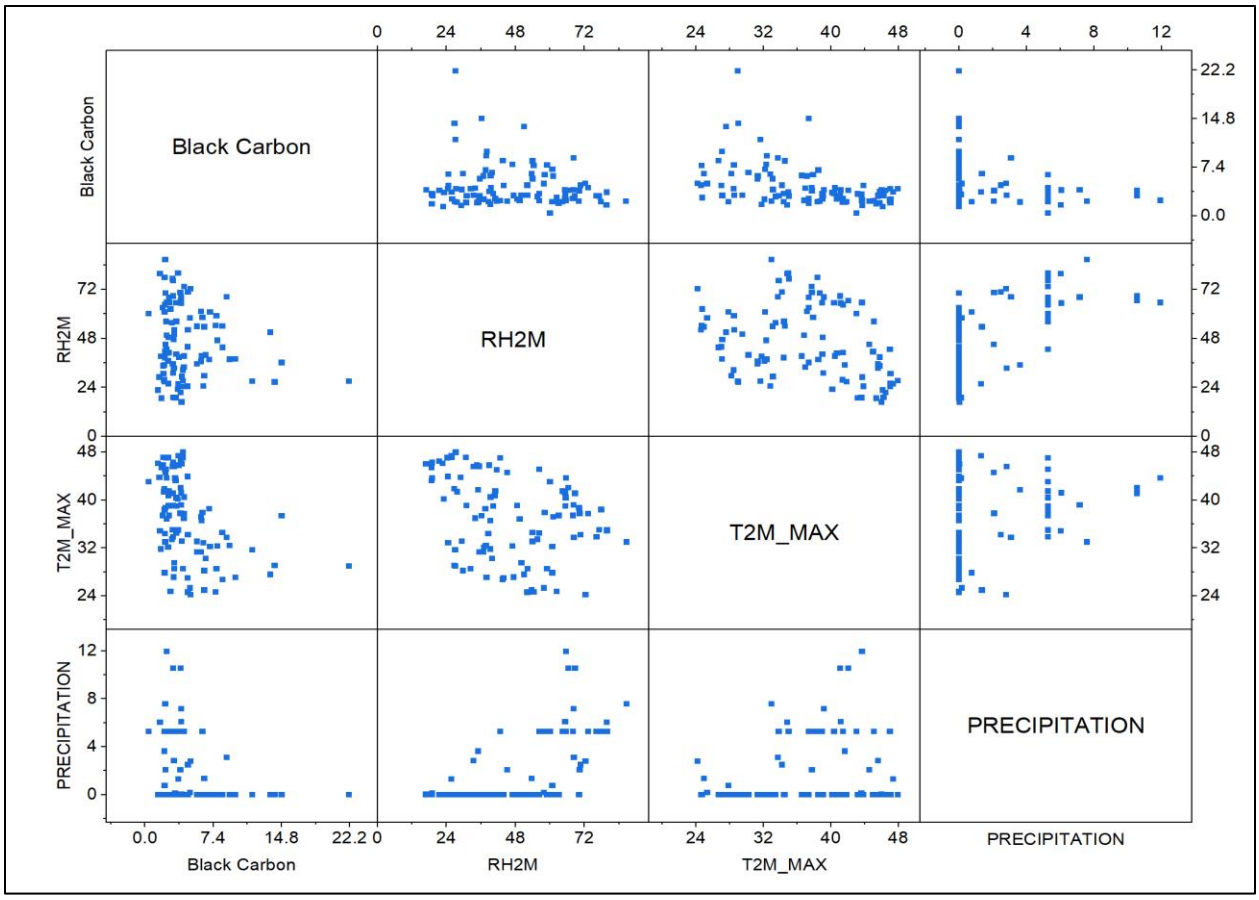

FIG 39: 4X4 Scatter Plot Matrix of Pearson Correlation for Black Carbon, RH2M, T2M_MAX and Precipitation in DELHI

Table 27: Pearson correlation coefficients for FIG 39.

Pearson Correlations	Black Carbon	RH2M	T2M_MAX	PRECIPITATION
Black Carbon	1			
RH2M	**-0.14272**	1		
T2M_MAX	**-0.44906**	-0.31167	1	
PRECIPITATION	**-0.23534**	0.64063	0.19073	1

Here in Table 27, Black Carbon shows weak negative, distinct negative and weak negative linear relationship with RH2M, T2M_MAX and PRECIPITATION respectively.

DELHI MONTHLY CARBON MONOXIDE(CO) VS METEROLOGICAL PARAMETERS SCATTER PLOT MATRIX

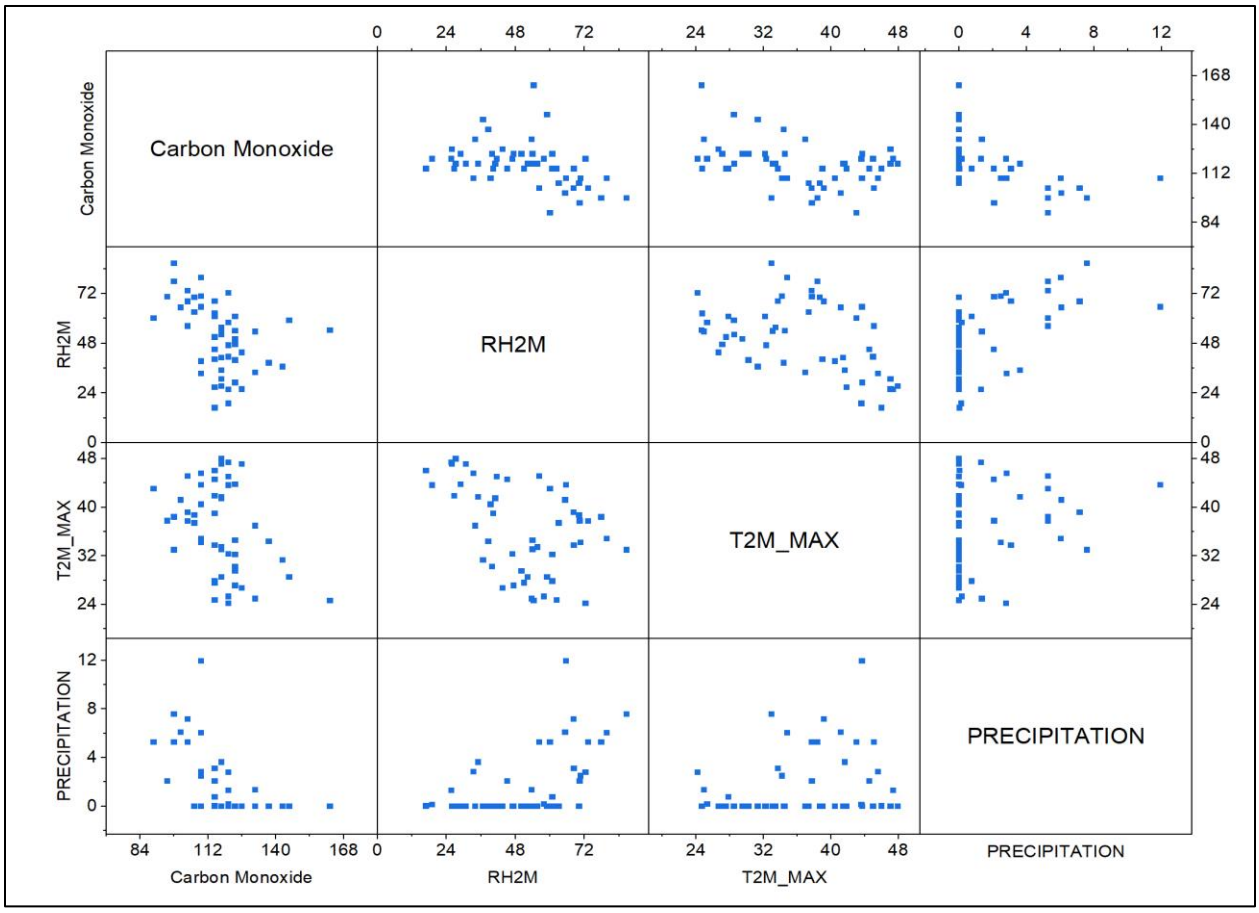

FIG 40: 4X4 Scatter Plot Matrix of Pearson Correlation for Carbon Monoxide, RH2M, T2M_MAX and Precipitation in DELHI

Table 28: Pearson correlation coefficients for FIG 40.

Pearson Correlations	Carbon Monoxide	RH2M	T2M_MAX	PRECIPITATION
Carbon Monoxide	1			
RH2M	**-0.39923**	1		
T2M_MAX	**-0.39111**	-0.43923	1	
PRECIPITATION	**-0.55075**	0.55328	0.21951	1

Here in Table 28, Carbon Monoxide shows distinct negative linear relationship with all three meteorological parameters i.e., RH2M, T2M_MAX and PRECIPITATION.

DELHI MONTHLY OZONE(O_3) VS METEROLOGICAL PARAMETERS SCATTER PLOT MATRIX

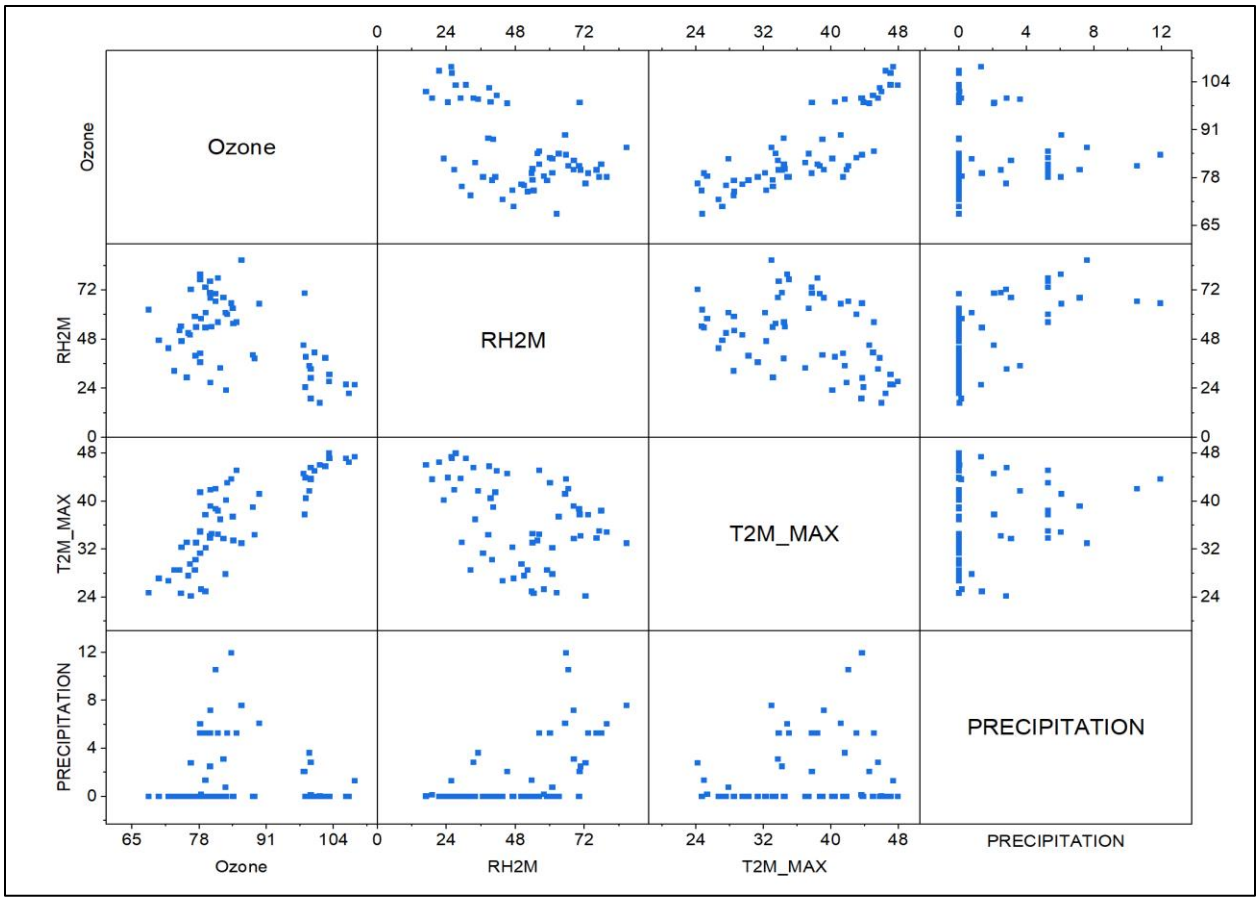

FIG 41: 4X4 Scatter Plot Matrix of Pearson Correlation for Ozone, RH2M, T2M_MAX and Precipitation in DELHI

Table 29: Pearson correlation coefficients for FIG 41.

Pearson Correlations	Ozone	RH2M	T2M_MAX	PRECIPITATION
Ozone	1			
RH2M	**-0.50841**	1		
T2M_MAX	**0.81797**	-0.42133	1	
PRECIPITATION	-0.07081	0.59244	0.18147	1

Here in Table 29, Ozone shows distinct negative and strong positive linear relationship with RH2M and PRECIPITATION respectively.

MOHALI MONTHLY BLACK CARBON VS METEROLOGICAL PARAMETERS SCATTER PLOT MATRIX.

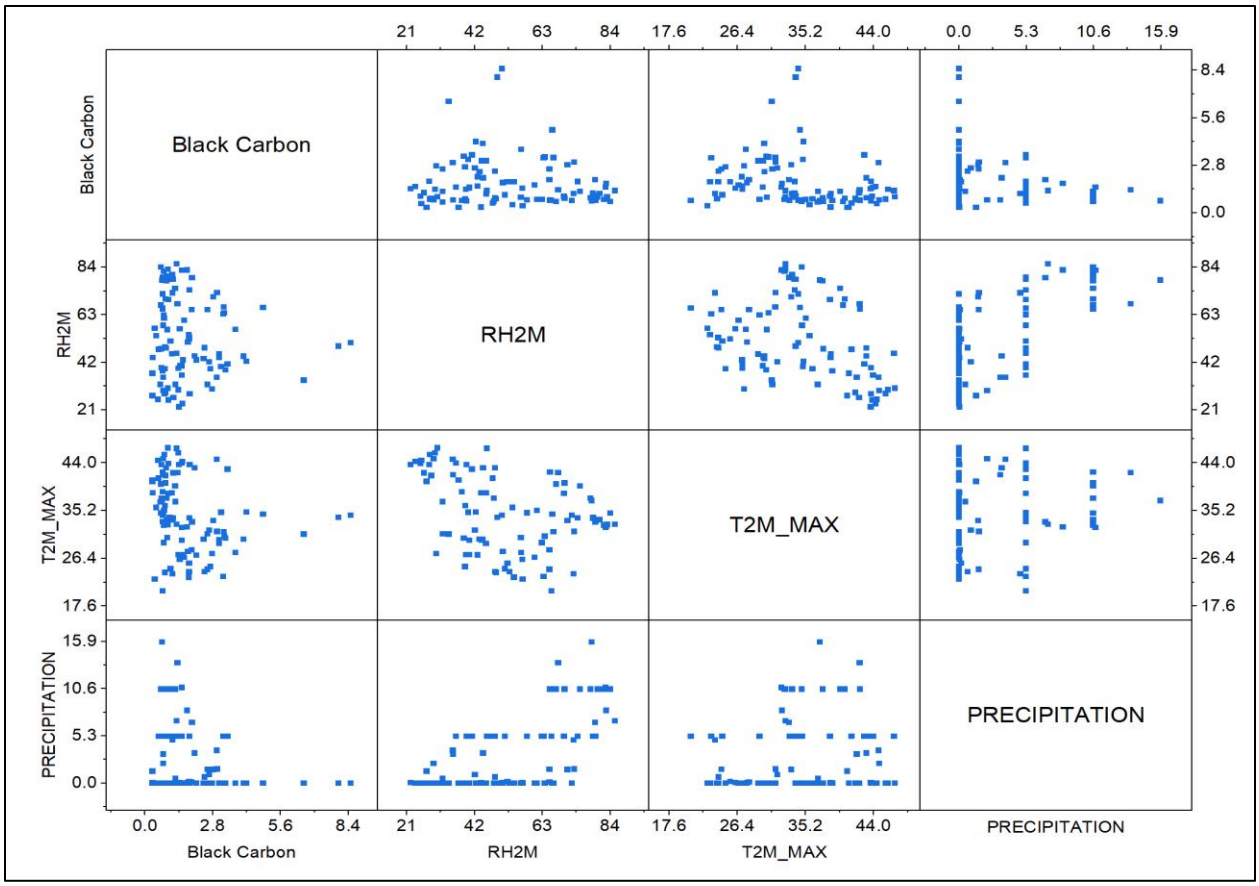

FIG 42: 4X4 Scatter Plot Matrix of Pearson Correlation for Black Carbon, RH2M, T2M_MAX and Precipitation in MOHALI

Table 30: Pearson correlation coefficients for FIG 42.

Pearson Correlations	Black Carbon	RH2M	T2M_MAX	PRECIPITATION
Black Carbon	1			
RH2M	-0.08611	1		
T2M_MAX	**-0.22912**	-0.33369	1	
PRECIPITATION	**-0.29252**	0.67013	0.17659	1

Here in Table 30, Black Carbon shows weak negative linear relationship with both T2M_MAX and PRECIPITATION respectively.

MOHALI MONTHLY CARBON MONOXIDE(CO) VS METEROLOGICAL PARAMETERS SCATTER PLOT MATRIX

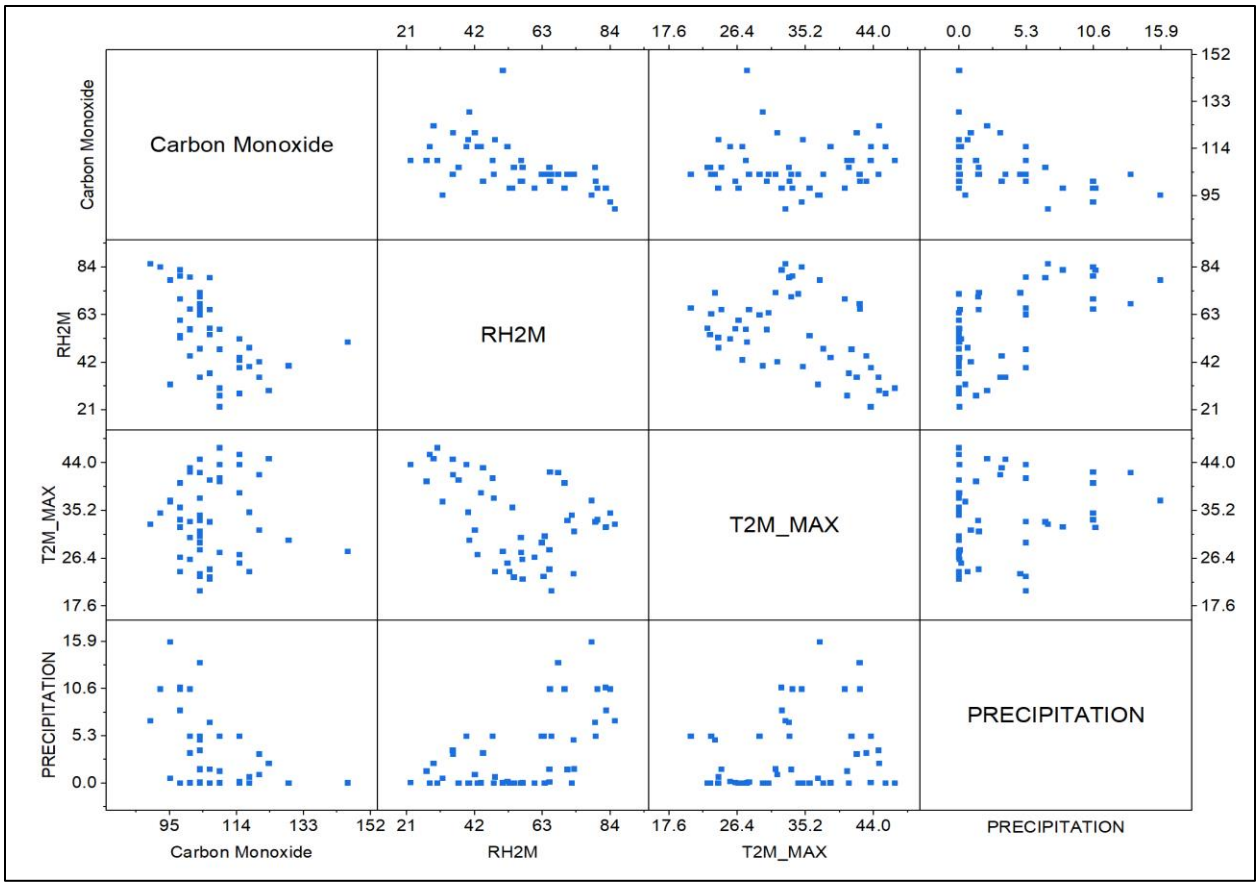

FIG 43: 4X4 Scatter Plot Matrix of Pearson Correlation for Carbon Monoxide, RH2M, T2M_MAX and Precipitation in MOHALI

Table 31: Pearson correlation coefficients for FIG 43.

Pearson Correlations	Carbon Monoxide	RH2M	T2M_MAX	PRECIPITATION
Carbon Monoxide	1			
RH2M	**-0.55014**	1		
T2M_MAX	0.02827	-0.41913	1	
PRECIPITATION	**-0.42587**	0.59837	0.20978	1

Here in Table 31, Carbon Monoxide shows distinct negative linear relationship with both RH2M and PRECIPITATION.

MOHALI MONTHLY OZONE(O_3) VS METEROLOGICAL PARAMETERS SCATTER PLOT MATRIX

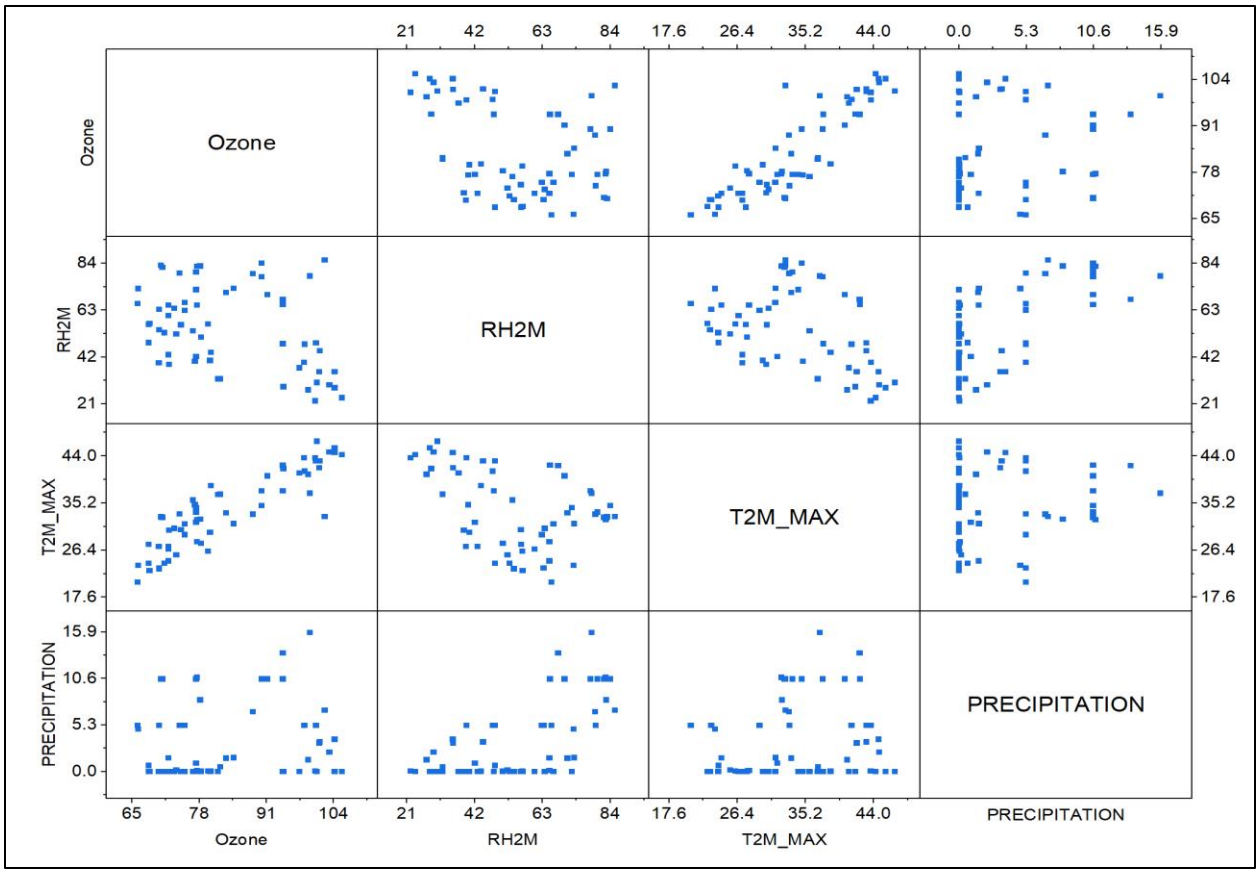

FIG 41: 4X4 Scatter Plot Matrix of Pearson Correlation for Ozone, RH2M, T2M_MAX and Precipitation in MOHALI

Table 32: Pearson correlation coefficients for FIG 44.

Pearson Correlations	Ozone	RH2M	T2M_MAX	PRECIPITATION
Ozone	1			
RH2M	**-0.37392**	1		
T2M_MAX	**0.88858**	-0.40935	1	
PRECIPITATION	**0.17747**	0.65061	0.17545	1

Here in Table 32, Ozone shows distinct negative, strong positive and weak negative linear relationship with RH2M, T2M_MAX and PRECIPITATION respectively.

For **Extreme Weather events**, we have taken the meteorological parameters for the **top 10** percentile and their respective pollutant concentration present at that time and ran the Pearson correlation coefficient and came up with the following numbers:

Table 33: PCC between Black Carbon and top 10 percentile meteorological parameters.

Pearson correlations	**Black Carbon**
Black Carbon	1
RH2M	-0.12693
T2M_MAX	0.12571
PRECIPITATION	0.21431

Table 34: PCC between Carbon Monoxide and top 10 percentile meteorological parameters.

Pearson correlations	**Carbon Monoxide**
Carbon Monoxide	1
RH2M	-0.24215
T2M_MAX	-0.32243
PRECIPITATION	0.00404

Table 35: PCC between Ozone and top 10 percentile meteorological parameters.

Pearson correlations	**Ozone**
Ozone	1
RH2M	-0.14927
T2M_MAX	0.72886
PRECIPITATION	0.16102

Here, from *table 33* it is evident that in the extreme weather cases (for top 10 percentile) of meteorological parameters Black Carbon has **weak positive relationship** with *T2M_MAX* (*Max temperature)* and *precipitation* whereas it showed **weak negative relationship** with *Relative humidity*.

In *table 34* we can see that Carbon monoxide showed **weak** and **distinct negative relationship** with *Relative Humidity* and *Max. Temperature* respectively.

And finally in *table 35*, Ozone showed **negative relationship** with *Relative humidity,* **strong positive relationship** with *max. temperature* and finally **weak positive relationship** with *Precipitation.*

6.3 Random Forest Regression

For regression tasks, a machine learning approach called random forest regression is employed. It is an expansion of the mostly-used-for-classification random forest algorithm.

In random forest regression, the algorithm predicts continuous values as opposed to classes as in classification. Throughout the training stage, it accomplishes this by creating a large number of decision trees. Every tree in the forest makes an independent prediction, and the overall forecast is the mean (or occasionally the median) of all the projections made by each individual tree predictions also known as Bootstrap aggregation of a group.

1. **Building Trees:** A decision tree "forest" is produced by the algorithm. Every tree is built using a randomly chosen subset of the input features and trained on a distinct subset of the training data.

2. Predictions: Based on the input attributes, every tree in the forest independently predicts an outcome for a new data point. The final prediction is then calculated by averaging (or aggregating via another technique, like taking the median) all of the trees' projections.

3. Managing Overfitting: By employing random subsets of each tree's characteristics and data, random forest regression works to reduce overfitting. Furthermore, compared to individual decision trees, the final prediction is typically more stable and less susceptible to noise in the data because it is the average (or median) of numerous forecasts.

Each decision tree has a significant variance, but when we aggregate them all at once, the variance that results shrinks because each decision tree is perfectly trained on that specific sample data. As a result, the outcome is dependent on numerous decision trees rather than just one. When dealing with a classification challenge, the majority voting classifier is used to determine the final output. The mean of all the outputs is the final result in a regression problem. This section is known as Aggregation.

The Random Forest Code in python was used to check the model consisting of Black carbon, CO, Ozone and **T2M_MAX**. An example of Code sequence has been furnished after this segment APPENDIX C.

Table 36: Comparison of Predicted values with Real values of T2M_MAX by RFR model

Predicted Values	Real Values
46.429	47.05
46.39613333	44.48
44.38466667	44.18
46.87686667	47.37
45.90286667	46.03
46.70253333	45.82
44.51126667	45.08
46.783	45.83

Mean squared error using RFR: 0.796121
Mean absolute error using RFR: 0.72079
Weightage of Black carbon, CO, Ozone for the model came out to be 0.070601, 0.055143 and 0.87425.

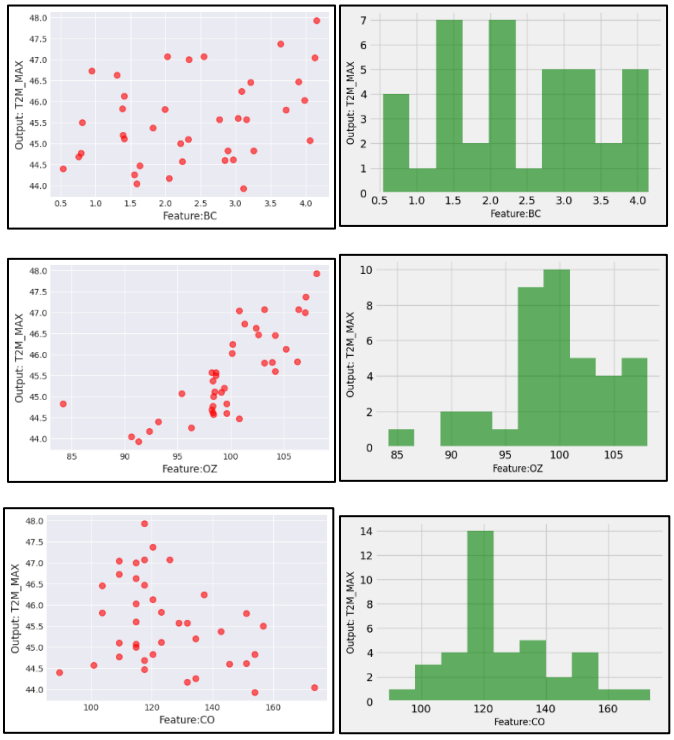

FIG 42 (a to f) L to R Plots between T2M_MAX vs pollutants.

Similarly, the code was run again for the model of Black carbon, CO, Ozone and **RH2M**

Table 37: Comparison of Predicted values with Real values of RH2M by RFR model

Predicted Values	Real Values
89.38794595	90.25
90.27167568	88.56
89.28221622	88.44
89.60751351	90.75
90.22935135	89.69
89.39054054	89.44
89.26902703	89.12
88.70951351	89.5

Mean squared error using RFR: 0.8284997
Mean absolute error using RFR: 0.7608445
Weightage of Black Carbon, CO, Ozone for this model came out to be 0.400337, 0.329723, 0.269940.

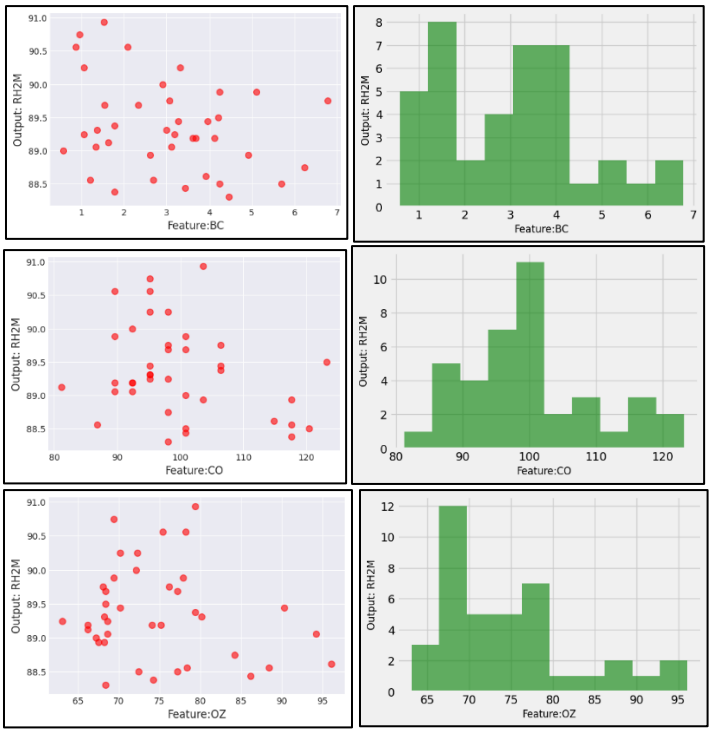

FIG 43 (a to f) L to R Plots between RH2M vs pollutants.

Finally, the code was run again for the model of Black carbon, CO, Ozone and **PRECIPITATION**

Table 38: Comparison of Predicted values with Real values of PRECIPITATION by RFR model

Predicted Values	Real Values
14.20882353	15.82
10.74294118	10.55
11.28882353	10.55
12.87470588	16.01
11.94705882	13.5
12.01	12.99
12.48529412	10.55
14.00529412	13.35

Mean squared error using RFR: 2.569480
Mean absolute error using RFR: 1.350220
Weightage of Black Carbon, CO, Ozone for this model came out to be 0.395870, 0.067778, 0.536352

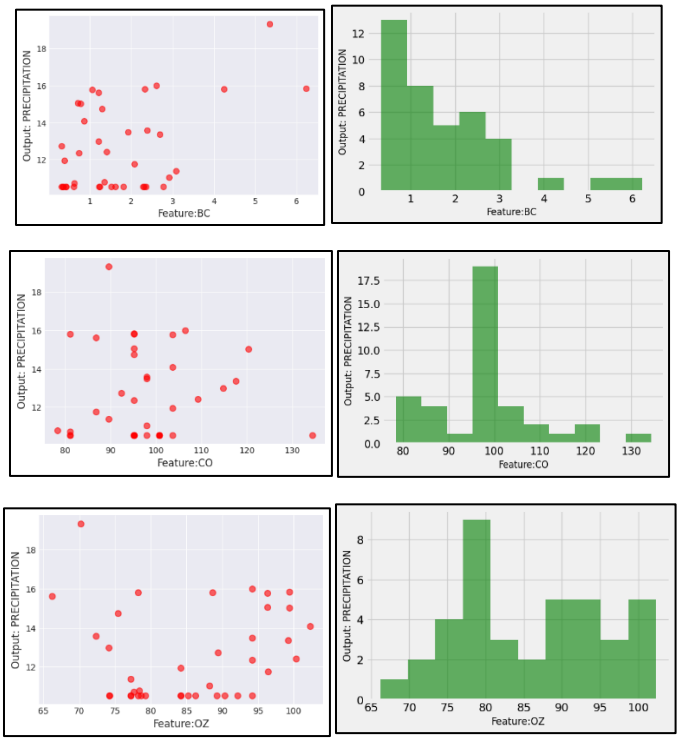

FIG 44 (a to f) L to R Plots between PRECIPITATION vs pollutants.

The artificial neural node model with an estimators value of 530 was trained in Random Forest regression for the Extreme weather cases (i.e., the top 10 percentile of the meteorological parameters). This model demonstrated the lowest mean squared error and lowest mean absolute error, with values ranging from 0.7 to 2.9.

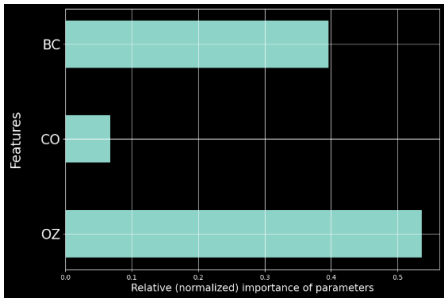

FIG 45: Relative importance of the factors in determining Precipitation by RFR model

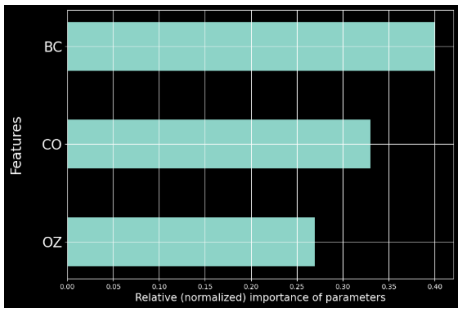

FIG 46: Relative importance of the factors in determining RH2M by RFR model

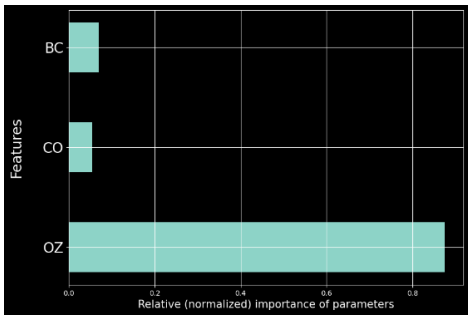

FIG 47: Relative importance of the factors in determining T2M_MAX by RFR model

From the above models, it can be observed that the model involving T2M_MAX and RH2M are efficient in predicting the corresponding pollutant parameters to a great extent as the mean absolute error and mean squared error are very low in these two cases. Therefore, it can be stated that Black Carbon, CO and Ozone can influence the RH2M. Though the reason behind it needs to be investigated further. Whereas in case of PRECIPITATION the model is not an efficient one for predicting the pollutant as the error terms are high. Hence it can be inferred that the pollutant parameters may not influence the Precipitation pattern.

6.4 DISCUSSIONS

6.4.1 Black Carbon and Meteorological parameters

By comparing the result of all the 27 scatter Plot matrix, out of 9 (nine) locations as earlier mentioned in the study area overview, in between *Black Carbon concentration* and *Relative humidity (RH2M),* it showed **weak negative correlation** in **4 (four locations)** and **distinct negative correlation in 1 (one) location**. Between *Black Carbon concentration* and *Max. Temperature (T2M_MAX),* it showed **distinct negative correlation in 5 (five) locations** and **weak negative correlation in 1 (one) location**. Between *Black Carbon concentration* and *Precipitation*, it showed **weak negative correlation in 6 (six) locations** and **distinct negative correlation in 3 (three) locations.**

6.4.2 Carbon Monoxide and Meteorological parameters

By comparing the result of all the 27 scatter Plot matrix out of 9 (nine) locations as earlier mentioned in the study area overview, in between *Carbon Monoxide concentration* and *Relative humidity (RH2M),* it showed **weak negative correlation** in **1 (one location)**, **distinct negative correlation in 3 (three) locations** and **strong negative correlation in 4 (four locations)**. Between *Carbon Monoxide concentration* and *Max. Temperature (T2M_MAX),* it showed **distinct positive correlation in 3 (three) locations, strong positive correlation in 1 (one) location** and **weak negative correlation in 2 (two) locations**. Between *Carbon Monoxide concentration* and *Precipitation*, it showed **weak negative correlation in 1 (one) location, distinct negative correlation in 3 (three) locations** and **strong negative correlation in 3 (three) locations.**

6.4.3 Ozone (Tropospheric) and Meteorological parameters

By comparing the result of all the 27 scatter Plot matrix out of 9 (nine) locations as earlier mentioned in the study area overview, in between *Ozone concentration* and *Relative humidity (RH2M),* it showed **distinct negative correlation in 5 (five) locations**. Between *Ozone concentration* and *Max. Temperature (T2M_MAX),* it showed **strong positive correlation in all 9 (nine) locations**. Between *Ozone concentration* and *Precipitation*, it showed **weak positive correlation in 3 (three) locations** and **distinct positive correlation in 2 (two) locations.**

For extreme weather events from the values in Table 34 and Table 35 showed only two possible correlation condition, i.e., between Carbon Monoxide and T2M_MAX where it showed between weak and distinct negative relationship. Whereas for Ozone and T2M_MAX it showed strong positive relationship. Further the probable correlation values were checked in Microsoft excel to establish any relation between the pollutant concentration and meteorological parameters.

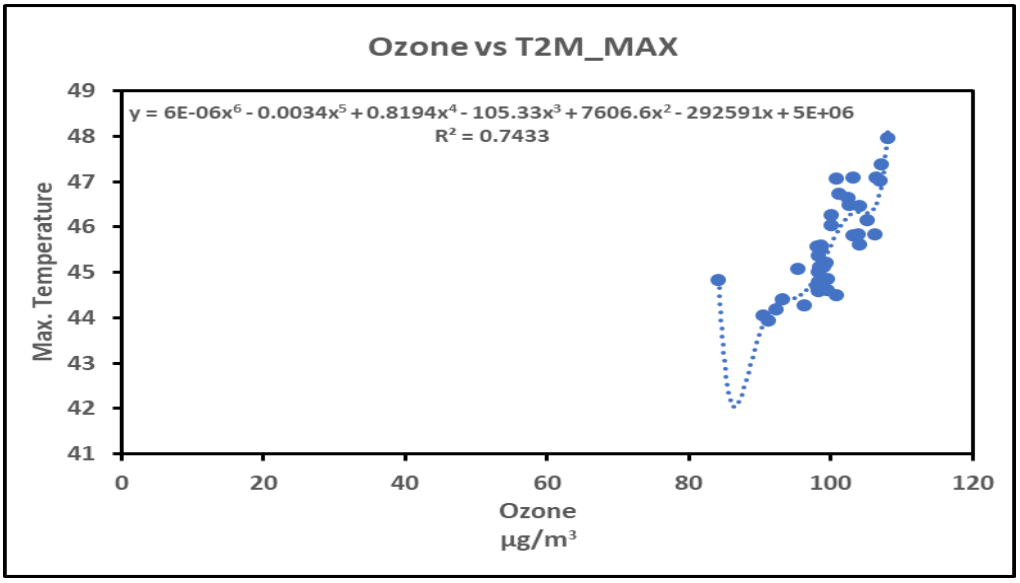

Fig 48. Polynomial trendline of degree 6 (R^2 = 0.7433)

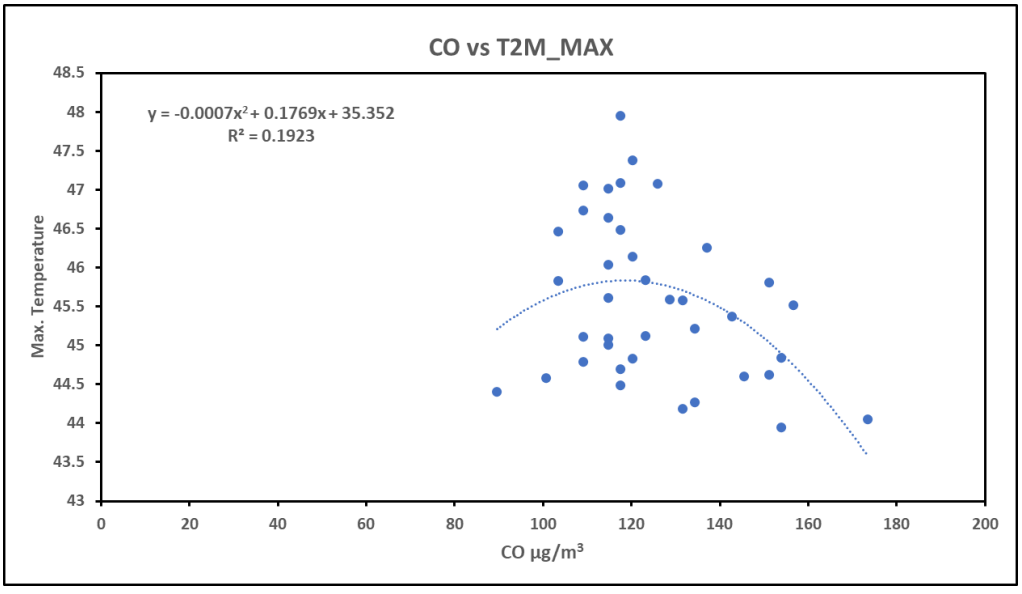

Fig 49. Polynomial trendline of degree 2 (R^2 = 0.1923)

7. Conclusions

Referring to the Results of the *Scatter Plot matrix* and Pearson tables mentioned earlier the *Black Carbon concentration* is **negatively** correlated to *all the meteorological parameters.*

Similarly, the *Carbon Monoxide concentration* showed **distinct** and **strong negative** correlation with both *Relative humidity and precipitation* whereas it showed both **distinct** and **strong** positive correlation with *max temperature*.

For *Ozone concentration* it showed **distinct negative correlation** with the *Relative humidity***, very strong positive correlation** with *max temperature* and **distinct** as well as **weak positive correlation** with *precipitation*.

For extreme cases in meteorological parameters i.e. taking the top 10 percentile and its corresponding pollutant concentration only two conditions showed probable correlation i.e., between Carbon Monoxide and T2M_MAX where it showed between weak and distinct negative relationship. Whereas for Ozone and T2M_MAX it showed strong positive relationship.

Furthermore, the CO when plotted against T2M_MAX, showed $\mathbf{R^2}$ value of **0.1062, 0.1923,0.2384,0.2495** for linear, polynomial of degree 2, degree 3, degree 4 respectively, when checked in Excel.

The Ozone when plotted against T2M_MAX, showed $\mathbf{R^2}$ value of **0.5817, 0.6788,0.6931,0.7433** for linear, polynomial of degree 2, degree 3, degree 6 respectively, when checked in Excel.

An artificial neural node model was created with Random Forest Regression taking the extreme weather cases (90 percentile) and the individual pollutant as independent variable, the model was able to predict the values with least mean squared error and least mean absolute error ranging between **0.7** to **2.9**. Hence, this model can be used to predict the values of meteorological parameters in extreme cases if the pollutant concentration values are known.

7.1 Future Scope of work

There is ample amount of correlation models that can be carried out between different kinds of air pollutants and meteorological parameters for better understanding the relationship between them as there is lack of research work in this field.

Synergistic effect between multiple pollutants and meteorological parameters should also be checked.

Furthermore, there are more and more options to compile huge datasets for in-depth studies because to developments in sensor technology and data collection techniques.

Numerous statistical and computational methods, such as regression modelling, machine learning algorithms, and correlation analysis, may be used in this kind of study. With the use of these techniques, it is possible to discern trends and relationships between various air pollutants and meteorological elements including temperature, humidity, wind speed, and air pressure. Comprehending these correlations can result in more focused measures and regulations aimed at diminishing air pollution and the related health hazards.

An ANN model having huge dataset can be used to train the model for prediction with least absolute and standard value, as the ANN model gives better prediction model when trained with bigger datasets. When training an ANN for air quality prediction, using a large dataset can indeed enhance the model's accuracy and reliability. With more data, the ANN can capture a broader range of scenarios and variations, leading to a more robust predictive model. Additionally, larger datasets help prevent overfitting, a common issue where the model performs well on training data but fails to generalize to unseen data.

8. REFERENCES

[1] World Health Organization (WHO), cited sources in academic writing. Retrieved March 4, 2022, from https://www.who.int/news-room/fact-sheets/detail/ambient-(outdoor)-air-quality-and-health

[2] EPA, cited sources in academic writing. Retrieved March 2022, from https://www.epa.gov/

[3] IPCC, cited sources in academic writing. Retrieved 12 November 2007 from https://www.ipcc.ch/report/ar4/syr/

[4] Dawson, J. P., Bloomer, B. J., Winner, D. A., & Weaver, C. P. (2014). Understanding the meteorological drivers of US particulate matter concentrations in a changing climate. *Bulletin of the American Meteorological Society*, *95*(4), 521-532.

[5] Live Science, cited sources in academic writing. Retrieved October 2, 2020, from https://www.livescience.com/22177-hurricanes-typhoons-cyclones.html

[6] SPC.NCEP. NOAA, cited sources in academic writing. Retrieved May 24,2023, from https://web.archive.org/web/20060929185156/http:/www.spc.ncep.noaa.gov/faq/tornado/

[7] Telangana today, cited sources in academic writing. Retrieved 26 May 2021, from https://telanganatoday.com/major-cyclones-that-hit-india-in-past-few-decades

[8] NOAA, cited sources in academic writing. Retrieved 16 October 2016, from https://psl.noaa.gov/marine-heatwaves/

[9] Anderson, G. B., Bell, M. L., & Peng, R. D. (2013). Methods to calculate the heat index as an exposure metric in environmental health research. *Environmental health perspectives*, *121*(10), 1111-1119.

[10] IPCC, cited sources in academic writing. Retrieved October 2021, from https://www.ipcc.ch/report/ar6/wg1/downloads/report/IPCC_AR6_WGI_SPM_final.pdf

[11] Australian Government Bureau of Meteorology, cited sources in academic writing, from http://www.bom.gov.au/info/wwords/

[12] Yale.edu, cited sources in academic writing. Retrieved 19 June 2008, from https://web.archive.org/web/20090411124535/http://e360.yale.edu/content/feature.msp?id=2010

[13] Holton, J.R (2004) Typical Scales of Atmospheric Motion Systems. Elsevier Academic Press.

[14] Bluestein, H., (1992) Synoptic-Dynamic Meteorology in Midlatitudes: Principles of Kinematics and Dynamics, Vol. 1, Oxford University Press.

[15] Shenfeld, L. (1970). Meteorological aspects of air pollution control. *Atmosphere*, *8*(1), 3–13.

[16] Zhang, X., Zhang, M., Cui, Y., & He, Y. (2022). Estimation of daily ground-received global solar radiation using air pollutant data. *Frontiers in Public Health*, *10*, 860107.

[17] National Weather Service (NWS), cited sources in academic writing, from https://www.ksfire.org/docs/weather/KDHE_Mixing-Height_Transport_Wind_Category_Day_Info.pdf

[18] NPS Influence of wind movement on pollutants, cited sources in academic writing. Retrieved 17 January 2018, from https://www.nps.gov/subjects/air/sources.htm

[19] Hamra, G. B., Guha, N., Cohen, A., Laden, F., Raaschou-Nielsen, O., Samet, J. M., ... & Loomis, D. (2014). Outdoor particulate matter exposure and lung cancer: a systematic review and meta-analysis. *Environmental health perspectives*.

[20] Warneck P., (2000) Chemistry of the natural atmosphere; RMS Academic Press.

[21] Reeves, C. E., Penkett, S. A., Bauguitte, S., Law, K. S., Evans, M. J., Bandy, B. J., ... & Kley, D. (2002). Potential for photochemical ozone formation in the troposphere over the North Atlantic as derived from aircraft observations during ACSOE. *Journal of Geophysical Research: Atmospheres*, *107*(D23), ACH-14.

APPENDIX A

RAW DATA of POLLUTANT CONCENTRATION

Monthly data of Black carbon concentration [µg/m^3] from 2015-2022

2015	Manali	Shimla	Dehradun	Haridwar	Durgapur	Burdwan	Kolkata	Delhi	Mohali
January	0.13	0.23	0.74	1.08	5.52	5.56	5.84	4.66	0.83
February	0.49	1.82	1.18	1.33	6.68	5.37	2.73	1.74	4.08
March	0.58	0.16	0.51	0.79	0.39	0.36	2.25	2.35	0.76
April	0.11	0.33	0.58	1.14	0.33	0.21	0.85	2.54	1.12
May	0.13	0.35	0.58	0.71	2.05	2.12	1.08	3.08	0.54
June	0.32	0.83	1.31	2.01	3.69	3.08	1.19	3.03	1.52
July	0.22	0.32	0.78	1.62	2.38	2.61	2.33	2.16	1.25
August	0.15	0.33	0.68	1.34	5.58	3.18	1.34	2.64	1.15
September	0.19	0.23	0.49	1.11	4.92	5.18	4.31	2.54	0.79
October	0.19	0.72	1.49	2.34	4.59	4.09	3.94	6.98	7.99
November	0.59	0.52	2.33	3.32	9.13	9.52	8.28	5.65	2.43
December	0.08	0.22	0.79	2.24	14.61	21.32	20.02	14.07	1.46

2016									
January	0.31	1.02	1.46	2.53	10.64	9.37	7.53	6.43	2.71
February	0.28	2.04	2.17	3.04	4.88	4.62	4.47	6.34	6.56
March	0.34	0.39	0.63	0.86	2.49	2.23	1.52	3.06	0.83
April	0.15	0.64	1.58	2.01	3.21	2.77	1.63	3.35	1.18
May	0.17	0.45	0.97	1.61	2.89	3.25	2.56	4.12	1.38
June	0.25	1.44	1.88	2.77	3.34	2.29	0.86	1.99	3.41
July	0.21	0.42	0.44	0.97	3.74	3.93	1.87	3.07	0.66
August	0.12	0.51	0.67	0.88	1.92	2.69	1.21	3.59	1.01
September	0.26	0.75	2.82	2.71	3.61	3.27	1.78	6.07	4.88
October	0.38	0.81	1.39	2.27	4.57	4.06	3.82	6.14	4.19
November	0.48	0.67	2.44	4.91	13.2	10.59	4.52	11.62	2.58
December	0.29	1.43	2.19	3.91	9.11	8.93	19.05	22.08	2.77

2017									
January	0.11	0.79	0.89	1.28	5.76	7.38	7.95	4.64	1.06
February	0.29	0.76	0.48	0.79	4.42	5.48	6.12	2.53	3.06
March	0.32	0.45	0.75	1.05	4.09	2.73	0.98	2.09	0.73
April	0.49	0.81	0.88	1.59	3.03	2.63	1.53	1.82	0.98
May	0.41	0.86	0.65	1.02	2.45	2.83	2.11	1.41	1.85
June	0.12	0.54	0.96	1.39	2.83	2.25	1.12	2.33	1.31
July	0.36	0.61	0.57	1.28	5.35	6.23	4.24	3.41	0.98
August	0.13	0.43	0.79	1.67	4.24	3.32	1.54	2.68	1.13
September	0.26	0.52	0.99	1.98	3.68	3.06	1.06	6.25	1.84
October	0.16	1.13	2.81	4.46	7.51	5.56	3.71	14.81	8.49
November	0.41	0.33	0.77	2.86	11.11	10.94	10.89	9.17	3.06
December	0.22	0.72	1.91	4.71	8.15	8.53	13.32	9.81	2.12

2018									
January	0.08	0.25	0.43	1.92	7.79	8.66	7.42	4.13	1.39
February	0.25	0.85	0.68	1.05	4.33	4.62	4.03	4.01	3.33
March	0.29	0.23	0.67	1.22	3.28	2.82	1.71	3.57	0.64
April	0.19	0.42	0.54	1.41	2.21	1.98	1.12	4.63	0.85
May	0.18	0.88	1.17	1.98	3.58	2.31	0.99	3.89	1.55
June	0.19	0.39	0.75	0.92	4.51	3.21	1.38	3.71	0.88
July	0.17	0.36	1.29	0.66	5.06	3.97	1.54	3.87	0.89
August	0.15	0.29	0.86	2.31	5.83	3.92	1.78	3.01	0.95
September	0.68	0.27	0.61	1.21	4.37	5.99	7.28	3.04	0.78
October	0.11	0.23	0.47	1.31	2.25	1.94	1.26	3.41	3.25
November	0.34	0.41	1.12	3.44	5.54	5.61	5.44	7.85	1.63
December	0.24	0.35	0.88	3.01	15.49	14.61	12.82	8.42	1.82

2019									
January	0.12	0.31	0.19	0.29	5.49	6.08	6.38	3.11	0.41
February	0.36	0.62	0.82	1.65	4.86	3.71	1.83	3.17	3.23
March	0.21	0.16	0.32	0.52	6.66	3.95	2.04	3.41	0.47
April	0.08	0.14	0.26	0.39	2.84	1.59	0.91	1.57	0.31
May	0.15	0.32	0.47	0.79	2.08	1.75	1.19	2.54	0.81
June	0.27	0.79	0.77	1.41	4.06	4.67	2.49	4.15	0.95
July	0.31	0.41	0.85	1.28	2.51	2.67	1.13	2.32	0.74
August	0.27	0.48	0.74	1.35	3.74	3.24	1.58	4.27	0.91
September	0.27	0.47	0.44	0.77	3.44	3.11	1.63	2.23	0.74
October	0.39	0.52	1.13	2.68	5.22	4.09	5.01	8.38	3.28
November	0.31	0.27	0.67	1.29	7.53	6.73	6.46	5.66	0.92
December	0.28	0.54	1.03	2.32	6.67	6.93	14.05	7.68	1.83

2020									
January	0.14	0.25	0.48	1.13	3.98	5.08	6.11	2.77	0.73
February	0.61	1.56	1.71	2.26	5.11	5.51	5.44	3.17	3.74
March	0.17	0.16	0.37	0.63	2.41	3.55	4.55	2.93	0.78
April	0.21	0.36	0.65	1.11	4.52	4.76	2.76	4.25	0.68
May	0.09	0.25	0.46	0.67	4.46	3.21	1.81	2.02	0.69
June	0.13	0.34	1.01	1.41	5.75	4.17	1.34	2.21	0.57
July	0.19	0.41	0.72	1.37	4.77	2.98	1.89	0.41	0.85
August	0.21	0.37	0.58	0.84	4.46	6.78	3.96	2.15	0.66
September	0.21	0.25	0.46	0.76	4.21	5.11	2.99	1.94	0.73
October	0.27	0.55	0.71	1.29	5.25	5.3	3.96	4.23	3.15
November	0.41	0.22	0.85	1.98	5.69	6.23	5.82	6.08	1.52
December	0.18	0.71	1.02	2.53	13.3	13.55	11.11	6.61	1.58

2021									
January	0.09	0.58	2.24	3.57	8.48	8.24	7.74	6.44	2.46
February	0.31	0.87	0.51	0.77	5.46	7.52	6.18	2.16	2.65
March	0.26	0.57	0.74	1.32	6.73	6.76	4.43	2.13	1.27
April	0.12	0.19	0.31	0.58	3.41	3.64	2.51	3.28	0.31
May	0.25	0.51	0.79	1.31	5.44	3.78	1.91	2.11	0.75
June	0.31	0.65	0.82	1.37	3.09	2.78	1.24	2.24	2.06
July	0.21	0.34	0.73	1.21	2.29	2.32	1.41	2.35	1.35
August	0.25	0.34	0.81	0.93	1.36	1.53	0.95	1.65	1.95
September	0.21	0.36	0.46	0.74	2.91	2.08	1.06	2.21	1.74
October	0.13	0.31	0.58	1.17	4.51	4.46	3.97	4.66	2.82
November	0.32	0.25	0.67	1.61	11.18	9.59	6.18	7.75	1.78
December	0.21	0.51	1.14	2.65	4.73	4.34	8.68	4.91	1.83

2022									
January	0.13	0.32	0.67	1.21	8.32	7.76	5.76	4.97	1.14
February	0.28	0.76	0.42	1.05	7.92	7.48	5.67	2.14	2.58
March	0.21	0.26	0.33	0.62	4.62	3.25	2.11	2.64	0.33
April	0.21	0.61	1.11	1.37	3.31	3.11	1.67	3.98	1.41
May	0.15	0.47	0.73	0.91	3.11	2.91	1.81	3.64	0.76
June	0.28	1.44	1.91	2.51	3.32	2.43	1.32	3.15	2.96
July	0.21	0.32	0.39	0.62	6.22	4.34	1.97	3.93	0.71
August	0.29	0.52	0.87	1.52	4.51	3.12	1.61	3.85	1.31
September	0.22	0.42	1.22	1.81	5.69	4.92	4.12	3.95	1.52
October	0.17	0.39	0.85	2.15	4.21	4.04	3.78	8.85	2.98
November	0.29	0.23	0.91	2.63	9.96	6.11	6.04	7.07	1.94
December	0.13	0.38	1.74	3.19	8.62	8.21	6.41	13.59	1.44

Monthly data of Carbon monoxide concentration [µg/m^3] from 2018-2022

2018	Manali	Shimla	Dehradun	Haridwar	Durgapur	Burdwan	Kolkata	Delhi	Mohali
January	0	0	0	0	0	0	0	0	0
February	0	0	0	0	0	0	0	0	0
March	0	0	0	0	0	0	0	0	0
April	0	0	0	0	0	0	0	0	0
May	0	0	0	0	0	0	0	0	0
June	0	0	0	0	0	0	0	0	0
July	0	0	0	0	0	0	0	0	0
August	0	0	0	0	0	0	0	0	0
September	0	0	0	0	0	0	0	0	0
October	0	0	0	0	0	0	0	0	0
November	61.6	64.4	89.6	98	114.8	123.2	128.8	120.4	98
December	64.4	72.8	92.4	100.8	145.6	131.6	137.2	126	106.4

2019									
January	70	72.8	98	103.6	142.8	128.8	137.2	123.2	106.4
February	70	70	95.2	106.4	148.4	126	137.2	117.6	103.6
March	86.8	72.8	92.4	100.8	154	131.6	142.8	114.8	98
April	70	81.2	103.6	109.2	151.2	128.8	134.4	123.2	106.4
May	72.8	86.8	109.2	114.8	142.8	131.6	128.8	126	114.8
June	78.4	92.4	114.8	117.6	137.2	134.4	123.2	117.6	109.2
July	75.6	78.4	100.8	103.6	98	100.8	98	103.6	100.8
August	72.8	81.2	98	95.2	95.2	100.8	100.8	103.6	98
September	70	78.4	98	98	95.2	123.2	98	106.4	100.8
October	64.4	70	98	100.8	123.2	114.8	120.4	123.2	103.6
November	67.2	72.8	92.4	103.6	137.2	120.4	131.6	117.6	100.8
December	61.6	67.2	86.8	98	142.8	137.2	131.6	162.4	98

2020									
January	72.8	75.6	92.4	106.4	148.4	137.2	142.8	114.8	103.6
February	61.6	72.8	100.8	114.8	145.6	134.4	145.6	123.2	109.2
March	61.6	75.6	95.2	103.6	145.6	137.2	134.4	117.6	103.6
April	72.8	78.4	98	106.4	137.2	134.4	142.8	109.2	103.6
May	64.4	81.2	106.4	117.6	131.6	128.8	123.2	117.6	114.8
June	81.2	89.6	109.2	103.6	134.4	137.2	109.2	120.4	109.2
July	64.4	81.2	95.2	100.8	95.2	92.4	89.6	89.6	98
August	64.4	81.2	95.2	100.8	95.2	92.4	89.6	98	92.4
September	70	78.4	98	106.4	100.8	98	98	106.4	103.6
October	67.2	78.4	103.6	114.8	117.6	120.4	117.6	131.6	117.6
November	70	75.6	103.6	117.6	128.8	123.2	134.4	142.8	128.8
December	64.4	72.8	95.2	109.2	162.4	151.2	148.4	123.2	114.8

2021									
January	61.6	78.4	109.2	117.6	170.8	151.2	154	131.6	117.6
February	67.2	86.8	114.8	120.4	156.8	145.6	154	137.2	120.4
March	67.2	75.6	100.8	109.2	173.6	151.2	156.8	114.8	95.2
April	64.4	86.8	109.2	114.8	162.4	154	154	120.4	109.2
May	67.2	92.4	114.8	117.6	137.2	126	123.2	117.6	120.4
June	70	81.2	98	100.8	120.4	114.8	117.6	114.8	100.8
July	70	86.8	103.6	106.4	103.6	98	95.2	109.2	103.6
August	75.6	89.6	100.8	106.4	106.4	103.6	95.2	109.2	106.4
September	61.6	78.4	89.6	95.2	95.2	95.2	89.6	98	98
October	61.6	72.8	89.6	98	134.4	117.6	114.8	109.2	103.6
November	53.2	70	92.4	106.4	142.8	123.2	131.6	145.6	145.6
December	53.2	72.8	92.4	95.2	134.4	120.4	134.4	120.4	114.8

2022									
January	58.8	70	89.6	98	142.8	134.4	128.8	120.4	103.6
February	53.2	70	92.4	103.6	137.2	123.2	131.6	114.8	106.4
March	64.4	81.2	106.4	114.8	151.2	134.4	142.8	117.6	114.8
April	64.4	81.2	114.8	114.8	154	131.6	145.6	114.8	109.2
May	70	86.8	114.8	117.6	137.2	134.4	134.4	120.4	123.2
June	67.2	92.4	109.2	114.8	126	128.8	131.6	109.2	103.6
July	72.8	81.2	86.8	98	89.6	86.8	86.8	100.8	95.2
August	61.6	81.2	92.4	95.2	95.2	86.8	89.6	95.2	89.6
September	64.4	75.6	92.4	95.2	106.4	106.4	100.8	103.6	98
October	53.2	67.2	81.2	92.4	109.2	98	103.6	114.8	103.6
November	50.4	64.4	86.8	92.4	128.8	117.6	128.8	123.2	103.6
December	47.6	64.4	86.8	95.2	151.2	134.4	142.8	114.8	100.8

Monthly data of Ozone concentration [µg/m^3] from 2018-2022

2018	manali	shimla	dehradun	haridwar	durgapur	burdwan	kolkata	delhi	mohali
January	47.5	49.5	61.2	63.5	77.8	78.6	77.9	73.2	70.2
February	49.5	53.2	62.6	66.2	83.2	81.2	79.6	75.6	72.2
March	63.2	68.6	77.6	76.2	88.6	89.5	89.6	83.2	81.6
April	79.2	73.2	83.6	81.2	102.2	105.6	103.2	98.5	94.3
May	98.6	99.6	101.2	101.8	106.6	103.5	105.2	107	105.6
June	96.3	98.6	96.9	99.6	93.1	95.4	88.2	102.4	100.6
July	82.3	84.2	88.6	89.2	72.1	77.6	74.9	81.2	90.1
August	68.2	77.2	78.2	74.2	67.2	68.2	63.1	78.2	70.6
September	69.2	78.2	79.2	77.2	68.4	68.6	67.5	80.1	70.9
October	70.1	79.2	80.6	78.2	70.3	70.6	68.6	81.6	75.2
November	65.6	77.5	80.4	74.2	68.2	68.3	61.3	74.6	72.1
December	64.2	74.6	78.2	70.2	66.8	64.2	60.3	72.1	70.3

2019									
January	48.2	50.2	60.2	64.1	74.6	77.5	77.6	70.2	68.4
February	46.5	48.2	58.6	59.4	77.6	80.2	84.2	74.2	70.3
March	60.2	66.2	70.2	74.6	80.2	84.3	90.1	88.4	76.8
April	84.2	77.6	82.1	77.8	98.6	101.3	100.4	99.6	97.4
May	99.4	101.2	101.4	100.9	105.4	103.4	100.4	106.4	104.2
June	94.5	99.6	94.2	100.2	98.1	98.4	94.2	103.1	100.8
July	88.4	85.2	94.2	90.1	77.6	78.4	79.4	85.2	94.2
August	70.2	74.2	84.2	77.4	68.2	69.4	62.1	79.2	77.4
September	70.2	77.4	80.2	78.4	68.6	70.2	68.4	81.2	74.2
October	74.2	80.2	81.2	74.5	71.3	72.3	70.6	80.4	73.2
November	66.3	75.2	81.2	77.2	68.4	70.5	68.3	77.4	74.5
December	68.2	77.6	84.2	72.4	68.4	68.6	65.2	74.5	71.3

2020									
January	44.2	51.2	60.4	66.4	77.2	78.4	74.2	68.2	66.1
February	51.2	49.2	59.2	60.2	78.4	81.2	85.2	76.2	68.2
March	61.3	68.4	71.2	76.4	82.3	88.4	92.3	84.6	75.2
April	88.4	69.4	80.3	76.4	97.6	99.4	98.4	98.6	94.2
May	88.4	100.3	100.8	103.2	104.5	101.2	100.7	103.2	98.3
June	93.4	94.2	98.6	106.4	99.3	99.4	88.4	100.3	98.4
July	87.5	86.2	92.1	95.2	74.2	66.2	68.2	83.4	91.2
August	71.3	78.6	90.3	88.4	75.2	77.9	68.1	81.6	90.1
September	71.2	72.4	81.4	79.5	69.4	72.1	68.4	84.5	77.4
October	77.4	81.2	88.4	77.6	72.4	75.4	72.4	82.1	77.2
November	68.1	74.2	78.4	78.6	72.4	71.2	68.2	78.2	80.1
December	69.2	76.2	77.4	73.1	67.6	65.2	68.4	77.3	72.1

2021									
January	48.2	53.1	62.1	68.4	79.4	80.3	88.4	79.2	68.2
February	58.4	76.2	77.4	79.2	89.2	90.1	92.1	88.7	77.4
March	61.8	64.2	70.4	77.2	77.2	96.3	99.1	80.2	82.1
April	85.2	62.3	74.2	78.2	99.4	97.2	98.2	99.6	99.1
May	89.4	99.4	98.4	101.2	103.2	99.4	98.2	99.3	101.2
June	88.6	89.3	88.4	99.4	102.3	100.3	89.4	98.2	101.3
July	88.2	88.2	96.3	94.2	77.2	74.1	66.2	84.2	94.2
August	70.3	79.3	88.4	90.2	76.2	79.4	69.4	78.2	88.4
September	77.2	77.4	83.2	83.2	72.3	75.4	70.2	86.2	78.2
October	78.3	83.4	89.4	78.6	77.2	76.4	74.2	80.1	83.2
November	66.3	74.9	76.4	77.4	70.2	65.3	64.1	77.2	78.4
December	66.3	77.4	78.4	75.2	68.2	68.9	70.2	78.4	73.6

2022									
January	46.3	50.2	66.1	64.2	80.4	79.4	82.5	76.4	66.2
February	55.2	74.2	72.1	78.4	88.4	81.2	90.2	83.1	72.1
March	68.1	66.3	77.3	78.2	78.6	94.2	80.2	78.2	80.3
April	88.3	68.4	77.2	83.1	100.3	99.4	99.3	101.3	100.4
May	96.3	99.9	99.6	103.2	101.4	100.3	103.2	108.1	103.2
June	94.2	92.3	96.3	101.2	106.8	103.2	106.7	99.6	104.2
July	94.2	96.3	99.4	99.2	79.3	77.2	65.2	89.6	99.4
August	77.2	84.2	96.1	95.2	84.2	88.2	78.4	98.4	102.3
September	69.1	76.3	94.2	96.4	80.2	79.4	77.2	80.2	77.6
October	67.4	75.2	77.1	84.2	79.4	68.4	71.9	82.7	84.7
November	68.7	78.3	79.7	79.3	71.8	66.9	67.2	79.3	77.6
December	63.9	72.1	77.9	73.7	69.7	72.7	72.9	75.9	79.7

APPENDIX B

RAW DATA OF METEOROLOGICAL PARAMETERS

Meteorological data (RH2M, T2M_MAX and PRECIPITATION) for Manali 2015 – 2022

PARAMETER	YEAR	JAN	FEB	MAR	APR	MAY	JUN	JUL	AUG	SEP	OCT	NOV	DEC
RH2M	2015	72.81	80.38	84.75	82.88	70.25	81.44	89.25	91.5	83.75	75.56	73.31	70.81
RH2M	2016	72.56	75.88	84	75.25	75.38	82.88	89.25	89.81	86.31	68.44	50.44	41.88
RH2M	2017	90.25	79	82.75	72.62	79.56	81.56	90.56	88.5	83.62	63.5	63.25	63.5
RH2M	2018	50	71.31	69.31	71.19	63.31	75.25	87.5	89.88	83.12	74.38	72.88	66.62
RH2M	2019	84.94	89.25	85.25	77.12	75.19	73.5	86.5	87.38	79.75	69.25	74.94	69.44
RH2M	2020	84.38	72.69	83.75	82.06	76.88	81.31	85.75	88.62	75.81	56.94	66.81	66.75
RH2M	2021	59.75	68.69	71.81	70.44	80.75	80.25	86.88	87.38	88.12	71.06	58.19	71.81
RH2M	2022	86	84.06	66.69	66.56	73.75	71.88	90.06	90.31	87.75	78.12	70.56	63.56
T2M_MAX	2015	3.05	3.65	6.8	7.62	10.67	12.51	16	14.24	10.3	9.44	5.75	5.44
T2M_MAX	2016	0.44	1.28	5.14	8.74	12.3	15.14	14.33	13.84	12.35	12.09	5.89	7.01
T2M_MAX	2017	-2.23	-0.51	6.95	9.95	9.59	14.19	13.98	13.88	12.82	11.02	6.65	5.33
T2M_MAX	2018	2.65	3.4	6.42	8.76	12.39	15.4	15.54	14.75	12.21	6.71	5.18	1.04
T2M_MAX	2019	-1.95	-2.95	4.04	8.65	10.53	12.26	15.77	14.67	13.84	7.54	4.26	1.14
T2M_MAX	2020	-3.42	0.33	2.48	7.37	11.47	12.99	14.24	14.62	13.94	10.75	5.4	1.38
T2M_MAX	2021	1.73	3.69	5.79	7.19	11.63	15.78	17.88	13.35	13.54	11.05	3.72	1.58
T2M_MAX	2022	-2.89	-3.61	8.86	10.14	11.91	15.9	15.3	14.83	12.06	9.01	5.53	2.4
PRECIPITATION	2015	0	0	5.27	0	0	5.27	10.55	5.27	0	0	0	0
PRECIPITATION	2016	0	0	5.27	0	0	0	5.27	5.27	0	0	0	0
PRECIPITATION	2017	5.27	0	0	0	0	5.27	5.27	5.27	0	0	0	0
PRECIPITATION	2018	0	0	0	0	0	0	5.27	10.55	5.27	0	0	0
PRECIPITATION	2019	0	5.27	0	0	0	0	5.27	5.27	0	0	0	0
PRECIPITATION	2020	5.27	0	5.27	0	0	0	5.27	5.27	0	0	0	0
PRECIPITATION	2021	1.19	0.94	1.19	4.53	2.29	2.49	7.42	3.74	5.74	1.56	0.02	0.66
PRECIPITATION	2022	4.04	2.46	0.21	0.41	1.87	2.03	9.02	7.75	4.68	1.31	0.77	0.19

Meteorological data (RH2M, T2M_MAX and PRECIPITATION) for Shimla 2015 – 2022

PARAMETER	YEAR	JAN	FEB	MAR	APR	MAY	JUN	JUL	AUG	SEP	OCT	NOV	DEC
RH2M	2015	50.12	48.56	62.12	51.12	30.06	40.44	78.56	81.5	64.12	52.75	47.12	43.12
RH2M	2016	43.25	39.31	46.5	34.5	35.31	45.62	71.38	81.44	71.44	45	33.31	31.56
RH2M	2017	54.06	47.19	44.12	31.75	34.81	50.94	72.56	83.75	74.38	49.81	46.06	42.69
RH2M	2018	38.19	40.56	36.94	35.44	28.44	50.38	79.44	85.56	82.62	66.38	60.12	53.44
RH2M	2019	59.56	67.06	60.38	44	34.75	34.81	68.38	82.81	81.5	64	57.06	50.38
RH2M	2020	65.62	57.12	65.25	53.94	44.56	52.38	72.62	85.38	74.19	41.81	42.38	41.94
RH2M	2021	45.56	45.31	38	34.25	40.69	48.69	69.81	81	83.75	70.31	48.56	51.81
RH2M	2022	71.25	65.88	47.25	27.25	33.19	38.19	81.31	87.31	85.44	73.12	62.5	55.69
T2M_MAX	2015	22.09	26.63	30.78	34.3	39.76	39.4	35.88	29.78	31.68	30.01	26.81	24.48
T2M_MAX	2016	21.36	27.3	31.78	37.01	41.02	39.73	35.88	30.76	30.41	31.07	28.35	24.98
T2M_MAX	2017	22.19	26.71	34.38	39.14	39.34	42.05	35.05	30.39	30.87	30.66	26.59	25.2
T2M_MAX	2018	24.56	26.48	32.49	37.24	39.67	39.27	34.51	29.43	29.82	27.48	23.86	20.01
T2M_MAX	2019	19.43	21.62	30.67	35.9	40.58	42.19	38.76	30.22	29.66	26.85	26.63	22.14
T2M_MAX	2020	19.94	25.19	25.39	33.37	39.14	37.01	36.98	31.6	31.16	31.81	27.8	24.94
T2M_MAX	2021	21.88	27.81	32.29	35.79	37.8	38.94	38.28	30	29.44	30.92	25.18	23.66
T2M_MAX	2022	21.59	21.55	34.57	38.87	40.6	40.24	33.62	30.31	29.01	28.51	24.96	23.15
PRECIPITATION	2015	0	0	5.27	0	0	5.27	10.55	5.27	0	0	0	0
PRECIPITATION	2016	0	0	5.27	0	0	5.27	10.55	5.27	0	0	0	0
PRECIPITATION	2017	5.27	0	0	0	0	5.27	10.55	10.55	5.27	0	0	0
PRECIPITATION	2018	0	0	0	0	0	5.27	10.55	10.55	10.55	0	0	0
PRECIPITATION	2019	0	5.27	0	0	0	0	10.55	10.55	5.27	0	0	0
PRECIPITATION	2020	5.27	0	5.27	0	5.27	5.27	10.55	10.55	0	0	0	0
PRECIPITATION	2021	0.68	1.13	0.68	2.49	3.15	3.76	11.05	6.5	7.79	1.3	0.02	0.32
PRECIPITATION	2022	5.22	2.15	0.09	0.1	2.56	3.5	15.77	8.82	8.5	1.29	0.23	0.06

Meteorological data (RH2M, T2M_MAX and PRECIPITATION) for Dehradun 2015 – 2022

PARAMETER	YEAR	JAN	FEB	MAR	APR	MAY	JUN	JUL	AUG	SEP	OCT	NOV	DEC
RH2M	2015	53.69	51.88	62.56	55.69	32.5	45.31	83.69	87.81	73.12	64.19	54.44	47.06
RH2M	2016	45.56	40.56	46.12	34.06	39.94	55.69	81.19	85.81	80.44	59.56	38.94	34.88
RH2M	2017	55.06	44.38	44.25	34.94	41.5	58.44	82.81	87.88	80.81	60.31	56.06	47.69
RH2M	2018	39.88	43.31	37.56	39.44	32.56	59.06	84.5	90.56	84.69	65.31	59.81	54.75
RH2M	2019	61.12	66.5	58.06	47	36.12	38.94	76.19	85.31	85.19	66.88	57.62	50.69
RH2M	2020	65.81	55.94	64.38	57.12	50.25	59.81	80.75	89	75.88	53.94	46.44	40.25
RH2M	2021	41.25	44.06	36.94	34.5	48.25	58.81	77.69	86.31	85.81	69.25	52.25	58
RH2M	2022	71.81	66.31	51	32.44	40.62	44.88	84.69	87.31	87.5	75.38	61.75	54.38
T2M_MAX	2015	20.92	26.56	27.4	30.12	35.65	36.37	31.57	26.78	27	25.84	23.87	21.95
T2M_MAX	2016	19.69	24.47	28.72	34.05	36.76	34.66	31.56	27.54	26.33	25.88	26.98	23.11
T2M_MAX	2017	20.16	25.4	32.58	35.33	35.49	38.18	29.43	27.75	27.51	25.98	21.68	22.52
T2M_MAX	2018	22.1	24.36	29.58	32.93	36.6	35.79	30.45	26.93	27.3	24.73	20.55	17.95
T2M_MAX	2019	17.81	18.86	27.08	33.16	37.4	37.95	34.96	28.05	27.19	23.71	22.99	18.59
T2M_MAX	2020	18.13	23.97	24.73	28.66	35.01	32.62	30.67	28.62	27.75	26.5	22.9	21.84
T2M_MAX	2021	20.86	25.14	29.11	32.6	33.69	35.53	34.04	27.87	26.73	26.42	20.86	19.39
T2M_MAX	2022	17.58	18.55	30.28	34.76	36.54	37.09	29.23	28.22	26.51	25.84	22.19	20.49
PRECIPITATION	2015	0	0	5.27	0	0	5.27	15.82	10.55	0	0	0	0
PRECIPITATION	2016	0	0	0	0	0	5.27	10.55	10.55	0	0	0	0
PRECIPITATION	2017	5.27	0	0	0	0	10.55	10.55	10.55	5.27	0	0	0
PRECIPITATION	2018	0	0	0	0	0	5.27	15.82	15.82	10.55	0	0	0
PRECIPITATION	2019	0	5.27	0	0	0	0	10.55	10.55	5.27	0	0	0
PRECIPITATION	2020	5.27	0	5.27	0	0	5.27	10.55	10.55	0	0	0	0
PRECIPITATION	2021	0.68	0.94	0.34	1.84	4.19	4.24	15.06	8.59	8.71	2.11	0.01	0.26
PRECIPITATION	2022	4.88	1.82	0.02	0.07	2.26	3.86	15.04	8.7	12.36	2.23	0.12	0.03

Meteorological data (RH2M, T2M_MAX and PRECIPITATION) for Haridwar 2015 – 2022

PARAMETER	YEAR	JAN	FEB	MAR	APR	MAY	JUN	JUL	AUG	SEP	OCT	NOV	DEC
RH2M	2015	50.69	44.38	56.81	45.69	24.69	36.88	77.5	83.75	69.31	53	45.62	41.38
RH2M	2016	37.56	32.12	35.12	23.12	29.69	43.25	73	81.56	73.06	46.31	34.75	32.06
RH2M	2017	47.5	39.62	34.94	24.06	29.25	46.25	73.12	82.69	79.12	53	46.12	43
RH2M	2018	38.69	37.19	28.12	28.31	23.19	49.5	79.06	86.44	84.25	67.56	63.94	55.81
RH2M	2019	55.94	60.12	48.12	35.62	24.56	30.31	66.88	81.06	81.25	63.25	51.94	50.25
RH2M	2020	62.44	54	59.62	44.5	39.62	48.88	74	87.12	76.81	46.75	41.19	41.06
RH2M	2021	44.81	40.38	30.25	23.75	37.38	49.56	71.62	84.5	82.56	72.44	59.44	61.5
RH2M	2022	76.06	67.81	46.62	23.69	30.94	37.12	77.38	83.88	83.5	76.94	68.88	62.81
T2M_MAX	2015	23.64	30.28	33.65	37.48	43.2	43.6	38.33	31.55	32.45	32.11	29.08	27.7
T2M_MAX	2016	25.02	29.83	35.53	41.58	43.67	40.94	38.37	32.15	32.12	33.41	30.48	27.26
T2M_MAX	2017	24.54	29.83	39.22	42.4	42.49	45.21	35.88	32.91	32.4	33.26	28.45	26.06
T2M_MAX	2018	27.94	29.18	36.32	39.88	43.61	42.19	37.05	31.16	30.72	29.55	25.52	21.57
T2M_MAX	2019	21.15	24.94	35.02	40.47	44.78	45.12	41.29	33.12	31.64	29.31	28.9	23.69
T2M_MAX	2020	20.41	28.06	30.93	36.12	43.04	39.94	36.56	32.99	31.75	31.89	28.49	26.33
T2M_MAX	2021	24.65	30.77	36.33	39.87	39.51	41.08	40.5	31.76	31.6	33.05	25.08	23.38
T2M_MAX	2022	19.87	23.18	37.05	42.09	43.55	43.66	36.3	32.49	31.14	29.89	25.44	24.97
PRECIPITATION	2015	0	0	5.27	0	0	5.27	10.55	10.55	0	0	0	0
PRECIPITATION	2016	0	0	0	0	0	0	10.55	5.27	0	0	0	0
PRECIPITATION	2017	0	0	0	0	0	5.27	5.27	10.55	5.27	0	0	0
PRECIPITATION	2018	0	0	0	0	0	5.27	10.55	10.55	10.55	0	0	0
PRECIPITATION	2019	0	0	0	0	0	0	10.55	10.55	5.27	0	0	0
PRECIPITATION	2020	0	0	5.27	0	0	5.27	10.55	10.55	0	0	0	0
PRECIPITATION	2021	1.02	0.75	0	0.93	3.9	3.38	16.01	7.81	8.61	2.62	0	0.13
PRECIPITATION	2022	4.1	1.43	0	0.03	1.94	3.65	13.35	5.86	11.75	3.16	0.04	0.01

Meteorological data (RH2M, T2M_MAX and PRECIPITATION) for Durgapur 2015 – 2022

PARAMETER	YEAR	JAN	FEB	MAR	APR	MAY	JUN	JUL	AUG	SEP	OCT	NOV	DEC
RH2M	2015	64.69	54.06	44	57.31	60.12	69.5	85.38	87.81	83.5	77.25	70.62	62.94
RH2M	2016	54.19	52.19	46.19	38.88	53.81	68.69	83.88	86.75	89.19	81.69	77.19	73.69
RH2M	2017	64.19	51.81	46.38	51.44	57.62	72.12	86.94	89.88	89.19	85.25	76.62	74.75
RH2M	2018	62.75	58.94	49.12	64.06	62	70.62	83.69	87.44	86.5	76.12	72.12	65.75
RH2M	2019	55.88	53.56	51.19	51.44	55.44	62.88	76.38	84.94	88.44	84.75	81.94	78.69
RH2M	2020	72.19	61.69	57.38	51.69	63.56	80.62	85.75	88.31	89.5	85.25	77.75	70.75
RH2M	2021	64.44	47.69	36.94	42	64.19	81.12	86.94	89.31	90	85.56	82.69	81.62
RH2M	2022	77.38	70.12	64.31	57.81	65.44	72.31	79.62	85.38	88.5	85	75	68.69
T2M_MAX	2015	27.97	33.9	38.11	42.41	44.18	43.38	35.22	32.88	33.55	33.15	29.94	29.51
T2M_MAX	2016	29.48	36.41	39.03	46.46	44.84	43.65	35.86	33.4	32.14	32.51	29.83	26.93
T2M_MAX	2017	28.63	34.01	42.8	42.63	42.75	43.16	34.05	32.32	33.26	33.03	29.05	27.4
T2M_MAX	2018	25.44	32.34	37.87	39.6	41.75	41.94	35.02	33.07	32.71	32.98	30.85	26.46
T2M_MAX	2019	28.9	34.57	39.12	44.6	43.81	45.08	37.14	34.87	33.44	31.08	29.02	26.53
T2M_MAX	2020	26.33	29.73	37.82	41.08	41.75	36.09	33.62	33.43	32.73	32.38	29.97	26.33
T2M_MAX	2021	29.23	35.77	42.51	41.87	42.12	38.81	34.1	33.12	32.72	32.53	27.98	26.03
T2M_MAX	2022	25.27	29.15	36.19	43.62	42.22	40.94	35.9	34.15	32.29	31.12	29.03	27.91
PRECIPITATION	2015	0	0	0	5.27	0	5.27	15.82	5.27	5.27	0	0	0
PRECIPITATION	2016	0	0	0	0	5.27	5.27	10.55	15.82	10.55	0	0	0
PRECIPITATION	2017	0	0	0	0	5.27	10.55	21.09	10.55	5.27	10.55	0	0
PRECIPITATION	2018	0	0	0	5.27	0	5.27	10.55	10.55	5.27	0	0	0
PRECIPITATION	2019	0	0	0	0	5.27	0	5.27	10.55	5.27	5.27	0	0
PRECIPITATION	2020	0	0	0	0	5.27	10.55	10.55	10.55	5.27	0	0	0
PRECIPITATION	2021	0	0	0.34	1.25	6.73	14.1	11.38	6.97	13.59	5.4	1.17	1.45
PRECIPITATION	2022	0.9	1.82	0.01	0.77	4.76	4.68	4.66	10.4	6.23	4.21	0	0

Meteorological data (RH2M, T2M_MAX and PRECIPITATION) for Burdwan 2015 – 2022

PARAMETER	YEAR	JAN	FEB	MAR	APR	MAY	JUN	JUL	AUG	SEP	OCT	NOV	DEC
RH2M	2015	63	54.62	46.25	62.69	64.81	74.5	88.94	89.25	85.81	78.88	73.19	64.19
RH2M	2016	54.62	55.06	56.38	49.19	60	76.19	86.25	88.56	89.44	83.25	79.19	76
RH2M	2017	63.62	50.94	53.56	57.69	60.81	76.44	88.75	90.25	89.75	86.19	79.12	79.5
RH2M	2018	65.44	61.69	51.56	64.31	65.06	76.75	86	88.62	87.5	76.88	72.94	64.94
RH2M	2019	52.75	51.75	60	57.25	61.69	69.44	77.88	86.25	89.06	85.31	82.88	78.81
RH2M	2020	73.19	62.38	58.88	55.88	70	85.38	88.12	89.75	89.88	86.31	80	73.5
RH2M	2021	64.56	46.81	40.94	48.69	66.62	85.44	88.19	90.94	90.56	86.5	83.38	82.81
RH2M	2022	79.06	70.75	64.31	57.5	68.38	76.25	82.38	86.44	88.94	86.12	76.31	67.94
T2M_MAX	2015	29.07	34.55	38.39	41.61	43.12	38.72	34.72	32.23	33.37	33.03	30.13	28.98
T2M_MAX	2016	30.42	36.49	38.34	45.57	44.83	42.3	34.85	33.22	32.33	32.76	30.21	27.23
T2M_MAX	2017	28.33	34.59	40.71	42.52	42.4	41.07	33.69	32.42	33.9	33	29.46	27.63
T2M_MAX	2018	25.09	33.31	38.52	39.82	41.98	40.36	34.56	32.87	32.66	32.92	30.71	27.52
T2M_MAX	2019	30.19	35.43	38.42	44.05	42.63	43.77	36.69	34.5	33.19	31.22	29.15	26.98
T2M_MAX	2020	26.44	30.43	37.95	41.52	40.58	34.23	33.4	33.4	32.99	32.75	30.08	26.4
T2M_MAX	2021	29.4	36.54	43.29	42.47	41.5	35.68	33.05	32.3	32.32	32.95	28.57	26.44
T2M_MAX	2022	25.42	29.55	37.04	43.94	39.7	38.8	34.53	33.87	32.87	31.71	29.78	28.64
PRECIPITATION	2015	0	0	0	5.27	0	5.27	21.09	5.27	5.27	0	0	0
PRECIPITATION	2016	0	0	0	0	5.27	5.27	10.55	15.82	10.55	0	0	0
PRECIPITATION	2017	0	0	0	0	5.27	5.27	21.09	10.55	5.27	10.55	0	0
PRECIPITATION	2018	0	0	0	5.27	0	5.27	10.55	10.55	5.27	0	0	0
PRECIPITATION	2019	0	5.27	0	0	5.27	5.27	5.27	10.55	10.55	5.27	0	0
PRECIPITATION	2020	0	0	0	0	10.55	10.55	10.55	10.55	5.27	5.27	0	0
PRECIPITATION	2021	0	0	0	0.87	8.19	12.43	12.99	8.47	14.75	5.66	0.77	3.12
PRECIPITATION	2022	0.87	1.83	0.02	0.59	5.92	4.24	5.51	8.96	7.22	3.94	0	0

Meteorological data (RH2M, T2M_MAX and PRECIPITATION) for Kolkata 2015 – 2022

PARAMETER	YEAR	JAN	FEB	MAR	APR	MAY	JUN	JUL	AUG	SEP	OCT	NOV	DEC
RH2M	2015	66.25	59.94	50	67.19	69.69	76.94	89.69	89.06	86.31	79.12	73.56	67
RH2M	2016	58.31	59.75	62.44	55.12	64.25	78.81	86.31	88.56	89.38	83.12	79.19	76.5
RH2M	2017	66.06	56.31	60.94	63.56	65.31	78.06	88.5	89.69	89.25	85.69	78.69	78.75
RH2M	2018	65	62.88	55.25	67.31	69.31	79.94	86	88.38	87.44	76.94	73.75	67.5
RH2M	2019	56.19	55.5	66.75	62.75	66.69	73.44	78.62	86.06	89.12	85.12	82.75	79.25
RH2M	2020	74.56	66.62	64.69	60.56	72.88	85.31	87.44	89.44	89.31	86.69	79.81	73.44
RH2M	2021	65.94	51.81	47.81	54.75	70.31	86.25	88.19	90.75	90.25	86.56	82.94	82.25
RH2M	2022	78.69	70.31	64.31	61	71.12	78.44	84.06	87.31	89.19	86.06	77.12	71.88
T2M_MAX	2015	28.8	34.44	38.56	40.56	42.39	37.4	33.84	32.08	33.19	32.81	30.18	29.24
T2M_MAX	2016	30.95	36.71	37.87	44.48	43.8	40.12	33.57	33.18	31.93	32.52	30.3	27.39
T2M_MAX	2017	28.2	34.41	38.29	42.07	41.69	38.6	34.13	32.41	33.66	32.81	29.7	28.05
T2M_MAX	2018	25.94	33.87	37.95	39.48	40.98	39.6	34.01	32.76	32.55	32.75	30.63	27.21
T2M_MAX	2019	30.27	35.6	37.36	42.8	41.29	42.23	35.86	34.41	32.9	31.46	29.13	27.26
T2M_MAX	2020	26.74	30.15	37.49	41.07	40.19	34.03	33.34	33.37	32.9	32.83	29.98	26.69
T2M_MAX	2021	29.6	36.71	43.83	41.9	40.55	34.74	33.33	32.25	32.13	32.75	28.7	27.05
T2M_MAX	2022	25.65	30.51	37.65	43.12	39.27	37.51	33.68	33.51	32.14	31.39	29.76	28.56
PRECIPITATION	2015	0	0	0	5.27	0	5.27	21.09	5.27	5.27	0	0	0
PRECIPITATION	2016	0	0	0	0	5.27	5.27	10.55	15.82	10.55	0	0	0
PRECIPITATION	2017	0	0	0	0	5.27	5.27	21.09	10.55	5.27	10.55	0	0
PRECIPITATION	2018	0	0	0	5.27	5.27	10.55	10.55	10.55	5.27	0	0	0
PRECIPITATION	2019	0	5.27	0	0	5.27	5.27	5.27	10.55	10.55	5.27	5.27	0
PRECIPITATION	2020	0	0	0	0	10.55	10.55	10.55	10.55	5.27	5.27	0	0
PRECIPITATION	2021	0	0	0	1.03	8.98	12.72	15.61	9.58	19.34	6.91	0.45	3.33
PRECIPITATION	2022	0.89	1.77	0.03	0.53	5.45	4.12	7.32	10.79	8.12	4.46	0	0

Meteorological data (RH2M, T2M_MAX and PRECIPITATION) for Delhi 2015 – 2022

PARAMETER	YEAR	JAN	FEB	MAR	APR	MAY	JUN	JUL	AUG	SEP	OCT	NOV	DEC
RH2M	2015	52.12	39.25	49.5	40.81	19.06	35.44	64.5	68	48.56	37.56	35.5	26.69
RH2M	2016	29.75	24.62	31	18.81	24.38	34.62	68.75	79.94	61.12	39.31	27	27.06
RH2M	2017	43.81	37	27.69	18.75	22.69	42.69	65.5	65.38	58.25	36.19	37.75	37.94
RH2M	2018	32.44	29.31	23.06	24.5	21.44	38.81	66.44	77.19	76.25	56.31	47	43.56
RH2M	2019	47.38	52.19	40.25	29	25.88	27.25	56.31	73.38	70.19	54	53.94	54.38
RH2M	2020	62.38	50.12	55.69	39.38	30.81	41.5	60.06	77.88	63.06	34	36.75	39.88
RH2M	2021	53.62	38.56	26.75	19	35.06	45.12	65.56	79.75	86.69	70.69	59.06	57.94
RH2M	2022	72.38	60.88	41	16.88	25.69	33.38	65.31	70.38	68.25	68.38	60.88	51
T2M_MAX	2015	24.58	31.8	36.81	40.72	46.25	45.6	41.47	37.39	39.05	38.51	31.32	29.03
T2M_MAX	2016	28.19	32.83	39.09	43.19	47.05	45.82	41.09	34.98	37.19	36.57	31.65	28.94
T2M_MAX	2017	27	32.12	41.37	45.37	46.13	47.01	40.39	38.98	37.9	37.37	32.42	27.07
T2M_MAX	2018	28.49	33.12	40.18	43.89	46.48	45.8	42.07	35.02	33.83	34.44	32.33	26.69
T2M_MAX	2019	27.13	28.52	38.99	43.75	47.07	47.94	45.11	37.72	38.69	34.55	33.08	24.65
T2M_MAX	2020	24.72	29.51	33.43	40.48	47.08	45	43.03	38.4	37.39	36.96	31.33	30.23
T2M_MAX	2021	24.95	34.39	41.85	43.62	41.67	44.58	43.69	34.83	32.98	34.19	28.51	25.33
T2M_MAX	2022	24.2	27.83	41.46	46.03	47.37	45.58	41.19	37.76	39.17	33.73	32.22	27.58
PRECIPITATION	2015	0	0	0	0	0	0	5.27	5.27	0	0	0	0
PRECIPITATION	2016	0	0	0	0	0	0	10.55	5.27	0	0	0	0
PRECIPITATION	2017	0	0	0	0	0	5.27	5.27	5.27	5.27	0	0	0
PRECIPITATION	2018	0	0	0	0	0	0	10.55	5.27	5.27	0	0	0
PRECIPITATION	2019	0	0	0	0	0	0	5.27	5.27	0	0	0	0
PRECIPITATION	2020	0	0	0	0	0	0	5.27	5.27	0	0	0	0
PRECIPITATION	2021	1.36	0	0	0.13	3.62	2.06	11.95	6.03	7.58	2.49	0	0.18
PRECIPITATION	2022	2.79	0.76	0	0.02	1.31	2.83	6.07	2.08	7.16	3.09	0	0

Meteorological data (RH2M, T2M_MAX and PRECIPITATION) for Mohali 2015 – 2022

PARAMETER	YEAR	JAN	FEB	MAR	APR	MAY	JUN	JUL	AUG	SEP	OCT	NOV	DEC
RH2M	2015	48.69	44.62	58.31	45.69	25.56	36.25	74.69	78.56	61.38	49.06	43.56	40.44
RH2M	2016	39.06	34.06	39.12	26.38	29.81	41.25	67.25	78.69	66.12	42.44	32.19	30.12
RH2M	2017	51.38	44.19	38.12	25.31	28.06	45.88	69.69	80.69	73.94	50.56	45.56	43
RH2M	2018	39.38	38.69	32.19	28.62	23.69	48.31	77.88	83.06	82.12	66.44	60.56	54.19
RH2M	2019	56.94	63.38	53.75	37.12	28.19	30.5	65.38	80.06	79.56	63.75	56.38	52.88
RH2M	2020	65.88	56.44	62.88	47.94	39.56	47.69	69.88	84	72.12	40.06	40.38	43
RH2M	2021	48.38	42.12	32.12	27.19	35.38	44.69	67.88	79.38	82.75	70.81	50.81	52.25
RH2M	2022	72.62	65.19	44	22.25	29.38	35.31	78.31	85.5	82.62	72.81	65.19	56.81
T2M_MAX	2015	23.8	29.89	34.76	38.48	44.4	43.91	39.69	33.79	35.24	33.94	29.9	27.05
T2M_MAX	2016	24.88	30.86	36.12	42.12	45.83	42.8	40.07	33.96	34.52	34.93	30.93	27.3
T2M_MAX	2017	24.48	29.77	38.66	43.83	43.65	46.63	38.37	33.49	33.85	34.3	29.12	26.98
T2M_MAX	2018	27.09	30.14	36.78	41.65	44.26	43.07	37.44	32.63	32.51	31.3	26.58	22.9
T2M_MAX	2019	22.58	23.06	35.75	40.83	45.51	46.73	42.24	33.51	33.15	30.46	30.24	23.96
T2M_MAX	2020	20.43	27.5	29.28	37.49	43.67	41.15	40.26	34.74	34.3	34.87	29.72	27.08
T2M_MAX	2021	23.97	31.56	36.83	40.57	41.81	43.05	42.2	33.1	32.15	33.36	27.67	25.52
T2M_MAX	2022	23.55	24.37	38.43	43.62	44.69	44.62	37.04	32.65	32.09	31.34	27.94	26.17
PRECIPITATION	2015	0	0	5.27	0	0	5.27	10.55	5.27	0	0	0	0
PRECIPITATION	2016	0	0	0	0	0	5.27	10.55	5.27	0	0	0	0
PRECIPITATION	2017	5.27	0	0	0	0	5.27	5.27	10.55	5.27	0	0	0
PRECIPITATION	2018	0	0	0	0	0	5.27	10.55	10.55	10.55	0	0	0
PRECIPITATION	2019	0	5.27	0	0	0	0	10.55	10.55	5.27	0	0	0
PRECIPITATION	2020	5.27	0	5.27	0	5.27	5.27	10.55	10.55	0	0	0	0
PRECIPITATION	2021	0.68	0.94	0.51	1.34	3.25	3.36	13.5	6.79	8.16	1.52	0.01	0.17
PRECIPITATION	2022	4.82	1.56	0.02	0.03	2.21	3.66	15.83	6.99	10.73	1.57	0.09	0.03

APPENDIX C

ABBREVIATIONS

1. PM – Particulate Matter
2. CO – Carbon Monoxide
3. O_3 – Ozone
4. SO_2 – Sulphur Dioxide
5. EF – Enhanced Fujita
6. HI – Heat Index
7. VR – Ventilation Rate
8. NAAQS – National Ambient Air Quality Standards
9. HAPs – Hazardous Air Pollutants
10. NRTI – Near Real Time
11. OFFL – Offline
12. RPRO – Reprocessing
13. API – Application Programming Interface
14. PCC – Pearson Correlation Coefficient
15. RH2M – Relative Humidity at 2 meters
16. T2M_MAX – Maximum daily temperature at 2 meters.
17. ANN – Artificial Neural Node.
18. RFR – Random Forest Regression.